From the Institute for Signal Processing (ISIP)
Director: Prof. Dr.-Ing. Alfred Mertins

Computational Modeling Approaches of Deep Brain Stimulation (DBS) in Parkinson's Disease (PD)

Dissertation For
Fulfillment of Requirements for the
Doctoral Degree of the University of Lübeck
- Department of Computer Sciences/Engineering -

Produced by

Felix Njap

Born in Douala, Littoral Province, Cameroon
Lübeck, 2012

First referee: PD. Dr. rer. nat. Jens Christian Claussen

Second referee: Prof. Dr.-Ing. E. Barth.

Date of oral examination: 25.01.2013

Approved for printing, Lübeck: 25.01.2013

"Modelers should not start building models without talking to a biologist, and ideally, experimentalists should have the input of computational modelers when planning and designing experiments."

—— Dr. Shayn Peirce

DECLARATION

I hereby declare, that this thesis is my own work and effort and that it has not been submitted anywhere for any award. Where other sources of information have been used, they have been acknowledged.

Lübeck,

—Felix Njap

Abstract

Parkinson's disease (PD) is a progressive neurodegenerative disorder that is often characterized by motor symptoms. Motor symptoms that can be relieved with medication or brain stimulation. Electrical high frequency stimulation (HFS) with 130 Hz represents an effective therapy (Obeso et al., 2001), however the mechanism mode of action is still under debate. Modeling this mechanism was first done with the Albin-Delong model (Albin et al., 1989), which assumed two discriminated feedforward projections, from the input stage striatum to the output stage internal globus pallidus (GPi) and substantia nigra pars reticulata (SNr). However, this influential contribution neither took motor control into account nor the evidence for a selective effect of high frequency stimulation.

Recently neurochemical findings provide initial evidence that HFS has a specific effect on GABAergic neuronal terminals resulting in an enhancement of extracellular GABA (Hiller et al., 2007; Li et al., 2006; Moser et al., 2003; Mantovani et al., 2006, 2009). In this thesis, we present our theoretical work that at least in part supports this hypothesis from modeling perspectives.

Firstly, we tackled the following question: From a computer simulation with some assumptions and restrictions, and, after processing, spike trains were produced. How do we validate or compare that simulation with real data? To attempt an answer to this question, we studied and investigated different spike similarity measures. Secondly, in another study, I investigated the GABAergic circuits in the basal ganglia and movement disorders and showed that a high concentration of the inhibiting neurotransmitter GABA together with electrical stimulation re-establishes faithful thalamocortical relaying which was broken in Parkinsonian conditions.

Finally, we used the mean-field techniques to study the oscillations patterns in the simple model of a coupled pair of glutamergic of the subthalamic nucleus (STN) and the GABAergic neurons of the external segment of globus pallidus (GPe) and showed that under certain circumstances, the network is capable of self -sustained oscillations without any external oscillatory input.

Contents

Acknowledgements

I would like to express my sincere gratitude to all those who have contributed directly or indirectly to this thesis. First and foremost, I would like to thank my thesis supervisor **Prof. Dr. rer. nat. Ulrich G. Hofmann** who guided me in this challenging, fascinating and exciting research field. I am grateful to him for all the scientific overviews, his modesty and infinite kindness, For the good person he is, who gives hope in humanity, I express my deep admiration.

A special thank goes to **Prof. Dr. med. Andreas Moser** for his deep scientific views, help and ideas on all the scientific writing and foolish things we worked on together. He has always been extremely friendly and helpful with me during these years. But above all, he has always found some time for me, despite all things that kept him busy. I really appreciated it.

I would like to express my gratitude to **PD. Dr. rer. nat. Jens Christian Claussen** for an incalculable number of suggestions and invaluable inputs during my PhD studies, and finally, for his motivational tête-*à*-tête.

I am thankful to **Prof. Dr.-Ing. Alfred Mertins**, the institute's director for the opportunity to carry out our project in the stimulating working environment. I extend my thanks to all institute staff and students especially to the secretary **Christiane Ehlers** for her multiple assistance and **Thomas Schnelle** for his technical support.

I am also grateful to **Prof. Roman Borisyuk** - University of Plymouth who gave me the chance to do the internship at his lab, and introduce me to the mean-field theory. It was an exciting experience.
I am indebted to **Robert Merrison** PhD student in computational neuroscience - University of Ply-

mouth for his precious bifurcation stuffs and to **Richard Taylor** my former landlord in Plymouth for both taking their time to read the earlier manuscript of this thesis and whose helpful comments were welcome.

I extend thanks to all my friends **Yijing**, **Simon**, **Amr** and **Mehrnaz** for their support, and timely suggestions. It has been a pleasure to work with all of you. A special thank goes to **Chen** for his precious matlab code suggestions. I also thank all the Graduate School students for the friendly environment and enlightening discussions during our formal/informal meetings and the good times spent over the past years.

This work would not have been possible without the support of the Graduate School for Computing in Medicine and Life Sciences funded by Germany's Excellence Initiative [Deutsche Forschungsgemeinschaft DFG- GSC 235/1]. I would like also to acknowledge the Fields Institute - Toronto for their generous travel support.

Last but not the least, I am extremely grateful to my mother for her affection and constant encouragement without which I would not have come to this position in my life.

—Felix Njap

Chapter 1

Introduction

1.1 Aim and scope of the thesis

Electrical high frequency stimulation (HFS) of the thalamus or the basal ganglia (BG) represents an effective clinical technique for the treatment of several medically refractory movement disorders (Benabid et al., 1996; Obeso et al., 2001). The mechanism of actions of electrical high frequency stimulation (HFS) with 130 Hz are, however, not fully elucidated (Vitek, 2002; McIntyre and Thakor, 2002). The main focus of the work presented in this thesis is Computational modeling approaches of electrical high frequency stimulation (HFS) in Parkinson's Disease (PD) to understand its influence on the motor symptoms of the diseases. The key hypothesis of this thesis is based on recently neurochemical on HFS rationale findings by (Moser et al., 2003; Mantovani et al., 2006; Feuerstein et al., 2011), according to which the electrical high frequency stimulation used for the treatment of neuropsychiatric diseases selectively induces GABA release, in other words GABA system is involved in the effectiveness of HFS.
To achieve this goal, this thesis addresses the following questions:

- Before assembling details of the models: *How should the models be compared?* This is a general difficulty in computational neuroscience, and before comparing data with models, or models with models, the means of comparison should be found and adapted to the type of models and data;

- *What could be the impact of extracellular neurotransmitter concentration GABA in thalamocortical relay fidelity?* The answer to this question can give clues about the selective release of GABA as possible explanation of the mode of action of HFS;

- *What favor the generation of oscillatory activities associated with some motor diseases?* The answer to this questions may help to understand and improve treatments during neuropsychiatric conditions.

1.2 Thesis Overview

This thesis is organized as follows:

Two introductory chapters review the neurophysiological and clinical background (chapter 1) and the models of computational neuroscience which form the methodical background (chapter 2) In the general introduction, we will provide literature review and background to the world of Parkinson's disease, which include the etiology or the cause of the disease, the pathophysiology and the therapy of the disease as well as the anatomy and physiology of the basal ganglia. Some models of the basal ganglia function in relation to PD will be presented, followed by an overview of electrophysiological and behavioral findings in PD patients and animal models of PD. The neurotransmitters glutamate and GABA will be presented, and we will emphasize on inhibitory GABAergic cells which is the core study of this work.

In **Chapter 2**: we provide a detailed description of the methods as applied in the different studies followed up with the presentation of each study in a separate chapter.

Chapter 3: investigates and applies different spike (dis)similarity measures to compare stochastically produce spike trains generated by one model to another.

Chapter 4: investigates the possibility of replacing deep brain stimulation (DBS) currents in an existing basal ganglia thalamocortical circuitry with a GABAergic current applied to the same target cell. This is illustrated by the changing ability of the thalamus to faithfully relay sensory input to the cerebral cortex.

Chapter 5: uses mean-field techniques to study the oscillatory patterns in the model of subthalamopallidal network of the basal ganglia, uses bifurcation analysis to get a deeper understanding of how oscillations can occur, and separates boundary regions of different dynamics.

The concluding **Chapter 6** discusses the results, summarizes the findings and points out limitations of the studies presented in this thesis.

1.3 Parkinson's disease

Parkinson's disease (PD) is a progressive neurodegenarative disease, that was first described by James Parkinson in his work *An Essay on the Shaking Palsy* (Parkinson, 1817). The disease is characterized by resting tremor, slowness of movement (bradykinesia), poverty of movement (hypokinesia) and rigidity (Burch and Sheerin, 2005). The degeneration or death of dopamine-generating cells in the pars compacta region of the substantia nigra leads to alterations in the activity of the neural circuits within the basal ganglia that regulate movement resulting in a difficulty to perform both voluntary and involuntary movements. Some evidence suggests that PD is involved in other non-motor diseases such as dementia, depression and sleep disturbances (Poewe, 2008), thus, resulting in long-term alteration of the quality of life.

PD affects about 0.3% of general world population but over 3% of people aged over 65 (De Lau and Breteler, 2006). Considered as the second prevalent neuropathology disorder after Alzheimer's disease (Nussbaum and Ellis, 2003). Approximately 60,000 people are freshly diagnosed with the disease per year. The average age of onset of symptoms is 60 but 5 to 10% of patients have symptoms before the age of 40. The Parkinson Society Canada reported that, over one million people have been diagnosed with PD in North America and over 100,000 Canadians are coping with the brain disease every day. With age the prevalence of the disease increases (Dorsey et al., 2007).

1.3.1 Cause of Parkinson's disease

The cause of the disease is still contentious, genetic predisposition, environmental factors, and excitotoxic cell death are suggested to be linked to the disease. Correlation between the loss of dopamine and severity of symptoms have been elucidated (Folley and Riederer, 1999). When $\sim$ 90% of cells producing dopamine in the brain area called the SNc are impaired, symptoms of PD appear (Marsden, 1990).

Lewy bodies

Accumulation of protein called alpha-synuclein into inclusions called Lewy bodies often characterized the pathology of the disease. Lewy bodies are found in neuronal populations in the brains of PD patients (Lang and Lozano, 1998), particularly in basal forebrain, cortex and brain stem. There is no clear relationship between Lewy bodies and symptoms of PD, since Lewy bodies are not only identified in PD but also in other neurodegenerative disorders (Tomiyama et al., 2007).

Genetics

Evidence shows that Parkinson's disease is associated with genetic factors (Betarbet et al., 2002; Klein et al., 2009a; Klein and Djarmati, 2011). Investigation in families with inherited forms of PD report that a few genes are associated with the disease. Consequently, family members with PD are more likely to develop the disease than relatives without any PD history (Klein and Westenberger, 2012; Klein and Lohmann-Hedrich, 2007; Klein et al., 2009b). Particularly, male relatives have a higher risk than female relatives. Many genetic mutations have been directly connected to the disease (Klein and Schlossmacher, 2007), but these have an effect only in some first-degree relatives.

Environmental factors

The epidemiology of the disease showed the existence of several factors as potential environmental factors, contributing to the disease (e.g. living in the rural area, potable water). A high risk of PD is associated with the exposure to an environmental toxin or injury and certain chemicals such as manganese and pesticides (Priyadarshi et al., 2001). There is no strong evidence that any environmental factor can be seen as the origin of the disease, since some people are exposed to toxin without developing the disease. The neurotoxin 1-Methyl-4-phenyl-1,2,3,6-tetrahydropyridine (MPTP) is one of the most notable ones that can induce parkinsonism. Environmental toxins and pharmacological agents have been helpful in studying experimental models of PD (Firestone et al., 2005; Werneck and Alvarenga, 1999; Wang et al., 1993).

Parkinson's Disease Symptoms

Three main classes of the disease' symptoms can be categorized: *The primary motor symptoms*, *the secondary motor symptoms*, and *the nonmotor symptoms*. The impairment and disability in patients with Parkinson's disease are evaluated using a rating scale called the Unified Parkinson's Disease Rating Scale (UPDRS). The scale is divided into different parts: Part I: *evaluation of mental activity, behavior, and mood*; Part II: *self evaluation of the activities of daily life (ADLs)* Part III: *motor evaluation*; Part IV: *Hoehn and Yahr stating of severity of Parkinson disease*; Part V: *Schwab and England ADL scale* (Goetz et al., 2008).

1.3.2 Primary Motor Symptoms

Tremor

Unilateral tremor consists of shaking or oscillating movements, appearing when the patient is at rest. During resting condition, patients' body shakes involuntary, when no conscious movement is performed and stops when patients begin conscious movement. PD's tremor can be worse, during stress condition. As the disease gradually progresses, tremor affects the other side of the body (Deuschl et al., 2000).

Bradykinesia/Akinesia

Bradykinesia often refers to slowness of movement resulting from an inability to produce the suitable quantity of muscle activity. Patients with PD may have difficulty performing daily activities (e.g. brushing teeth, buttoning a shirt, cutting food) due to bradykinesia. People who experience bradykinesia may walk by dragging their feet along or without lifting them fully from the ground (Berardelli et al., 2001). Akinesia refers to the lack or paucity of spontaneous movement resulting from an inability to combine cognitive and motor processes (Lee, 1989).

Rigidity

An increase in muscle tone often characterizes rigidity. Different forms of rigidity can be seen in various forms of movement disorders, such as PD. *Leadpipe* rigidity appearing as a consequence of an increase in muscle tone gives rise to a sustained resistance to passive movement throughout the whole range of motion, with no fluctuations, whereas *Cogwheel* rigidity is a combination of leadpipe rigidity and tremor which appears as irregular resistance to passive movement as muscles tense and relax. Finally, *Spasticity* is a special form of rigidity that is only present at the start of passive movement (Lee, 1989).

Balance

Postural instability is one of the sign easily noticed. It is characterized by a tendency to be unstable when in a vertical position. Patients suffering from postural instability have lost the reflexes necessary to prevent a fall or to keep an upright posture, and may topple backwards if pushed even slightly. At the advanced stage of the disease loss of coordination and postural instability are the most debilitating symptoms impacting on the patient's quality of life (Williams et al., 2006).

1.3.3 Secondary Motor Symptoms

Freezing

Freezing is characterized by an inability to move muscles in any desired direction, is one of the potentially dangerous problem in PD since it may increase the risk of falling and fractures. Freezing is an important sign of PD that does not have any clear explanation. Patients with freezing symptoms will be reluctant before moving forward. Generally, it occurs in clearly identified situations walking, pivoting, crossing an entrance to a room or building through a door (Lamberti et al., 1997).

Other Secondary Motor Symptoms

Micrographia refers to skrinkage in handwriting that advances in individuals with Parkinson's disease. It happens as a consequence of bradykinesia, which is at the origin of difficult repetitive actions. Dribbling saliva uncontrollably from the mouth is a result of reduced swallowing movements. In addition to above secondary motor symptoms, some patients living with Parkinson's disease will individually experience one of these, dystonia, speech problem, sexual dysfunction, poverty of movement, saliva drooling (Lees et al., 2009).

1.3.4 Nonmotor Symptoms

The majority of patients living with PD, exhibit nonmotor symptoms, that do not involve movement, coordination, physical tasks or mobility. These symptoms can cause difficulty, impair their quality of live more than the visible motor symptoms of PD.

For the treatment of PD, dopaminergic medication and deep-brain stimulation with electrical high frequency stimulation therapy are widely used, despite the fact that the treatment is not able to reverse the effects of the disease. The first therapy aims at replacing dopamine, the degeneration of dopaminergic cell in the SNc, whereas electrical stimulation of the globus pallidus (GPi), the subthalamic nucleus (STN) aims at changing the temporal firing pattern within the basal ganglia (Arle et al., 2008) as well as the output signals from the the basal ganglia (BG) (Meissner et al., 2005).

1.3.5 Dopamine Medication

The dopamine precursor levodopa (L-dopa) was discovered in the 1960's (Cotzias et al., 1967) and is the most potent drug for controlling PD symptoms. As mentioned in section 1.3.1, PD is diagnosed when ($\sim 90\%$) of dopaminergic cells in the SNc are impaired, hence the primary medication to alleviate PD symptoms consists of replenishment of striatal dopamine through oral administration of levodopa. In contrast to dopamine, L-dopa can cross the blood-barrier. L-dopa is taken up by remaining dopaminergic neurons in striatal terminals and changed into dopamine by the enzyme aromatic L-amino-acid decarboxylase. With long-term levodopa medication, the therapy's effect is reduced and instead patients develop involuntary movement (dyskinesia) (Gerlach et al., 2011). There is a controversial debate among researchers about whether lovodopa causes the progression of the disease or not? (Fahn, 2005). Other scientists claim that levodopa has a strong impact on learning ability (Hall et al., 2012).

1.4 Basal ganglia

The basal ganglia (BG) are a group of subcortical nuclei consisting of the striatum, the substantia nigra (SN), the globus pallidus (GP), and the subthalamic nucleus (STN) (Fig.1.1). BG nuclei play a major role in voluntary and involuntary movement control and are associated with cognitive functions. The striatum is the main BG input structure divided into the caudate and putamen which are separated by the internal capsule (Fig.1.1). The STN is also thought as input structure to the BG, because similar to the striatum it receives direct input from the cerebral cortex (Fig.1.2). The globus pallidus (GP) is divided into the internal segment (GPi) and external segment (GPe). Both divisions of the GP have distinctive functionallity and differ from their inputs and outputs. In a similar way, the SN is divided into the pars compacta (SNc) and pars reticulata (SNr). SNc and SNr have the same input but have different outputs and have neurochemical distinct neurons types. A black staining of dopaminergic neurons characterizes the SNc in post-morten tissue. The GPi and SNr are the main output nuclei of the BG through which the BG project to the thalamus, the superior colliculus and the pedunculopontine nucleus (PPN) (Fig.1.2) (Tepper et al., 2007). There are no direct outputs from the BG to spinal or brainstem motor neurons. The BG influence motor, sensory and cognitive cortical information through the thalamus (Kandel et al., 2000). Head and eye movements are also influenced through the superior colliculus (Hikosaka et al., 2000), and spinal cord processing and locomotion and postural control features through PPN (Takakusaki et al., 2004). BG disorders are associated with several debilitating clinical

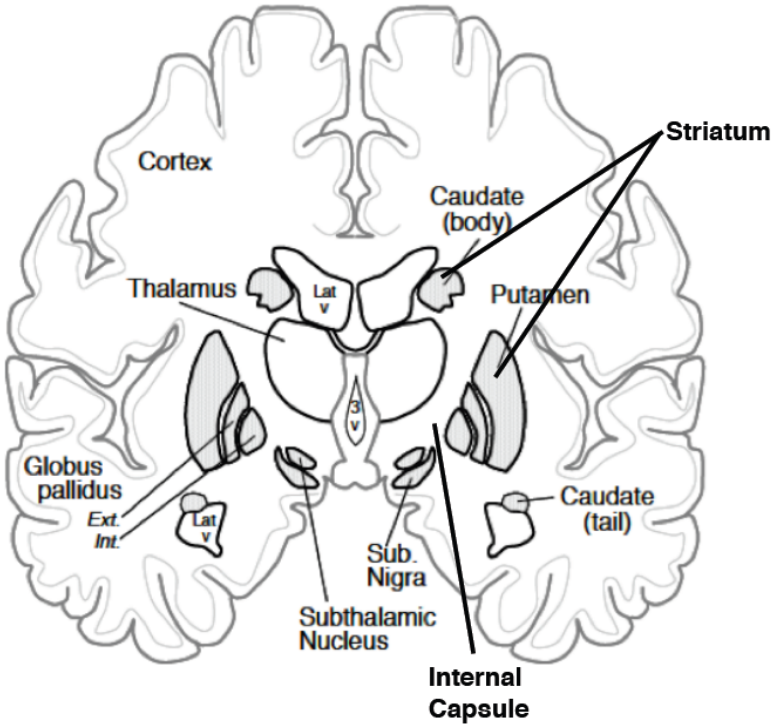

Figure 1.1: Coronal section of basal ganglia and associated structures, modified from:

http://www.neuroanatomy.wisc.edu

conditions whose most easily perceived are movement disturbances. These disturbances can be seen not only in movement disorders such as Parkinson's disease, Huntington's disease and dystonia but also in diseases such as obsessive-compulsive disorder (OCD), schizophrenia and various addictive behaviors. Many of these abnormalities, including PD, have cognitive and affective parts.

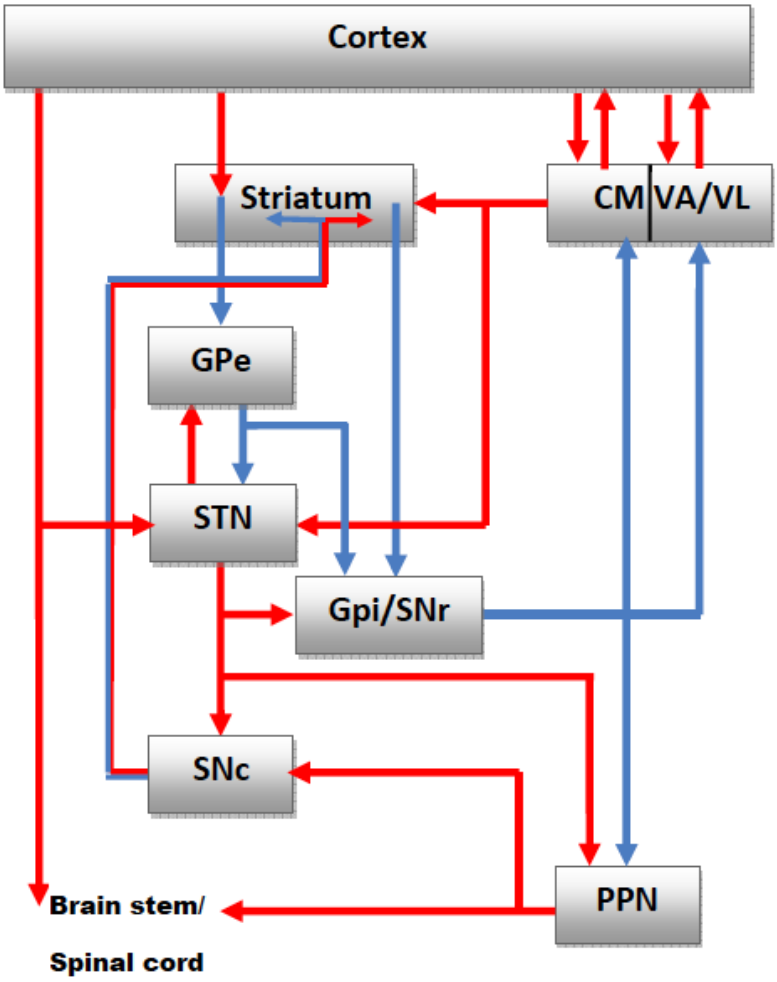

Figure 1.2: The basal ganglia thalamocortical circuitry with associated structures. These structures are connected via a complex network of excitatory (red) and inhibitory (blue) connections. Their external connections include cortical areas, the thalamic centtromedian (CM), ventral anterior (VA) and ventral lateral (VL) nuclei, and the pedunculopontine nucleus (PPN).

1.4.1 Substantia nigra

Located to the dorsal cerebral peduncle in the ventral midbrain (see Fig.1.1), the SN play an important role in reward, addiction and movement (Chakravarthy et al., 2010b). Even though it appears as an unbroken band in brain, SN is divided of two anatomical parts having different connectivity and functionality, namely pars compacta and pars recticulata. Cells of the pars compacta are dopaminergic (dopamine-producing) and also contain neuromelanin, a dark pigment derived from dopamine. Neuromelanin gathers with age in lysosomal granules of the cells and accounts for the dark color of this structure (Tzedek, 2008).

Substantia nigra pars compacta

The striatal neurons send GABAergic input to the SNc which is downregulating, and the striatum receives dopaminergic input from the SNc which is an activating connection. Additionaly, collaterals of the nigrostriatal axons supply extrastriatal dopaminergic innervation of the pallidum and STN. The flow of information is modulated through the dopaminergic neuron of the SNc (Bevan et al., 1996). Aebischer and Schultz show that in healthly monkeys dopaminergic neurons present a relatively low discharge rate $0.5-8Hz$ and long impulse duration $\sim 2.05ms$ on average (Aebischer and Schultz, 1984). These neurons are not related to movement, but in response to rewards during procedural learning and conditioned stimuli change their activity (Schultz, 1986). Besides striatal input, dopaminergic neurons are innervated by other BG nuclei. In rat, these neurons receive massive GABAergic inputs from neurons in the GP and from axon collaterals of SNr projection neurons (Smith and Bolam, 1990). In vivo experiments by (Paladini et al., 1999) shows that electrical stimulation of GABAergic pathways originating in the striatum, GP or SNr produces inhibition of SNc dopaminergic neurons mediated by the $GABA_A$ receptor subtype. Interestingly, the discharge pattern of SNc dopaminergic neurons in vivo can be modulated by local application of $GABA_A$ and $GABA_B$ receptor antagonists according to circumstances. Bicuculline, gabazine and picrotoxin which are $GABA_A$ antagonists considerably produce burst firing in dopaminergic neurons, whereas $GABA_B$ antagonists cause a moderate move to a regular firing 50% of the cases (Paladini and Tepper, 1999). Hence, this suggest that dopaminergic neurons are under tonic GABAergic inhibition mediated by $GABA_A$ receptors. Findings by (Chergui et al., 1993) support that STN stimulation actively causes burst discharge in a subpopulation of SNc neurons, most likely via NMDA receptors, thus suggesting that excitatory inputs to midbrain dopaminergic neurons may be involved in the control of the dopamine release in target areas (Chergui et al., 1993).

Substantia nigra pars reticulata

The substantia nigra pars reticulata (SNr) is the second principal output nucleus of the basal ganglia. It receives afferents from other basal ganglia nuclei and provides efferent connections to the thalamus and brainstem (Fig.1.2). The inhibitory inputs come from the striatum and GPe while the excitatory input from the subthalamus (Hedreen and DeLong, 1991; Bevan et al., 1996). Pars reticulata neurones are also GABAergic and exert firm inhibitory control over parts of the thalamus and brainstem including the superior colliculus, pedunculopontine nucleus and medullary reticular formation (Chevalier and Deniau, 1990).

1.4.2 Striatum

The striatum is major recipient structure of the BG from the cerebral cortex, the thalamus and the brain stem. The striatum can be subdivided into, the *caudate nucleus*, the *putamen* and the *ventral striatum*. Its neurons project to the GP and to the recticular position of the substantia nigra. The caudate nucleus and putamen appear as one structure at the rostral end and are separated by the internal capsule.
The main output neurons of the striatum are GABAergic, also known as *medium spiny neurons* (MSNs). They account for at least 90% of striatal neurons (Bolam et al., 1981). The medium spiny neurons project to the GP and SNr, and send local axon collaterals to other striatal medium spiny neurons. MSNs can be classified according to their projection target and the content of neurotransmitters, even though MSNs are GABAergic. MSNs projecting to SNr and GPi constitute the *direct pathway* and express GABA and substance P, whereas MSNs projecting to the GPe constitute the *indirect pahway* expressing GABA and enkephalin (Albin et al., 1989).

1.4.3 Putamen

The putamen is somatotopically organized throughout its rostrocaudal extent and receives cortical projection for the most part from somatosensory motor areas. It has been associated to execution of movement or proprioceptive information in primates (Alexander and DeLong, 1985).

1.4.4 Caudate nucleus

The caudate nucleus plays a role in associative functions such as planning and prediction of forthcoming events. It receives input from prefrontal cortex and parietal association area (Apicella et al., 1991).

1.4.5 Globus pallidus

The globus pallidus is also comprised of two parts : the internal medullary lamina globus pallidus (GPi) and the external globus pallidus (GPe). The cells of the GPi, like the cells of the SNr use the inhibitory neurotransmitter GABA. The GPi plays a major part in sensorimotor processing and is one of the targets for deep brain stimulation. In rodents, the homologue of the GPi is the entopeduncular nucleus (EPN) that is surrounded by the fibres of the internal capsule, and the GPe is referred to as the GP (Nambu, 2007).

Globus pallidus externus(GPe)

The GPe sends inhibitory GABAergic projections to many BG nuclei including the STN, GPi, SNr and striatum (Bolam and Smith, 1992), that terminate on the soma and proximal dendrites. In the striatum, GPe axons terminate on a spiny interneurons and the dendritic shafts of spiny projection neurons (Sato et al., 2000). A small number of GPe neurons also projects to the dorsal thalamus, reticular thalamic nucleus, inferior colliculus and the PPN (Kita, 2007).

Globus pallidus internus (GPi)

The GPi plays a key role in the BG network as it includes information from the striatum, GPe and STN. The GPi is part of the indirect pathway (**Cortex** $\rightarrow$ **Striatum** $\rightarrow$ **GPe** $\rightarrow$ **STN** $\rightarrow$ **SNr/GPi** $\rightarrow$ **Thalamus** $\rightarrow$ **Cortex**) and the direct pathway (**Cortex** $\rightarrow$ **Striatum** $\rightarrow$ **SNr/GPi** $\rightarrow$ **Thalamus** $\rightarrow$ **Cortex**). The GPi receives inhibitory input from the substance P-containing striatal neurons and excitatory input from the STN (Parent and Hazrati, 1995). Unlike GPe neurons that exhibit pauses of activity, GPi neurons fire spontaneously with a mean rate of $60-80\,Hz$ without pauses (DeLong, 1971).

1.4.6 Subthalamic nucleus

The subthalamic nucleus is mostly composed of glutamatergic projection neurons and has a biconvex-shaped morphology. Evidence shows the existence of interneurons as a result of collaterals. The STN plays a key role in BG ganglia organization since STN receives input from, and projects to, many nuclei (Alexander and Crutcher, 1990).

In primates, STN can be divided into three different functional subdivisions. Two *rostral-third* and a *caudal-third*. The rostral two-thirds can be further divided into medial third and lateral two-thirds.

The medial part of the rostral two-thirds is comprised by the limbic and the part of the associative territories. The ventral feature of the lateral part of the rostral two-thirds comprises the additional part of the associative territory. Some evidence suggest that the dorsal portion of the lateral part of the rostral two-thirds and the caudal third are associated to motor circuits.

The STN is broadly divided into a dorsolateral sensorimotor part and a ventromedial associative part. The dorsolateral region is shown to be somatotopically organized in primates. The lateral fraction contains neurons that respond to arm movements and the more medial fraction neurons that respond to leg movement (Wichmann et al., 1994; Rodriguez-Oroz et al., 2007), whereas the ventromedial part of the STN is involved in oculomotor and associative aspects of motor behaviour, and neurons are activated during visual and oculomotor tasks (Matsumura et al., 1992).

1.5 Neurodegenerative disorders and Basal ganglia

Several neurodegenerative pathologies associated with the basal ganglia structures produce severe movement disorders that can give rise to akinetic or hyperkinetic syndromes. These disorders are characterized by increase or reduce basal ganglia output, GPi and SNr activity leading to an excessive inhibition or disinhibition of the thalamorcortical circuitry respectively (Fig.1.3). This thesis focusses on PD, a hypokinetic disorder due to progressive degeneration of the dopaminergic neurons of SNc (Marsden, 1990).

1.6 Deep Brain Stimulation

Ablative surgery of the motor thalamus and the internal segment of the globus pallidus were often performed in the early 1950's (Kringelbach et al., 2007). Electrodes were inserted in the target area, using stereotactic neurosurgical techniques, and lesions were created using radiofrequency current (Osborne, 2009). With the introduction of L-dopa, the amount of ablative surgery started to decrease in 1969 (Wichmann and DeLong, 2006). With the shortcomings of L-dopa in the early 1990's, and the better comprehension of the the globus pallidus and the subthalamic nucleus in the organization of normal motor control and PD, there was an increasing use of pallidotomy, which was efficient in reducing L-dopa induced dyskinesias (Narabayashi et al., 1997).

Benabid performed successfully the first deep brain stimulation with HFS into thalamic ventralis intermedius (Vim) in 1987 (Benabid et al., 2005) to treat tremor. Nowadays, device consists of three

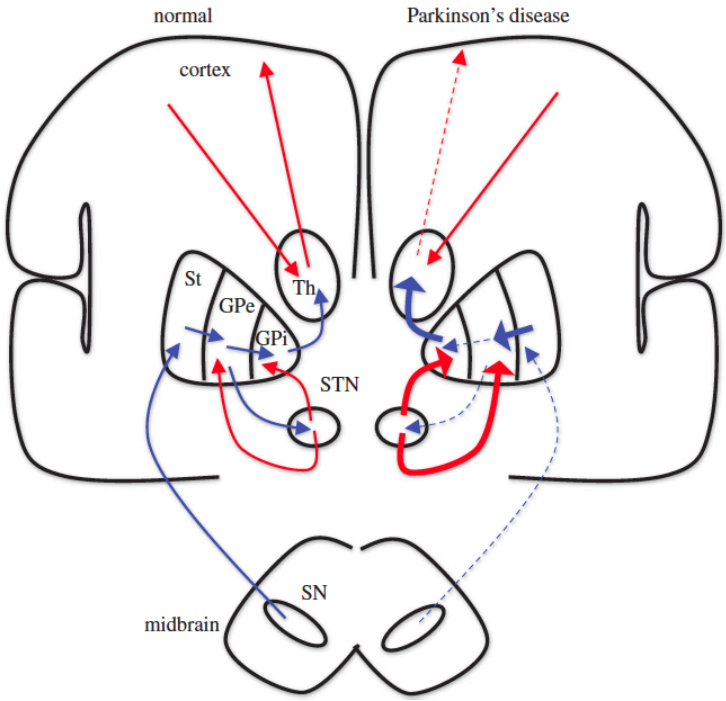

Figure 1.3: An imbalance network in Parkinson's disease. Blue arrows shows inhibitory projections while red arrows indicates excitatory projections. The figure shows the strikingly difference between the normal (left) and Parkinson's disease (right) state. The thickened (thinned) lines indicate an increase (decrease) in excitation (red) or inhibition (blue), taken from (Schiff, 2010).

main components, the electrode, extension wires and a battery-operated medical device called a neurostimulator. The electrode lead is connected with an extension wire to the neurostimulator, which is a programmable pulse generator implanted below the clavicle (Fig.1.4). The therapy consists of implantating the neurostimulator that sends electrical impulses to the target part of the brain (which may be VIM, STN or GPi) (Feuerstein et al., 2011). The surgical technique presents several advantages compared to neuroablation. DBS electrodes can be implanted unilaterally or bilaterally with minor side effects (Bastian et al., 2009). Patients may still continue to take L-dopa medication with the implanted device. DBS is an established procedure to treat patients with dystonia as well (Vercueil et al., 2001; Tagliati et al., 2004). Investigations for the potential treatment of other neurological disorders such as obsessive-compulsive disorder (OCD) (Hodaie et al., 2002), epilepsy (Gabriels et al., 2003), Tourette syndrome, chronic pain, depression are currently underway.

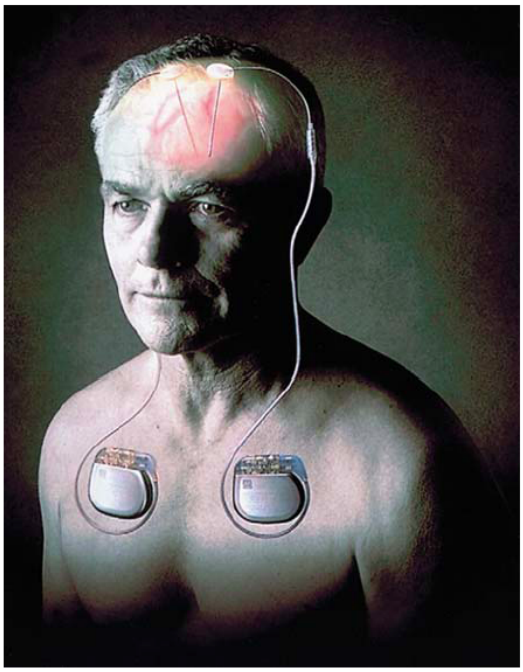

Figure 1.4: Deep brain stimulation placement. The image shows bilateral electrodes, extension wires and neurostimulator, taken from (Mogilner et al., 2001).

Electrical stimulation of GPi or STN have been efficient for most of the symptoms of PD (Tronnier et al., 1997). One of the most remarkable effect in GPi or STN is the reduction in L-dopa dyskinesias. GPi-DBS puts an end to L-dopa-induced dyskinesias, whereas STN-DBS helps patients to decrease their

L-dopa intake, thus reducing dyskinesias (Moro et al., 1999). For the reasons above, STN-DBS and GPi-DBS are preferred treatment options. In particular to treat dystonia, GPi-DBS is preferred. Despite being an invasive procedure, DBS is recommended to patients with L-dopa allergy and those exposed to complication and motor fluctuations that cause severe disability (Vercueil et al., 2001). Even though thalamic stimulation has been effective for PD tremor, it is rarely recommended since its theurapeutic effect on other main PD symptoms is not beneficial (Lozano et al., 2000).

Positive and negative effects

Reported findings on postoperative bilateral STN-DBS with HFS symptomatic therapy are in most cases encouraging and favorable. Such studies are summarized in (Ashkan et al., 2004). Overall it shows significant improvement in motor function and L-dopa induced dyskinesia as defined by the UPDRS.

1.6.1 Mechanisms of electrical HFS

Hypotheses

According to (Heida et al., 2008; McIntyre et al., 2004b), various hypotheses on the mechanisms of actions of HFS have been reported, currently there exist four general hypotheses to explain the therapeutic mechanisms(s) of HFS:

- **Depolarization blockade**

  Stimulation-induced alterations in the activation of voltage-gated sodium and calcium ions channels that block neural output near the stimulating electrode (McIntyre et al., 2004a; Lozano et al., 2002; Beurrier et al., 2001);

- **Synaptic inhibition**

  Indirect inhibition of neuronal output by means of activation of axon terminals that make synaptic connections near the stimulating electrode (Dostrovsky et al., 2000);

- **Synaptic depression**

  Lack of successful synaptic transmission of the efferent output of stimulated neurons as a result of transmitter depletion caused by excessive stimulation by the electrode (Urbano et al., 2002);

- **Modulation of pathological network activity**

  Stimulation-induced interruption of pathologic network activity (Montgomery and Baker, 2000).

Depolarization blockade and synaptic inhibition represent hypotheses that explain the similarity between ablative therapy and DBS. To support both of theses hypotheses, single-unit recordings of local cells in the stimulated target were used (Beurrier et al., 2001; Dostrovsky et al., 2000; Benazzouz et al., 2000). The main drawback of these hypotheses is the lack of the possible independent activation of the efferent axon of local cells. As a result of this, it is not clear why impulses are still being generated around the area of the electrode.

Depolarization blockade means that the membrane is depolarized so that spike activity decreases, and finally disappears, owing to inactivation of voltage-gated sodium current. Some scientists claim that the STN spike amplitude does not change in the initial part of the train and the firing rate does not increase before activity decreases, therefore this hypothesis has been refuted (Limousin et al., 1997; Hashimoto et al., 2001). Besides, the response of the soma does not inevitably represent the output of the axon during HFS (McIntyre et al., 2004a). Consequently, while synaptic inhibition and/or depolarization blockade may be occurring in the soma, the functional effect of these phenomena may have limited significance in the therapeutic mechanism(s) of HFS.

Alternatively, the synaptic depression represents the most attractive connection between the functional effects of electrical HFS and ablative surgery. However, several in vivo experimental studies have shown increases in transmitter release (Hiller et al., 2007; Moser et al., 2003; Li et al., 2006; Mantovani et al., 2006, 2009) and sustained changes in firing of neurons of efferent nuclei compatible with activation of neurons near the stimulated electrode and subsequent synaptic action on their targets during electrical HFS (Hashimoto et al., 2003; Anderson et al., 2003; Windels et al., 2003). Consequently, in spite of the fact that some level of synaptic depression is taking place throughout the stimulated network of neurons, this phenomenon does not seem to be sufficient to block signal transmission between nuclei (Li et al., 2005).

Finally, the stimulation-induced modulation of pathological network activity is the general theory that is consistent with the current available data. Alteration in the network activity could have the same effects as ablation therapy induces (Bergman et al., 1998; Deuschl et al., 2001; Vitek and Giroux, 2000). However, this theory does not explain much. It simply states that neural network is altered by the electrodes simulations. The question under debate is how or why the network is altered (McIntyre et al.,

2004a)?

1.6.2 Inhibitory and excitatory effects of HFS

Inhibitory effects of HFS

The subthalamic nucleus (STN) has been recognized as the potential target of choice for the neurosurgical treatment for patients with advanced parkinson's disease. For that reason, a huge amoung of data about STN-HFS has been reported. Most of the recordings immediately after interruption of electrical HFS account for a post-stimulus period of reduced neuronal firing activity followed by the slow recovery of spontaneus activity. In rat brain slice preparation, it has been shown that electrical HFS -STN produces extended disruption in the activation of voltage-gated sodium and calcium (Beurrier et al., 2001). In rats, (Benazzouz et al., 2000) found that a 5 sec electrical HFS train in the STN induced a decrease in STN neuronal activity for 30-90 sec after the stimulation was stopped. There has been evidence

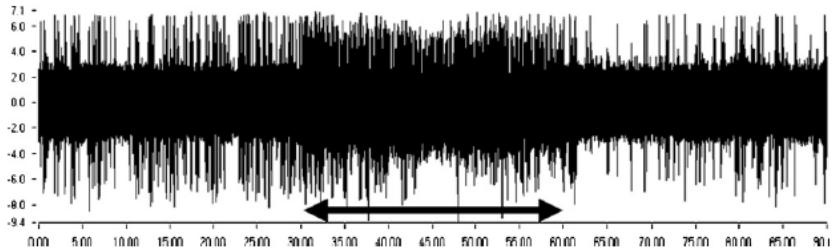

Figure 1.5: Multi-recording of GPi neurons during 30 sec before, during (indicated by the horizontal arrow) and after STN DBS. We can notice the increased activity followed by a reduction. Taken from (Montgomery and Gale, 2007).

that stimulation at higher frequencies (50-200 Hz) and with higher currents produced inhibition lasting for 50 to over 500 msec after the stimulus train in many cells (Dostrovsky and Lozano, 2002). In a similar way, significant work revealed that electrical HFS at frequencies above 50Hz in the STN of patients under DBS (Lozano et al., 2002; Filali et al., 2004), in vivo rat STN (Burbaud et al., 1994) and in vitro rat STN slices (Garcia et al., 2003; Beurrier et al., 2001) produces a period of neuronal silence of hundreds of milliseconds to tens of seconds (Fig.1.5). The inhibitory neurotransmiter γ-aminobutyric acid (GABA) was recognized as a potential key player to convey synaptic inhibition and its role was clearly established (Benabid et al., 2002). Neurochemical studies in the caudate putamen of the rat showed that GABAergic interneurons with functional $GABA_A$ receptors are necessary to

elicit a neurochemical effect of electrical high-frequency stimulation (Moser et al., 2003). Also, increased GABA release from GABAergic interneurons was characterized as an immediate effect of electrical high-frequency stimulation (Li et al., 2004). Beyond that, a certain type of neuronal pre-activation was associated as a prerequisite for successful electrical high-frequency stimulation applied in vitro and in vivo (Li et al., 2006; Mantovani et al., 2006; Hiller et al., 2007).

Excitatory effects of HFS

The effect of HFS is not only inhibitory, some findings support that HFS-induced excitation, thus modifying the pathological spontaneous activity. These studies solely focus on electrophysiology data, not biochemical to support or not the activation theory. (Maurice et al., 2003) findings show that there is an increase level in SNr activity at high-intensity STN-HFS, but a decreased activity at low-intensity STN-HFS, whereas other studies use both electrophysiology and biochemical explanations to cite evidence in support of activation theory. However discriminating spikes from stimulation artifacts, could probably explain the controversy of both inhibition and activation theory. An alternative solution to this controversial matter was the replacement of electrical stimulation with the use of chemicals instead. They found an increase of spontaneous STN neurons activity, when injecting the monkey STN with gabazine, an allosteric inhibitor of $GABA_A$ channel (Kita et al., 2005). On the other hand microinjection of bicuculline into the rat STN excites the efferents SNr, whereas muscimol, $GABA_A$ receptor agonist produces the opposite effect. Finally, neural activation is a fundamental component of DBS. This in turn led to more intense study of which neural elements are directly stimulated by DBS and how is activation dependent on the stimulation parameter settings (i.e. frequency)

Currently, test studies are underway to investigate DBS with HFS beyond PD conditions. Meanwhile, alternative brain stimulation techniques are now being investigated. The neuronal desynchronization counteract pathological synchronization using *electrical coordinated reset stimulation* (Tass, 2003; Hauptmann and Tass, 2009, 2010) and *closed-loop stimulation* using microelectrodes recording to trigger stimulation (Rosin et al., 2011) are effective, but more studies need to be carried out before they can be used in human patients.

1.6.3 Functional organization of the basal ganglia

The main neurotransmitter in the BG is GABA and the majority of neurons in BG are projections neurons. The striatum, GPi, GPe and SNr are composed of GABAergic projections neurons, whereas the STN contains glutamatergic projection neurons and SNc mainly consist of dopamine generating cells. The striatum consists of populations of interneurons, all but one (the cholinergic interneurons) of which are GABAergic. Fig 1.6 shows a classical basal ganglia pathway information and associated structures. Briefly, the BG receives major excitatory input from the cerebral cortex and the intralaminar thalamic cell nuclei. These afferents are glutamatergic and terminate in the Striatum and STN. The BG (GPi and SNr) send output back to the cortex via the ventrolateral thalamus.

In 1989 (Albin et al., 1989) and 1990 (DeLong, 1990) proposed the famous "box-and-arrow" model of BG connectivity and physiology so-called the *direct pathway* and *indirect pathway* and is still the most influential and accepted contribution. Cortical information is transmitted to the output nuclei of the BG through these pathways. In the direct pathway, striatal GABAergic neurons monosynaptically inhibit the GABAergic output neurons in GPi and SNr, whereas it is assumed that striatal neurons inhibit the GABAergic neurons of the GPe. GPe neurons innervate GPi/SNr via direct projections and indirectly by innervating the glutamatergic neurons of the STN that excite GPi/SNr. In contrast with the direct patway, the indirect pathway excites GPi/SNr. Significantly, the discrimination between these two pathways is not absolute. Anatomical findings show that individual striatal neurons can be involved in both pathways (Levesque and Parent, 2005). Besides the direct and indirect patway, evidence show the existence of a cortical glutamatergic *hyperdirect* pathway to STN. Excitation of GPi/SNr neurons is done through activation of this pathway.

1.6.4 Dopamine role

The balance between these two projections is controlled by a difference between actions of dopamine, from SNc, on striatal neurons. The striatal neurons giving rise to these two projections have the same electrophysiology and morphology properties, but are different in their neurochemical features. Neurons containing substance P preponderance of dopamine receptor D_1-type make *direct* contact with the BG output nuclei, whereas striatal neurones containing Enkephalin mainly express D_2-type make *indirect* contact with output nuclei via GP and STN (Aubert et al., 2000).

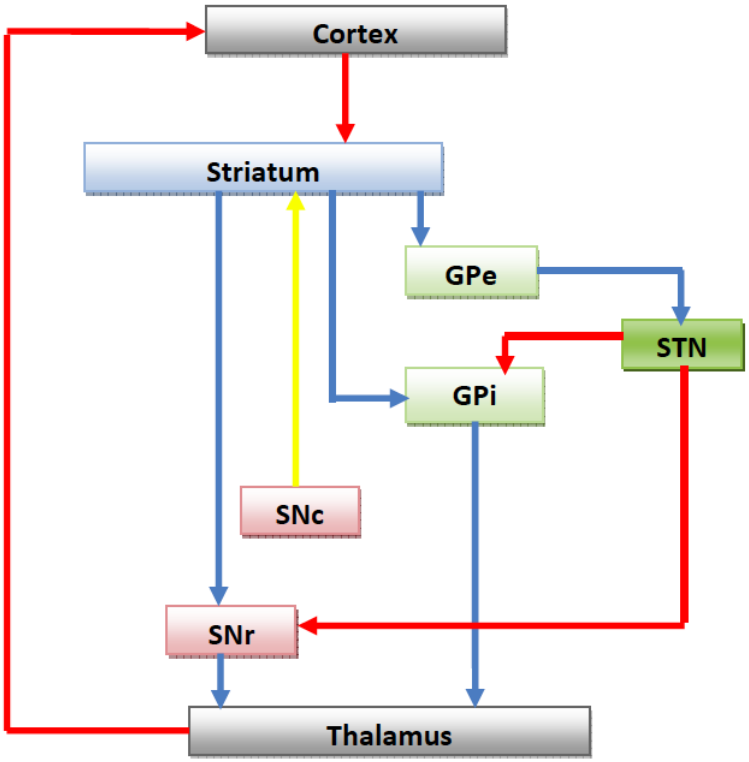

Figure 1.6: Classic connectivity diagram of the Basal Ganglia, showing glutamatergic pathways as red, dopaminergic as yellow and GABA pathways as blue.

1.6.5 External architecture

Besides the internal BG nuclei organization described in the above section 1.6.3, BG nuclei also have distinct circuits with the external nuclei, the thalamus, the pedunculopontine nucleus and large region of cortex. This functional organization may allow the BG to play role in motor and non-motor functions of the cerebral cortex (Alexander and Crutcher, 1990).

1.7 Associated structures

1.7.1 Thalamus

The thalamus is situated between the cerebral cortex and midbrain, it plays the major role in relaying sensation and motor signals to the cerebral cortex, along with the regulation of consciousness and sleep. Thalamic nuclei have strong reciprocal connections with the cerebral cortex, forming thalamo-cortico-thalamic circuits that are believed to be involved with consciousness. Damage to the thalamus can lead to permanent coma. According to the Albin and Delong's model, the loss of dopaminergic innervation of the striatum is linked with an immoderate tonic inhibition of thalamic motor nuclei (DeLong, 1990).

1.7.2 Cortex

From a macroscopical point of view, the cortex is roughly a sheet of tissue that makes up the outer layer of the brain. There are two hemispheres of the brain, separated by a central fissure. Each hemisphere is then made up of four lobes. The *frontal lobe* located anterior to the central sulcus, the *parietal lobe* found dorsally to the same central sulcus, the *temporal lobe* on the most lateral part of the cortex and the *occipital lobe* which occupies the most occipital part of the cortex.

1.7.3 Pedunculopontine nucleus (PPN)

The pedunculopontine nucleus (PPN) is located in the brainstem, caudal to the substantia nigra and adjacent to the superior cerebellar peduncle. It has two divisions, one containing cholinergic neurons, and one containing mostly glutamatergic neurons.

1.8 Models of the basal ganglia

Models of basal ganglia circuitry have provided piece of evidence into the pathophysiological mechanisms of movement disorders and reasons that disruption of parts of the circuit by lesion or deep brain stimulation might improve motor function. In this section, we will review the main three models: the classical *rate model* proposed over 20 yeas ago by Albin and Delong, the *centre-surround* model by Mink and recently the *oscillatory model* by Brown (Weinberger, 2009).

1.8.1 Rate model

The rate model was first proposed by Albin (Albin et al., 1989) and Delong (DeLong, 1990). According to this model, the basal ganglia facilitate and inhibit movement through changes in firing rates in its nuclei. This model, which is largely based on the serial connections between BG nuclei (see Fig. 1.6), provides a coherent explanation of opposing movement disorders (i.e. hypo and hyperkinetic) (DeLong, 1990). Albin and Delong's model suggest that activation of the direct pathway gives rise to decreased activity in GPi/SNr and facilitation of movements through a process of disinhibition of thalamocortical relay neurons. On the other hand, activation of the indirect pathway disinhibits the STN and causes increased activity in GPi/SNr, therefore leading to suppression of movements. In other words, the rate model predicts that decreased GPi/SNr activity would result in movements that are fast and large and that increased GPi/SNr activity would result in movements that are slow and small (Alexander and Crutcher, 1990).

1.8.2 Centre-surround model

The centre-surround model suggests that the basal ganglia functions through centre-surround mechanisms (Mink, 2003; Nambu, 2005; Nambu et al., 2000, 2002). Although the centre-surround model has some appealing features, there is no direct physiological support for it. The model predicts a positive correlation between the discharge of pallidal neurons that participate in the same action, and a negative correlation between pallidal neurons that participate in competing actions. Physiological studies, however, have failed to reveal such relationships between simultaneously recorded basal ganglia neurons (Jaeger et al., 1994).

1.8.3 Oscillatory model

Findings in PD patients and animal models of PD have suggested that loss of dopamine in the striatum leads to excessive synchronized oscillatory activity in the BG which may underlie the clinical features of PD (Brown, 2003) such as akinesia/bradykinesia (Brown, 2006) and limb tremor (Levy et al., 2000).

The oscillatory model for basal ganglia action proposed by Brown (Brown, 2003) suggests that basal

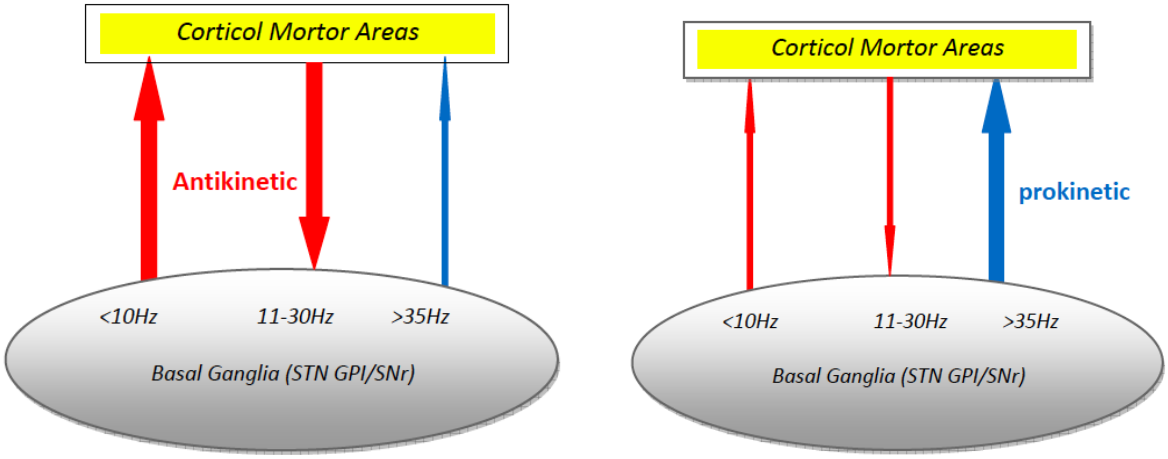

Figure 1.7: Basal ganglia oscillatory model in healthy patient "PD off" (left) and in parkinsoniam patient "PD on" (right). The death of dopamine-generating cells in the pars compacta region of the substantia nigra leads to pathological oscillations activity in the basal ganglia which occurs regularly. Rest tremor activity characterizes by oscillations in $\alpha - band$ (3-7Hz) become apparent in basal nuclei and spread to the cortex to produce (antikinetic) effect, whereas STN is characterized by oscillations in $\beta - band$ (11-30Hz), assumed to be antikinetic. Finally, oscillations in the $\gamma - band$ (>35Hz) facilating movement (prokinetic) are absent in Parkinson's disease. Modified from (Hutchison et al., 2004).

ganglia activity may be synchronized in multiple frequency bands, each with different functional significance. In this model, beta activity plays an *anti-kinetic* role that originates from the cortex while gamma activity, originating from the BG, is *pro-kinetic* by virtue of its facilitation of motor cortical interaction in the $\gamma - band$ (>35Hz) (Fig. 1.7). This theory resolved the paradox of pallidotomy by suggesting that pallidotomy removes abnormally high BG output in the $\beta - band$ (11-30Hz) and $\gamma-$ band and therefore ameliorates motor symptoms in both types of disorders.

Taking together, the three models discussed above, none of these models is truly exclusive. Another

approach to modelling the BG puts forward that the normal dopaminergic system supports segregation of the functional subcircuits within the BG, and that breakdown of this independent processing (by increased synchronization between neurons) could play an important role in the pathophysiology of PD. Many studies have revealed that PD is associated with dramatic loss of spatial selectivity in various regions within the BG-thalamocortical circuit including the STN, GP, thalamus and cortex.

1.9 Neurotransmitters

The main transmitters associated with cortical neurons are glutamate and GABA ($\gamma - aminobutyric\ acid$). A good rule of thumb is that glutamate excites the postsynaptic cell, whereas GABA inhibits it. However, the reversal potential of some GABA receptors is mainly dependent on chloride concentration, so it can be close to rest and even above rest.

1.9.1 Glutamate receptors

The neurotransmitter glutamate activates 2-amino-3-(3-hydroxy-5-methyl-isoxazol-4-yl)propanoic acid (AMPA) and N-Methyl-D-aspartic acid (NMDA). AMPA is very fast and NMDA is involved in memory and LTP of synapses. Both receptors excite the membrane.

AMPA/Kainate

A fast AMPA current synapse is given by 1.1:

$$I_{AMPA} = \overline{g}_{AMPA} s \left(V - V_{AMPA}\right). \tag{1.1}$$

AMPA receptors on inhibitory interneurons have rise and fall times about twice as fast as those on excitatory neurons (Ermentrout and Terman, 2010).

NMDA receptors

NMDA receptor responds quick to glutamate but has effects that last considerably longer than those of AMPA. The NMDA current is given by 1.2:

$$I_{NMDA} = \overline{g}_{NMDA} s B\left(V\right)\left(V - V_{NMDA}\right). \tag{1.2}$$

where s obeys 1.8 and 1.9 and $B(V)$ represents the magnesium block (Jahr and Stevens, 1990) given by:

$$B(V) = \frac{1}{1 + e^{-0.062V}\left[Mg^{2}+\right]/3.57}. \tag{1.3}$$

Clearly as:

$$B(V) = \frac{1}{1 + e^{(V - V_t)/16.13}}. \tag{1.4}$$

where V_t is the half activation and is modelled as:

$$V_t = 16.13 \ln \frac{\left[Mg^{2+}\right]}{3.57}. \tag{1.5}$$

Sometimes it is convenient to implement the NMDA channel so that there is greater flexibility in the rise time. In this case, the channnel is modeled by the two variables,

$$\begin{aligned} \frac{dx}{dt} &= \alpha_1 T(V)(1 - x) - \beta_1 x. \\ \frac{ds}{dt} &= \alpha_2 x(1 - s) - s/\tau. \end{aligned} \tag{1.6}$$

so that the first-order s in 1.2 is replaced by the s in 1.6.

1.9.2 GABA receptors

GABA is the principal inhibitory neurotransmitter in the central nervous system. Two main GABA receptors can be distinguished : $GABA_A$ and $GABA_B$. $GABA_A$ receptors are responsible for fast inhibition and AMPA similar to NMDA receptors, requires a single presynaptic spike to be evoked (Ermentrout and Terman, 2010).

$GABA_A$ receptors

The current is:

$$I_{GABA_A} = \overline{g}_{GABA_A} s \left(V - V_{GABA_A}\right). \tag{1.7}$$

where s obeys

$$\frac{ds}{dt} = a_r [T](1 - s) a_d s \tag{1.8}$$

and

$$[T](V_{pre}) = \frac{T_{max}}{1 + exp\left(-\left(V_{pre} - V_T\right)/K_p\right)} \tag{1.9}$$

a_r characterizes the rise rate of the synaptic conductance and a_d charaterizes the decay. Many modelers assume $a_r = a_d$. The GABA current is conveyed by chloride (among other ions) depending on physiological conditions and the developmental stage of the neurons (Koch and Segev, 1998).

$GABA_B$ receptors

The $GABA_B$ receptor has an indirect effect: transmitter binds to a receptor protein which activates an intracellular complex, a G-protein, which in turn activates a potassium channel to hyperpolarize the membrane.

The model for $GABA_B$ is given by 1.10:

$$\begin{aligned} I_{GABA_B} &= \overline{g}_{GABA_B} \frac{s^n}{K_d + s^n} (V - E_K). \\ \frac{dr}{dt} &= a_r [T] (1 - r) - b_r r. \\ \frac{ds}{dt} &= K_3 r - K_4 s. \end{aligned} \tag{1.10}$$

The nonlinearity in 1.2 means s must become large enough for the synapse to take effect. $GABA_B$ receptors are more effective when several action potentials occur in a row hyperpolarizing (Ermentrout and Terman, 2010).

1.10 GABA in the basal ganglia

The majority of neurons in the basal ganglia use GABA as their major neurotransmitter (Bolam et al., 2000), as a result nearly all basal ganglia neurons receive extensive GABAergic inputs derived from various sources. To better understand the GABA roles in the basal ganglia, it is essential to determine exactly where these receptors are located vis-à-vis to some familiar and recognized neuron subtypes and afferents. This section will be devoted on ionotropic $GABA_A$ and metabotropic $GABA_B$ receptors localization in the basal ganglia, the primary objective is to describe the distinctive nature of the subcellular localization of GABA receptors in different nuclei of the basal ganglia. Different approaches have been used to define the precise localization of neurotransmitter receptor at the regional, cellular and subcellular levels including ligand binding, in situ hybridization, various molecular techniques and immunocytochemistry. In Table 1.1, we summarize some of these immunocytochemical techniques and present their limitations and advantages (Baude et al., 1993; Bernard et al., 1997).

1.10.1 GABA in the striatum

$GABA_A$ receptors

It is not surprising that the $GABA_A$ receptor subunits is heterogeneous due to the existence of cellular heterogeneity in the striatum (Table 1.2). Immunolabelling for the α_1 subunit is kept to GABAergic

Table 1.1: Immunocytochemical Techniques

Method	**Fluorescence Immunolabelling**	**Immunoperoxidase labelling**	**Diffusion reaction**	**Immunogold labelling**	**Freeze-fracture replica**
Advantages	High resolution Ease Rapid Multiple immunolabelling	High sensitive Multiple labelling Appropriate Permanent marker	Excellent spatial resolution Ease quantification Precise localization	**Pre-embedding**:High sensitive Clearly visible **Post-embedding**:Overcome pre-embedding dificulty Multiple immunolabelling	Quantitative analysis High sensitivity Superb resolution
Limitations	Not permanence marker Inappropriate at microscopic level	Not suitable Complicate Peroxidase reaction diffuses		Required small particles Lost of spatial resolution False-negative labelling Post-embedding: Antigenicity	

interneurons that convey parvalbumin, whereas α_3 convey with cholinergic interneurons. (Caruncho et al., 1996). The medium spiny projection neurons, show immunoreactivity for both α_2 and α_3 (Waldvogel et al., 1999). Repartition of $\beta_{2/3}$, and γ_2 subunits is notably homogeneous, apparently mirroring their association with $GABA_A$ receptors having different α subunits. Subcellular repartition of $GABA_A$ receptors data is limited to the α_1, $\beta_{2/3}$ and γ_2 subunits. Immunogold particles coding for these subunits are throughout the striatum when performing analysis using the post-embedding method, with the most noticeable labelling at symmetrical synapses. Even though much effort is needed to unambiguously attribute the labelling to presynaptic and postsynaptic membrane in this type of process, the importance from in-situ hybridization and pre-embedding labelling in the striatum (see Fig.1.8) and other regions of the basal ganglia is that $GABA_A$ receptors are mainly held together, if not solely with postsynaptic structures. The greater number of $GABA_A$ receptor-positive synapses in the striatum express immunolabelling for the $\beta_{2/3}$ subunit, with insignificant number positive for α_1 and γ_2 subunits.

$GABA_B$ receptors

$GABA_B$ receptor subunits immunoreactivity has been described at the light miscroscopic level in rats, monkeys and humans, showing no significant differences between species. $GABA_{B1}$ and $GABA_{B2}$ immunoreactivity is relatively homogeneous throughout striatum (Boyes and Bolam, 2007) with the immense majority of striatal neurons expressing both subunits. (Yung et al., 1999) have reported that double labelling studies for $GABA_B$ receptor subunits is associated with the significant subpopulations of striatal neurons. Medium spiny neurons show insufficient labelling for $GABA_{B1}$, with sufficient labelling seen in large cholinergic interneurons. Localization of $GABA_B$ receptor subunits in the striatum has been analysed in monkeys using the immunoperoxidase method (Charara et al., 2000, 2004) and in rats using the pre-embedding immunogold method (Lacey et al., 2005). Immunolabelling for $GABA_{B1}$ and $GABA_{B2}$ are important in axon terminals forming asymmetrical synapses.

1.10.2 GABA in the globus pallidus: External and Internal

$GABA_A$ receptors

In the GPe, GPi/EP, a sightly different pattern for $GABA_A$ receptor subunits can be observed at the light microscopic level. Neurons and dendritic processes show a significant label for the α_1, $\beta_{2/3}$, and γ_2 subunits in both regions (Fritschy and Mohler, 1995). Immunostaining for the α_3 subunit has been seen in all species inspected. In agreement with reported data in other regions of the basal ganglia, immuno-

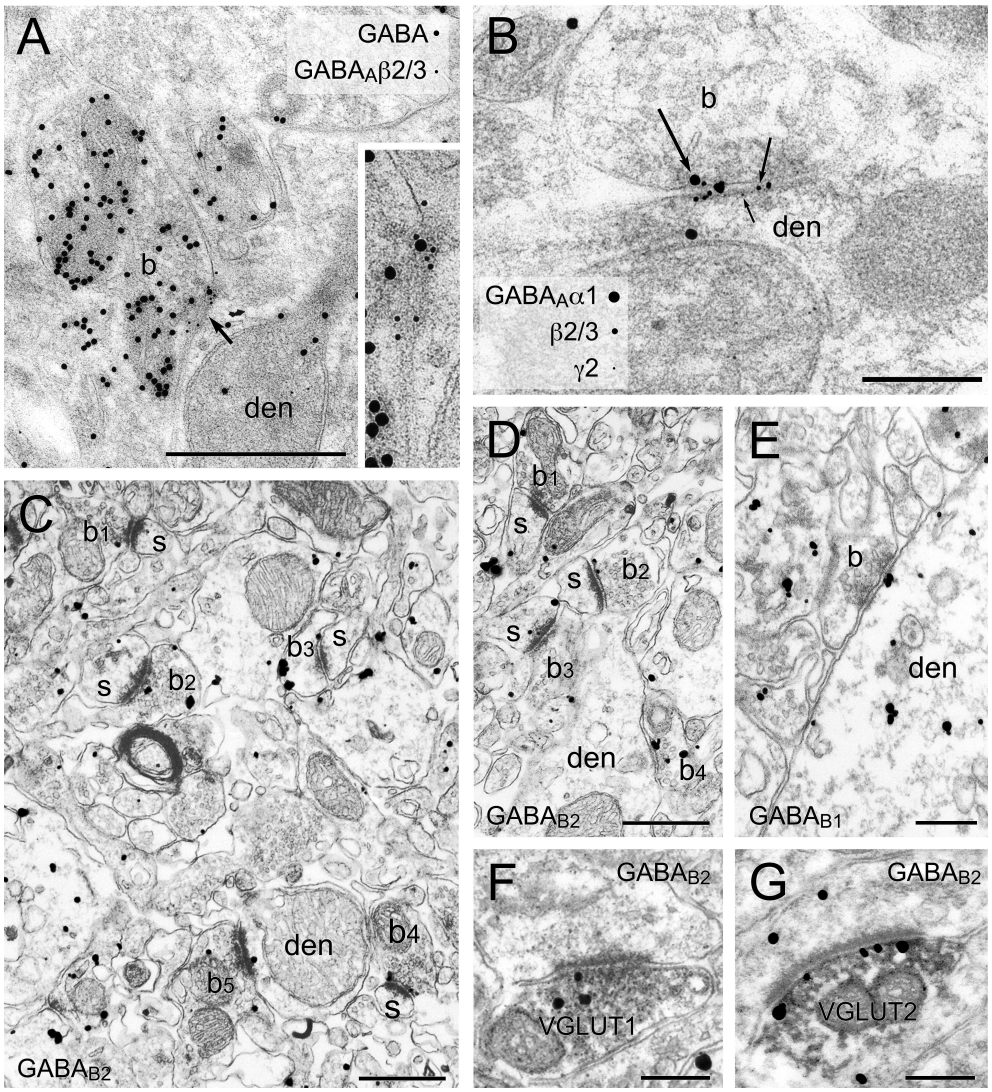

Figure 1.8: GABA receptors in the striatum. (A) post-embedding immunolabelling for GABA, (B) Co-localization of $GABA_A$, (C) Pre-embedding immunolabelling for $GABA_{B2}$, (D) Pre-and postsynaptic immunolabelling for $GABA_{B2}$, (E) Immunolabelling for $GABA_{B1}$, (F) and (G) Presynaptic $GABA_{B2}$ labelling of glutamate. From (Boyes and Bolam, 2007), Image used with written permission of the author.

labelling for $GABA_A$ receptor units is mostly localized on membranes and at symmetrical synapses (Fig. 1.9), whereas in rat the greater number of terminals constituting $\beta_{2/3}$, subunits-posiive synapses in the GP and EP are immunoreactive for GABA.

In Table 1.2 we display a summary of in situ hybridization studies of GABA receptors subunits in different regions of the rat basal ganglia. $GABA_A$ receptor subunits data are derived from (Chadha et al., 2000) and (Wisden et al., 1992); and $GABA_B$ receptor subunits data are derived from (Bischoff et al., 1999).

Table 1.2: In situ hybridization studies of GABA receptors in the rat BG.

Reproduced from (Boyes and Bolam, 2007) with written permission of the author.

	$GABA_A$										$GABA_B$	
	α_1	α_2	α_3	α_4	β_1	β_2	β_3	γ_1	γ_2	γ_3	R_1	R_2
Striatum	(+)	+++	+	++	(+)	(+)	++	(+)	+	+	++	0
GP	+++	++	+	0	(+)	+++	+	++	+	0	+	+
EP	+++	(+)	0	0	0	+++	0	0	+	0	+	+
STN	+++	0	0	0	0	++	(+)	(0	++	(+)	++	++
SNr	+++	(+)	+	0	0	++	(+)	(+)	+	+	+	+
SNc	(+)	0	+	+	(+)	(+)	+	(+)	+	(+)	+++	++

Note: 0 (not detectable), +++ (very strong signal).

$GABA_B$ receptors

Immunolabelling for $GABA_B$ receptor subunits in the GPe is the same in primates and rats. $GABA_{B1}$ and $GABA_{B2}$ labelling are held together with cell bodies and proximal dendrites, and also neuropil, with the magnitude for $GABA_{B1}$ (Charara et al., 2000; Chen et al., 2004). The subcellular repartitions of $GABA_B$ receptor subunits have been described by pre-embedding immunogold labelling in the GP in rats (Chen et al., 2004) and the GPe, GPi in monkeys (Charara et al., 2005). Immunolabelling $GABA_{B1}$ and $GABA_{B2}$ is seen in presynaptic and postsynaptic elements in every part of the GP, whereas in rat, labelling is generally seen in terminals symmetrical GABAergic synapses, comprising striatopallidal terminals.

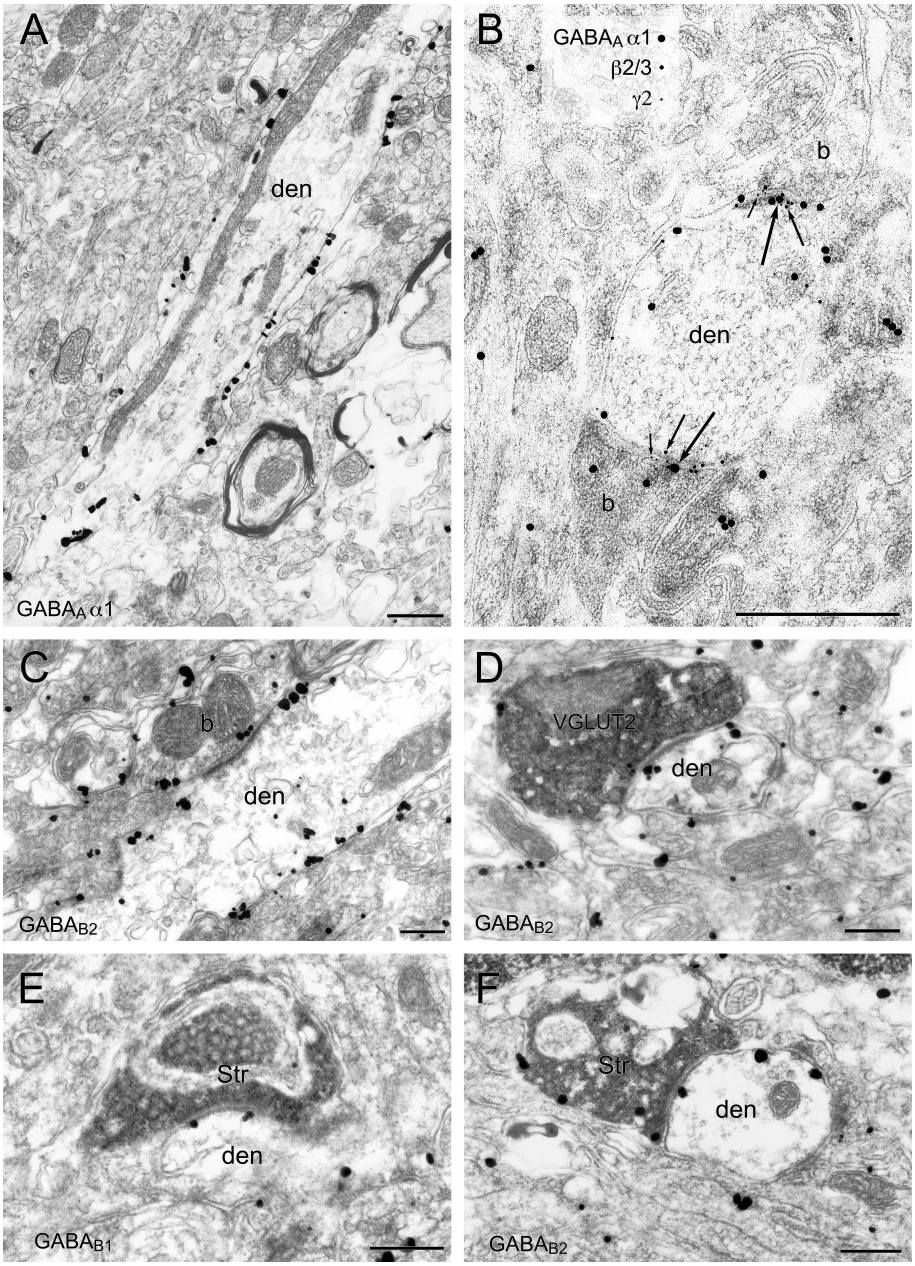

Figure 1.9: GABA receptors in the globus pallidus. (A) post-embedding immunolabelling for $GABA_A$, (B) Co-localization of $GABA_A$, (C) Pre-embedding immunolgold for $GABA_{B2}$, (D) Immunolabelling for $GABA_{B2}$, (E) and (F) Anterogradely labelled striatal boutons. From (Boyes and Bolam, 2007), Image used with written permission of the author.

1.10.3 GABA in substantia nigra

$GABA_A$ receptors

The pattern of $GABA_A$ receptor subunits in the SNr is similar to that which can be observed in the GP, with emphasis on α_1 , $\beta_{2/3}$ and γ_2 subunits. All other regions of BG, strikingly different from neurons in the SNc, supposed to be dopaminergic, show insignificant immunoreactivity for both α_1 and α_2 subunits, but label relatively significant for the α_3 subunit. Other $GABA_A$ receptor subunits showed in the SNc include α_4, β_2, γ_2 and γ_3 (Table 1.3) (Fritschy and Mohler, 1995). Compared to the striatum and GP immunolabelling for $GABA_A$ receptor subunits α_1 , $\beta_{2/3}$, and γ_2 in the substantia nigra is accumulated at the symmetrical synapses and terminals establishing $GABA_A$ subunit-positive synapses are immunoreactive for GABA.

$GABA_B$ receptors

Immunocytochemical studies in rats and primates show that $GABA_{B1}$ and $GABA_{B2}$ are expressed in SNc and also SNr neurons, with a clear difference between the two regions (Table 1.3). Hence, supposed dopaminergic neurons in the SNc are considerably immunoreactive for $GABA_{B1}$ and, to not so great extent, $GABA_{B2}$. Cells in the SNr show only light staining for $GABA_{B1}$ and $GABA_{B2}$, with immunoreactivity mostly deprived to the neuropil. The subcellular repartitions of $GABA_B$ receptor subunits have been reported in monkeys using the immunoperoxidase method (Charara et al., 2000) and in rats using pre-embedding immunogold method. The model of immunolabelling for $GABA_{B1}$ and $GABA_{B2}$ in the SN is similar to those observed in the GP, with both subunits localized in presynaptic and postsynaptic elements, and most labelling at intracellular sites or associated with extrasynaptic sites on the plasma membrane.

In Table 1.3 we display a summary of in situ hybridization studies of GABA receptors subunits in different regions of the rat basal ganglia. Data for $GABA_A$ receptor subunits derived from (Fritschy and Mohler, 1995); data for $GABA_B$ receptor subunits derived from (Charles et al., 2001).

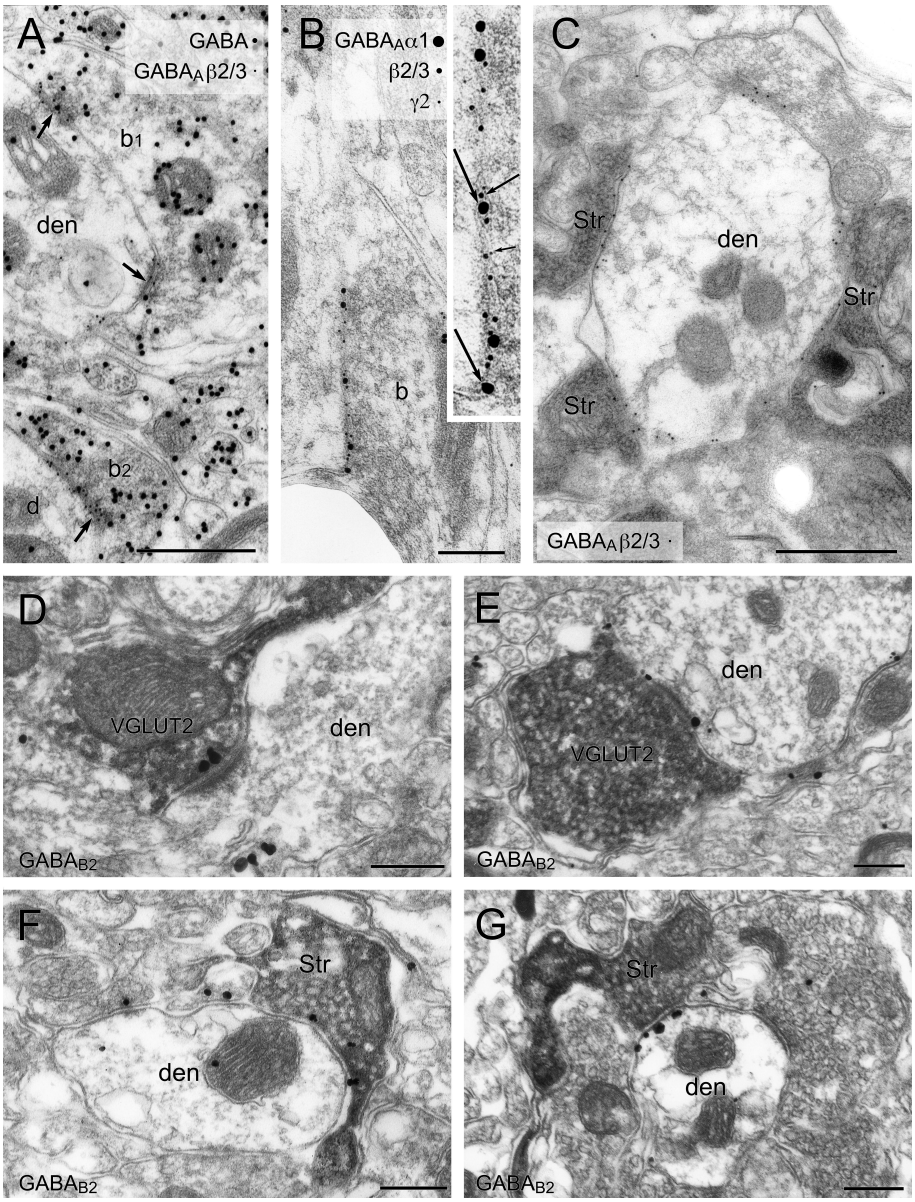

Figure 1.10: GABA receptors in the substantia nigra. (A)-(C) post-embedding immunolabelling for $GABA_A$, (D) and (E) Pre-embedding immunolabelling for $GABA_{B2}$, (F) and (G) Pre-embedding $GABA_{B2}$ immunolabelling. From (Boyes and Bolam, 2007), Image used with written permission of the author.

Table 1.3: Immunohistochemical studies of GABA receptors in the rat BG.

Reproduced from (Boyes and Bolam, 2007) with written permission of the author.

	$GABA_A$												$GABA_B$	
	α_1	α_2	α_3	α_4	α_5	β_1	β_2	β_3	γ_1	γ_2	γ_3	δ	R_1	R_2
Striatum	+	+++	+	++	+	+	+	+++	(+)	++	(+)	+	++	++
GP	+++	+	+	(+)	(+)	0	+++	(+)	++	++	(+)	0	+	+
EP	+++	+	+	0	0	(+)	+++	(+)	+	+++	0	0	+	-
STN	++	+	+	0	(+)	0	+	+	0	++	(+)	(+)	++	-
SNr	+++	0	(+)	0	(+)	(+)	++	0	+	+++	+	0	+	+
SNc	+	(+)	++	(+)	+	(+)	+	0	+	++	++	+	+++	++

Note: 0 (not detectable), +++ (very strong staining), - (not reported)

1.10.4 GABA in subthalamic nucleus

The localization $GABA_A$ and $GABA_B$ receptors (Fig. 1.11) in the STN are not clearly studied (Galvan et al., 2004). Overall contributions mainly resemble those in other regions of the BG. Therefore, $GABA_A$ receptor subunits are improved at symmetrical synapses formed by GABA-positive terminals that probably originate from the GPe. Some of these synapses co-express the α_1 , β_2, β_3 and γ_2 subunits. Immunolabelling for $GABA_B$ receptors is largely conveyed in neuronal perikarya and dendrites in the STN as well as in the ultrastructural level localized at both presynaptic and postsynaptic sites (Charara et al., 2000; Galvan et al., 2004).

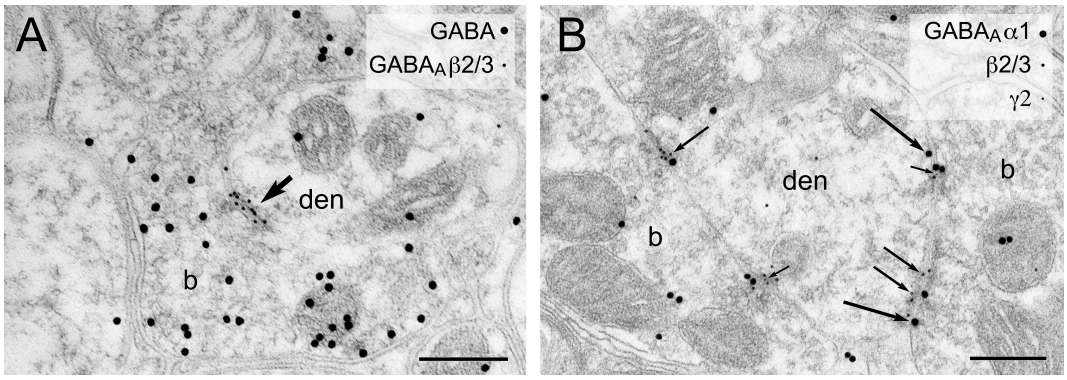

Figure 1.11: GABA receptors in the subthalamic nucleus. (A) post-embedding immunolabelling for $GABA_A$, (B) Boutons (b) forming $GABA_A$ receptor From (Boyes and Bolam, 2007), Image used with written permission of the author.

All regions of basal ganglia, $GABA_A$ receptor subunits are localized at symmetrical synapses formed by

GABA-containing terminals, and are also expressed at extrasynaptic areas, although at less significant densities than at synapses. Synases that express the α_1, $\beta_{2/3}$ and γ_2 subunits of the $GABA_A$ receptors are largely distributed in the network of the basal ganglia. $GABA_B$ receptors are widely distributed than $GABA_A$ receptors, in presynaptic and postsynaptic sites.

1.11 GABA for DBS mechanism

The mechanism of action of electrical high frequency stimulation is still under debate. The number of available parameters, applied in many brain regions to alleviate or treat neuropsychiatric disorders, increase the complexity of unique mechanism associated with the HFS therapy. Improving or optimizing the HFS technology will consist of investigating and identifying a unique parameter. Experimental evidence indicate that only axonal membranes are target of HFS, not other membranes of the neuron. On the other hand excitatory glutamatergic and inhibitory GABAergic are involved and they are active in all clinical conditions where HFS works effectively. For this reason, glutamatergic and GABAergic fibers are considered as primarly, potential mediators of a single HFS mode of action, whereas monoaminergic or cholinergic and other fibers type neurons are highly unlikely to be candidates. Evidence based on pathophysiology of several neurological disorders under deep brain stimulation suggest that selective GABA release may play a key role during electrical high frequency stimulation (Feuerstein et al., 2011).

As mentioned in 1.6, Benabid was the first to perform successfully the first deep brain stimulation into thalamic ventralis intermedius (Vim) in 1987 (Benabid et al., 1987). Parameter settings to produce the most therapeutic benefits of HFS, are frequency stimulation 120 -180 Hz, pulse duration 60-200μs and currents <1 mA (McIntyre et al., 2004b). These parameters are unique and suggest a possible mode of action for all clinical conditions treated with HFS in many brain regions. More than two decades later, HFS mechanism mode of action still elusive. Table 1.4 summarizes various clinical condtions under deep brain stimulation and associated brain areas.

From table 1.4, excitatory glutamatergic and inhibitory GABAergic axons take place in all HFS target neurons, whereas other cells are not present in a particular circumstance. Does this absence supports the assumption of another fiber type other than excitatory glutamatergic and inhibitory GABAergic? A unique mode of action could be valid for glial cells since these are possible targets for HFS in all brain

Table 1.4: Deep brain stimulation (DBS) in CNS disorders

Partially reproduced from (Feuerstein et al., 2011)

Clinical conditions	**Brain region**	**Stimulation**	**Neurons involved**	**Sources**
Parkinson's disease	STN	HFS	Glu-neuronal cell bodies and nerve endings of axon collaterals, GABA-axons with terminals.	(Benabid et al., 1994)
Abnormal involuntary movement	GP_{med}	HFS	Glu-axons with terminals, GABA-neuronal cell bodies and nerve endings of axon collaterals.	(Peppe et al., 2001)
Tremor	Centrum medianum+ ncl. parafascicularis thalami ncl. ventralis intermedius thalami	HFS stimulation (20Hz)	Glu-neuronal cell bodies and nerve endings of axons collaterals, GABA-axons withs terminals, ACh-axons	(Peppe et al., 2008) (Benabid et al., 1987)
Dystonia	GP_{med}	HFS	Glu-axons with terminals GABA-neuronal cell bodies and nerve endings of axons collaterals	(Peppe et al., 2001)
Essential tremor	Ncl. ventralis intermedius thalami	HFS	Glu-neuronal cell bodies and nerve endings of axons collaterals, GABA-neuronal cell bodies and nerve endings of axon collaterals	(Papahill et al., 1999)

areas as refered in table.

In section 1.6.1, we review the possible mechanism of electrical HFS. Among these hypotheses, the activity modulation is widely accepted as a possible hypothesis to explain clinical benefits observed during deep brain stimulation. It is generally assumed that HFS generates network-wide effects having self-contradictory elements with blockage or inhibition of the stimulated nucleus. A recent contribution by (Hammond et al., 2008) suggests that spontaneous pathological patterns of neuronal networks are corrected during HFS. In contrast with this, the firing pattern model of the pathophysiology of Parkinson's disease is under debate. Some findings suggests that oscillatory activity observed during PD comes after parkisonian motor symptoms become visible or noticeable, but this specific characteristic does not support the firing pattern model, which is the basis underlying the activity modulation. Some authors suggest that HFS mode of actions could be explained by a combination of several phenomena (McIntyre et al., 2004b), whereas others assume that the uniqueness of the constellation of HFS parameters suggests a unique mechanism mode of action. Previous hypotheses that contradict, depolarization blockage, the synaptic inhibition, the synaptic depression and the stimulation-induced modulation are: **HFS inactivates stimulated structures** by (Beurrier et al., 2001). Experiments conducted in awake monkeys, and patients with dystonia show that this is inconsistent with the GPe-HFS decreasing the activity of thalamic neurons. The decreased activity observed in the thalamic neurons can be clearly described as a consequence of an increased GABA release. **HFS activates stimulated structures** by (Montgomery and Baker, 2000). Experiments conducted in STN-HFS indicate that the STN firing rate are reduced and increased activity in PD patients. Similarly, (Benazzouz et al., 2000) found that in anesthetized state, the greater number of neurons recorded downstream from the stimulated site during HFS in the STN are inhibited, whereas the decline of excitatory glutamatergic output occurs as a consequence of deactivation of SNr neurons.

1.11.1 HFS-induced selective GABA release

In vitro evidence

Recent neurochemical findings on DBS rationale have shown that in human neocortical slices, HFS targets axons solely and selectively inducing the release of GABA, thus including $GABA_A$ autoreceptors (Mantovani et al., 2006, 2009). This in vitro evidence supports the hypothesis of the mechanism of action of HFS. Findings by (Mantovani et al., 2009) revealed the impossible release of glutamate, associated with that of GABA. HFS does not directly have any effects on nerve terminals. Experiments in striatal

slices of rat caudatoputamen, instead of STN, show a selective GABA release due to HFS in vitro earlier stage (Li et al., 2006).

Initial in vitro evidence indicating HFS-induced selective GABA release was done in rat striatum (Moser et al., 2003; Li et al., 2006). Activating $GABA_A$ heteroreceptors on dopaminergic terminals inhibit the release of DA. During HFS, findings show that GABA release increases and DA release decreases, with bicuculline injection, this effect is reversed, leading to the assumption of activation of $GABA_A$ heteroreceptors by endogenous GABA. Moreover the stimulation frequency (130 Hz) considerably decreases the extracellular DA concentrations, whereas the stimulation frequency (80 Hz) insignificantly altered DA while stimulation at 4 Hz does not have any effect at all.

In vivo evidence

Other in vivo evidence in the striatum of freely moving rats indicates that HFS considerably increased GABA release, without affecting glutamate levels using simultaneously and co-localized microdialysis and HFS (Hiller et al., 2007; Loffler et al., 2008). These findings do not contradict in vitro evidence and also supports the hypothesis of the mechanism of action of DBS-HFS, with the observation that HFS produces the same behavioural effect as $GABA_A$ receptor agonist muscimol local injection both experimentally and clinically (Temel et al., 2007). The only discrepancy between in vivo and in vitro experiments was the HFS time duration. In vivo duration was three times in vitro (i.e. 30 min) sufficient to reflect the steady state GABA concentrations with an operative presynaptic autoregulation.
There are additional biochemical reasons in favor of HFS-induced glutamate release is the measure of cGMP concentration in GPi of STN-HFS treated PD patients. A higher amount of cGMP concentrations was explained as evidence for a local increase in glutamate release since the the level of glutamate concentration was regarded as insensitive to STN-HFS. A decrease in the GABA concentration in the nucleus ventralis anterior thalami, one of the projection of the GPi was reported in line with the view of a reduced GABAergic neurotransmission in the GPi (Stefani et al., 2006, 2005; Galati et al., 2006).

The paragraph above supports the hypothesis that selective GABA release is correlated with HFS in the different target of brain region. **Are there some evidences from computational modeling perspectives?** The answer to this question will be discussed in **Chapter 3** and **Chapter 4**. Before, we introduce the modeling techniques in **Chapter 2**.

Chapter 2

Computational Modeling of Neurodynamics

In this chapter, we briefly provide the descriptions of the modeling methods presented in this thesis, for more insights we suggest the following textbooks (De Schutter, 2009; Izhikevich, 2010; Koch and Segev, 1998; Dayan and Abbott, 2001; Gerstner and Kistler, 2002). A consequent approach to study the brain therapy starts from identification of key features of its basic components, neurons and synapses, from which a simplified or complex functional model neural network can be constructed.

2.1 Neural Modeling

The brain is organized into regions, each region has a large groups of neurons. The neuron's role as the primary functional unit of the CNS was first recognized through the work of the spanish histologist Ramon y cajal. He proposed that neurons were discrete cells acting as metabolically distinct units communicating via specialized circuits and junctions (Ramon, 1890). A characteristic of neuron (also called a nerve cell) consists of, the cell body or soma, one or more dendrites and an axon. Fig. 2.1 (Left) shows the basic parts of a neuron. Each of these parts has a distinct role in generating electrical signals. Neurons are highly specialized for generating electrical signals in response to chemical and other inputs, and transmitting them to other cells. Each of these regions has a distinct role in the communication or generation of signals. The entire cell is surrounded by a thin nerve membrane, any of these elements may be missing. Neurons receive a large number of inputs from thousands to hundred of thousands,

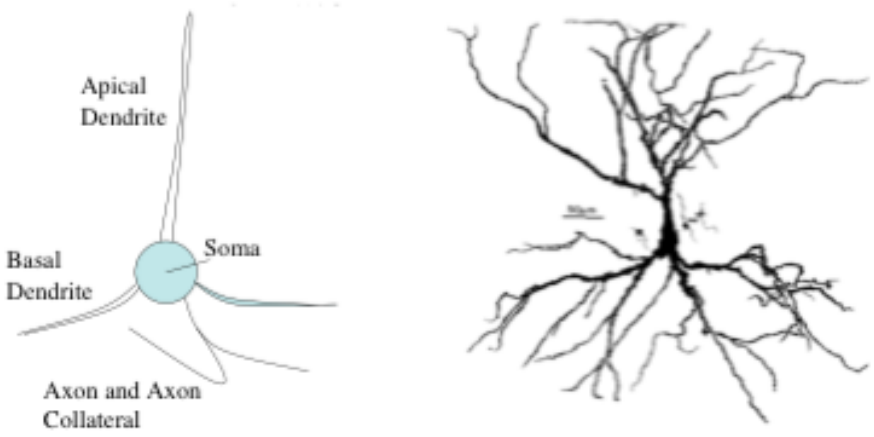

Figure 2.1: Platonic neuron (Left) and a real pyramidal neuron (Right) (Bower and Beeman, 1998)

as in the cerebellar Purkinje cell (De Schutter and Bower, 1994). The soma is the central processing unit (CPU) and performs an important non-linear processing step; if the total input exceeds a certain threshold, then an output signal, the action potential is generated.

The electrically relevant signal for the single neuron system is the potential difference across the soma membrane. Under resting conditions, the potential inside the cell mebrane is about -70 mV relative to that of the surrounding bath, conventionally defined to be 0 mV, and the cell is said to be depolarized. A current has to flow to maintain such a potential difference. This current is uphelp by the ions pumps located in the cell membrane which carry ions to maintain ionic concentration gradients. For most of the play, sodium, potassium, calcium and chloride are the ionic species involved. The concentrations of Na^+ ions is higher outside than inside a neuron, whereas, ion K^+ is more concentrated inside the cell than in the extracellular medium. Ions flow according to their concentration gradient through a variety of ions channels which open and close in response to voltage changes as well as to internal or external signals. Current flowing outside the cell, making the membrane potential more negative is *hyperpolarization*. Inverse current will *depolarize* the cell. If a neuron is sufficiently depolarized, i.e the voltage across the membrane passes a threshold, a positive feedback is initiated and the neuron generates an action potential.

2.2 Neuron Models

A variety of research approaches have so far been considered to study and model neural activity. Electrophysiological recordings of neuronal activity, biochemical analyses, images studies and computational modelling have all shown some strengths and weaknesses. We present through a set of mathematical formulations how neurons are modeled. In the next lines Hodgkin and Huxley, Morris Lecar, FitzHugh-Nagumo, Integrate and Fire and Izhikevich neuron models and a population-based neuron approach model by Wilson and Cowan are reviewed. For the purpose of this thesis, we will only consider the earliest work of Hodgkin and Huxley to represent the process of action potential generation in the squid giant axon (Hodgkin and Huxley, 1952) and the population level modeling by Wilson and Cowan (Wilson and Cowan, 1972).

2.2.1 Hodgkin and Huxley Model

The main electrophysiological features of the neurons were obtained by the pioneering works of Hodgkin and Huxley (Hodgkin and Huxley, 1952). Their paper summarizes the studies on the giant squid axon and proposes an analytical model of ionic currents affecting the neuronal dynamics. Three major currents:*voltage-gated persistent* K^+ current, *voltage-gated transient* Na^+ current with three activation gates and one inactivation gate and *ohmic leak current* I_L, which is carried mostly by chloride ions Cl^-. They showed how these currents account for important features of the neurons such as the generation of action potentials. The basic electrical relation between the membrane potential and the currents of Fig. 2.2 is given by:

$$C_m \frac{dV}{dt} = I(t) - I_{Na} - I_K - I_L \tag{2.1}$$

where C_m is the membrane capacitance, V_m is the intracellular potential (membrane potential). Eqn 2.1 considers the linear model of $I - V$ relations. Each ionic current depends on a driving force and on permeability coefficients which vary according to the potential $V(t)$ across the membrane capacitor. The model of voltage-gated channels can be written by Eqn. 2.2 as :

$$C_m \frac{dV}{dt} = I(t) - \bar{g}_K n^4 (V - E_K) - \bar{g}_{Na} m^3 h (V - E_{Na}) - \bar{g}_L (V - E_L) \tag{2.2}$$

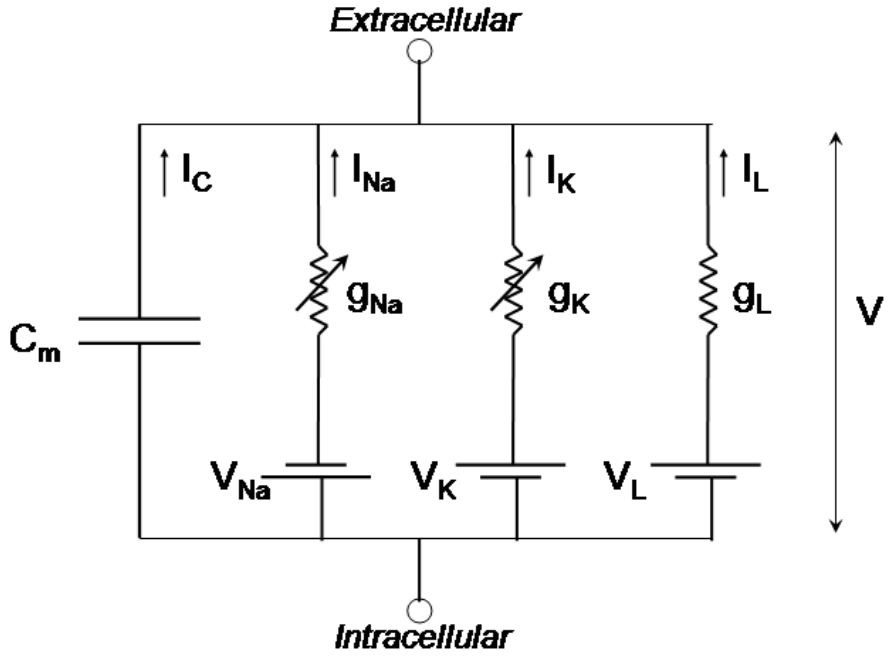

Figure 2.2: Electrical scheme for the conductance-based neuron model by Hodgkin and Huxley

To describe the behavior of g_{Na} and g_K, they introduced three gating variables m, n and h accounting for the probability that a channel is open.

$$\begin{aligned} \frac{dn}{dt} &= \alpha_n(V)(1-n) - \beta_n(V)\,n \\ \frac{dm}{dt} &= \beta_m(V)(1-m) - \beta_m(V)\,m \\ \frac{dh}{dt} &= \alpha_h(V)(1-h) - \beta_h(V)\,h \end{aligned} \tag{2.3}$$

Hodgkin and Huxley estimated the rate constants (α_i and β_i) by fitting empirical functions of voltage to the experimental data. The functions α_i and β_i result of instantiations of the steady-state activation and inactivation functions and of the time constant functions. The related steady-state (in)activation functions of the variable x simply reads $x_\infty = \alpha_x/(\alpha_x + \beta_x)$ and its time constant $\tau_x = 1/(\alpha_x + \beta_x)$.

These functions are :

$$\begin{aligned}
\alpha_m &= \frac{-0.1\,(V - V_r - 25)}{exp\,[-\,(V - V_r - 25)\,/4] - 1} \\
\alpha_n &= \frac{-0.01\,(V - V_r + 10)}{exp\,[-\,(V - V_r + 10)\,/10] - 1} \\
\alpha_h &= 0.07\,exp\,[-\,(V - V_r)\,/20] \\
\beta_n &= 0.125\,exp\,[-\,(V - V_r)\,/80] \\
\beta_m &= 64\,exp\,[-\,(V - V_r)\,/18] \\
\beta_h &= \frac{1}{1 + exp\,[-\,(V - V_r + 30)\,/10]}
\end{aligned} \tag{2.4}$$

In the original model proposed by Hodgkin and Huxley, these functions and constant are set as in table 2.1. The Hodgkin and Huxley model is widely used in the neuroscience community. It is quite precise

Table 2.1: Parameters of Hodgkin-Huxley model.

Ions	$E_{ion}\,(mV)$	$\bar{g}_{ion}, mS/cm^2$
Na	115	120
K	-12	36
L	10.6	0.3

and has the advantage of being based on the main biophysical principles it emulates. This model presents very interesting phase portrait and even chaos. Its main drawback is high complexity and dimensionality that prevent analytical studies and efficient simulations.

2.2.2 Morris and Lecar Model

One of the simplest models for the generation of action potentials is a model proposed by Kathleen Morris and Harold Lecar (Morris and Lecar, 1981). This model has three channels: a *potassium*, a *leak* and a *calcium* channels. In this model, the calcium depends instantaneously on the voltage. Thus, the Morris-Lecar equations have the form given by eqn. 2.5:

$$\begin{aligned}
C_m \frac{dV}{dt} &= I_{app} - g_L\,(V - E_L) - g_K n\,(V - E_K) \\
-g_{Ca} m_\infty\,(V)\,(V - E_{Ca}) &\equiv I_{app} - I_{ion}\,(V, n) \\
\frac{dn}{dt} &= \phi\,(n_\infty\,(V) - n)\,/\tau_n\,(V)
\end{aligned} \tag{2.5}$$

where

$$\begin{aligned} m_\infty(V) &= \frac{1}{2}\left[1+\tanh\left(\left(V-V_1\right)/V_2\right)\right] \\ \tau_n(V) &= 1/\left[1+\cosh\left(\left(V-V_3\right)/2V_4\right)\right] \\ n_\infty(V) &= \frac{1}{2}\left[1+\tanh\left(\left(V-V_3\right)/V_4\right)\right] \end{aligned}$$

Here V_1, V_2, V_3 and V_4 are parameters chosen to fit voltage-clamp data.

2.2.3 FitzHugh-Nagumo Model

FitzHugh and Nagumo (FitzHugh, 1960; Nagumo et al., 1962) was probably the first to propose a discussion for generation of action potential. This model reduces the Hodgkin-Huxley model to a two-variable model for which phase plane analysis can be applied. This reduction was based on the fact that the gating variable n and h have slow kinetics relative to m. Moreover, for the parameter values specified by Hodgkin and Huxley, $n+h$ is approximately 0.8. This led to a two-variable model, called the fast-slow phase plane model, of the form given by eqn. 2.6:

$$\begin{aligned} C_m\frac{dV}{dt} &= I_{app}-g_K n^4\left(V-E_K\right)-g_{Na}m_\infty^3(V)\left(0.8-n\right)\left(V-V_{Na}\right)-g_L\left(V-V_L\right) \\ n_\omega(V)\frac{dn}{dt} &= n_\infty(V)-n \end{aligned} \tag{2.6}$$

This model gives a phase qualitative explanation of the generation and decay of action potential. On the other hand the V-nuclines have the shape of a cubic function whereas the n-nuclines could be approximated with straight line, both within the physiological range of the variables. Consequently a model polynomial can be suggested with the following equations 2.7:

$$\begin{aligned} \frac{dv}{dt} &= v\left(v-\alpha\right)\left(1-v\right)-\omega+I \\ \frac{d\omega}{dt} &= \varepsilon\left(v-\gamma\omega\right) \end{aligned} \tag{2.7}$$

where v represents the fast variable, ω the slow variable. α, γ and ε are constant with $o<\alpha<1$ and $\varepsilon \ll 1$. Both Morris-Lecar and FitzHugh- Nagumo models are bidimensional approximations of the original Hodgkin-Huxley model based on quantitative observations and are more tractable. One of their main advantages is the low dimensionality allowing one to perform a phase plane analysis.

2.2.4 Leaky Integrate -and-Fire Model

The leaky integrate-and-fire (LIF) neuron (Knight, 1972; Tuckwell, 1988) is the drastic simplification of the Hodgkin-Huxley model reducing the number of equations involved from four to one. The LIF is described by a membrane potential variable with the following features time constant, a stable resting potential, a membrane potential threshold for spike generation, a reset for membrane potential after a spike is emitted, and refractory period. The model is characterized by the membrane potential V, which behaves as a passive integrator of synaptic inputs in the subthreshold range:

$$C\frac{dV}{dt} = -g_L\left(V - E_L\right) + I_{syn}\left(t\right) \tag{2.8}$$

where C is the neuron capacitance, g_L is the leak of conductance, E_L is the leak (or resting) potential, and $I_{syn}\left(t\right)$ are the synaptic inputs. The equation for membrane potential dynamics is often rewritten as

$$\tau_m\frac{dV}{dt} = -\left(V - E_L\right) + \bar{I}_{syn}\left(t\right) \tag{2.9}$$

where $\tau_m = C/g_L$ is the membrane time constant and $\bar{I}_{syn}\left(t\right) = I_{syn}/g_L$ describes the synaptic inputs in the units of voltage. A simple model of the LIF has been proposed, the so-called *perfect integrate-and-fire* neuron (Knight, 1972).

2.2.5 Izhikevich Model

The Izhikevich (Izhikevich, 2003) model neuron was developed as an efficient, powerful alternative to the integrate and fire model. It is described as a two-dimensional system of ordinary differential equations 2.10:

$$\begin{aligned} \frac{dv}{dt} &= 0.04v^2 + 5v + 140 - u + I \\ \frac{du}{dt} &= a\left(bv - u\right) \end{aligned} \tag{2.10}$$

with the auxiliary after-spike resetting

$$if\ v \geqslant 30\ mV, \quad then \quad \begin{cases} v \leftarrow c \\ u \leftarrow u + d \end{cases} \tag{2.11}$$

where I is weighted inputs, u and v are dimensionless variables a, b, c and d are dimensionless parameters.

2.2.6 The Wilson and Cowan Model

In most part of the brain it is possible to divide neurons into excitatory and inhibitory depending on the effect of their output on other neurons. The former form predominantly excitatory connections with their postsynaptic neurons, the latter predominantly inhibitory connections. Wilson and Cowan proposed in their original paper a model of two population dynamics for excitatory-inhibitory (EI) neural networks (Wilson and Cowan, 1972).

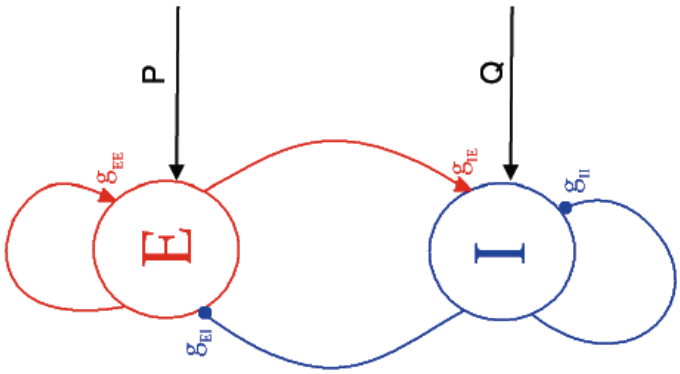

Figure 2.3: Excitatory-Inhibitory network

Two Population Models

A localized neural population composed of an excitatory subpopulation and an inhibitory subpopulation. The evolution of the activity of the neural population is described by the system of two nonlinear differential equations (Wilson and Cowan, 1972):

$$\tau_e \frac{dE}{dt} = -E + (k_e - r_e E) \cdot f_e \left(\omega_{EE} E - \omega_{EI} I + P\right) \tag{2.12}$$

$$\tau_i \frac{dI}{dt} = -I + (k_i - r_i I) \cdot f_i \left(\omega_{IE} E - \omega_{II} I + Q\right) \tag{2.13}$$

Here $E(t) = 0$ and $I(t) = 0$ are the averaged activities of the excitatory and the inhibitory subpopulations, the resting states which represent a low-level background firing or a spontaneous cells firing rate. Therefore, small negative values of these variable represent a suppression of resting activity. r_e and r_i are the refractory constants, P and Q are the external inputs to the excitatory and the inhibitory subpopulations, k_i and k_e are constants, and ω_{EE}, ω_{EI}, ω_{IE}, ω_{II} are the strengths of connections between subpopulations Fig.2.3. f_j is the activation function or response function representing the proportion

of cells firing in a population for a given level of input activity eqn. 2.14, and τ_j represents the time constant of the change in the proportion of non-refractory cells which are firing in a population. k_j is defined to be the maximal value of the functions f_j such that $k_j = f_j(\infty)$.

$$f_j(x) = \frac{1}{1+\exp(-b_j(x-\theta_j))} - \frac{1}{1+\exp(-b_j(\theta_j))} \tag{2.14}$$

where b_j and θ_j are parameters.

Population models are useful method of looking at the nonlinear dynamics involved in neuronal activity and allow the global effect of the manipulation of connections to be observed. More importantly, they allow exploration of the nonlinear dynamics of a system based solely on the connectivity. However, there are a number of signifcant drawbacks that ought to be considered, not only when deciding whether to use population models, but also when considering the results obtained from such models. The main benefit is the ability to utilize bifurcation analysis to investigate the nonlinear dynamics of the model within the parameter space. The main criticism of this method lies in the choice of parameters; there is often deficient data about the number of synapses and their strength and reliability of synaptic transmission, which mediate various connections in the brain (Yousif, 2005). Despite the lack of biologically plausible details, the population-level approach provides a method of examining the dynamics of neuronal networks and allows us to explore systems and produce coherent and testable hypotheses. (Denham and Borisyuk, 2000) used such method to build a model of the septo-hippocampal circuitry and investigated network theta frequency oscillations (Yousif, 2005).

2.3 Spike trains and Point process

Neurons carry information through trains of spikes. Even spikes from the same neuron may display differences in shape; however, they are typically assumed to be identical. Spike trains can be represented using only the time of spike occurrence, i.e. *point process*. A train of n actions potentials occuring in a time window $(0, T]$ is thus defined by the times t_i with $i = 1, ..., n$. The spike sequence can be seen as a sum of infinitesimally narrow Dirac δ functions (Dayan and Abbott, 2001).

$$\rho(t) = \sum_{i=1}^{n} \delta(t - t_i) \tag{2.15}$$

where $\rho(t)$ is the neural response function. The number of spikes occurring in the time window $(0, T]$, also called spike count, is the integral of $\rho(t)$ up to time T,

$$\int_{i=0}^{T} \rho(t)\,\delta(\tau) = n. \tag{2.16}$$

Because the neuronal response is not identical from trial to trial, it is randomly treated.

A **point process** is a stochastic process which generates series of events, such as action potentials. It provides a rigorous framework to model neural activity (Pazienti, 2007). In the next section I will introduce statistical measures that using this framework, allow to quantify the correlations between neurons.

2.4 Quantifying neuronal spike trains

In this section we review different measures, derived from wide spectrum of disciplines including statistics, signal processing, information theory and physics, and investigate the robustness and reliability of those measures by means of surrogate data consisting of two spike trains. In Ch. 3, we apply those measures to compare neuronal responses in a modified Rubin and Terman model under noise pertubations and their original. In this work, we quantify neuronal responses as spike trains which refers to a sequence of neuronal action potentials, with a specific assumption that the shape of the spike and the background activity do not contain relevant information, only the timing of individual spikes. The majority of spike train distances rely on a paramter which controls the temporal scale in the spike trains to which the distance are sensitive. These distances are sensitive to the difference in spike number in a single point of the parameter space, and detects coincidences in the other point. These boundaries represent the features of a rate code which assumes that a neuron's response is completely characterized by its time-varying mean firing rate (Hsu et al., 2004). In experimental setting, neural responses are often recorded from a set of stimuli, and neural coding are accessible through application of clustering approach to the pairwise spike train for different parameter values of the time scale for which the reponses are well identified. The most prominent time-scale dependent measures are discussed in the following lines. A comparison of these measures on simulated data are reported by (Paiva et al., 2010; Chicharro et al., 2011).

2.5 Review of similarity measures

In this section, we successively review and discuss different metrics, the Victor-Purpura distance metric, the Van Rossum similarity Measure, the Schreiber et al. similarity Measure, the Event synchronization, the Stochastic Event Synchrony, the InterSpike Interval distance, the Mahalanobis Distance, the Mutual information.

These measures are applied in a surrogate data and their similarities and differences on the basis of synchrony are investigated.

2.5.1 Victor-Purpura distance

The Victor-Purpura distance metric (Victor and Purpura, 1997), mathematically discussed in ch.3, sec. 3.3.4 is a cost based metric, costs assigned to adding or deleting spikes, moving spikes.

2.5.2 Van Rossum metric

The Van Rossum distance measure was described in (Van Rossum, 2001). Given x and x' two spikes train with spiketimes $t_i\,(t_i) > 0$.

$$x\,(t) = \sum_{i=1}^{N} \delta\,(t - t_i)$$

$$x'\,(t) = \sum_{i=1}^{M} \delta\,(t - t_i)$$

Each time event x and x' is convolved with an exponential function $exp\,(t - x_i/\tau_R)$ with $(t_i > x_k)$ resulting in time series $s\,(t)$ and $s'\,(t)$, the Van Rossum distance measure is computed according to 2.17:

$$D_R = \frac{1}{\tau_R} \int_t \left[s\,(t) - s'\,(t)\right]^2 dt \tag{2.17}$$

If x and x' are identical, $D_R = 0$. τ_R determined the time scale of the Van Rossum measure.

2.5.3 Schreiber et al. metric

The Schreiber et al. distance metric was described in (Schreiber et al., 2003). Given x and x' two spikes train, each time event is convolved with a filter (Gaussian or exponential) with a certain width τ_S resulting in time series $s\,(t)$ and $s'\,(t)$. Then the pairwise correlation is readily computed as:

$$S_S = \frac{\int_t s\,(t)\,s'\,(t)\,dt}{\sqrt{\int_t s^2\,(t)\,dt}\sqrt{\int_t s'^2\,(t)\,dt}} \tag{2.18}$$

The width τ_S of the filter defines the time-scale. If x and x' are identical, $S_S = 1$.

2.5.4 Event synchronization

The Event synchronization was described in (Quiroga et al., 2002; Dauwels et al., 2009b). It defines similarity in terms of coincident events. Two events are coincident if their timing offset is smaller than

a maximum lag τ_Q derived from the two time event x and x':

$$\tau_Q = (k, k') = \min\left(x_{k+1} - x_k, x_k - x_{k-1}, x'_{k+1} - x'_k, x'_k - x'_{k-1}\right)/2 \tag{2.19}$$

The number of times an event appears in x after appearing in x' is computed as:

$$d\left(x/x'\right) = \sum_{k=1}^{N} \sum_{k'=1}^{N'} J_{kk'} \tag{2.20}$$

where

$$J_{kk'} = \begin{cases} 1 & \text{for } \; 0 < x_k - x'_{k'} \leq \tau_Q \\ \frac{1}{2} & \text{for } \; x_k = x'_{k'}, \\ 1 & \text{for } \; elsewhere \end{cases} \tag{2.21}$$

On the same lines, $d\left(x'/x\right)$ can be defined as in eq. 2.20. Therefore, the event synchronization is given by eq. 2.22:

$$S_Q = \frac{d\left(x'/x\right) + d\left(x/x'\right)}{\sqrt{NN'}} \tag{2.22}$$

$S_Q = 1$ if and only if events in x and x' are coincident.

2.5.5 Stochastic Event Synchrony

The Stochastic Event Synchrony was described in (Dauwels et al., 2009b,d). It is quantified by the following three parameters (δ_t, s_t, ρ), respectively time delay, variance of the timing jitter, fraction of "non-aligned" events.

2.5.6 InterSpike Interval distance

The InterSpike Interval distance (ISI-distance) was described in (Kreuz et al., 2007). Discussed in ch.3, sec. 3.3.3 is based on the instantaneous interspike intervals. For two identical spikes the quantity ISI-distance becomes 0, and approaches 1 or -1 respectively, if the first or the second spike train is much faster than the other.

2.5.7 Mahalanobis distance

The Mahalanobis distance was described in (Wright et al., 1999). Discussed in ch.3, sec. 3.3.1. If $\vec{x}$ and $\vec{y}$ are two random vectors, of the same distribution, The Mahalanobis distance is readily given by:

$$d(\vec{x}, \vec{y}) = \sqrt{\sum_{i=1}^{p} \frac{x_i - y_i}{\sigma_i}} \tag{2.23}$$

2.5.8 Mutual information

The Mutual information was described in (Guiasu, 1977; Papoulis, 1984), Discussed in ch.3, sec. 3.3.1, the mutual information measures the mutual dependence between the joint distribution X and Y.

Most of the above measures depend on a parameter that defines the time scale of the interaction between the point processes.

2.6 Application to surrogate data

Previous contributions have shown the differences between some measures on the basis of firing rate, phase in firing rate modulation and synchronous firing for different kernels functions (see Fig. 2.5 and 2.6). Reference spike train was first generated as a realization of a Poisson process, then the spike trains was derived from the reference by copying spikes with a certain probability and by adding jitter noise to each spike time. The operation was done independently for each spike, whereas (Dauwels et al., 2009c) randomly generated 10,000 pairs of one-dimensional point processes (x, x') according to the procedure displayed in Fig. 2.4. The above study provides a systematic evaluation of the discrimination

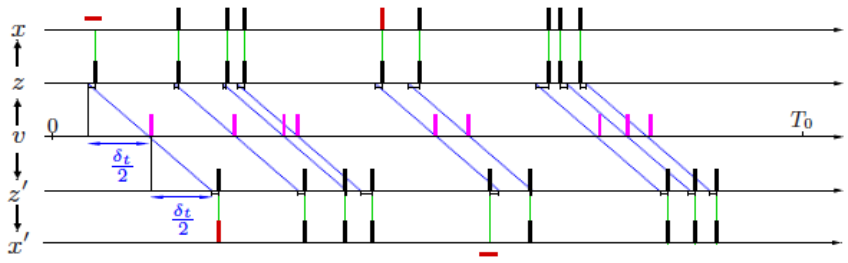

Figure 2.4: Procedure relating time event x and x'. Reproduced from (Dauwels et al., 2009c)

characteristics, fundamental for understanding the behavior of each measure and deciding which might be more appropriate, finally in both studies of specific surrogate data, the measure were reliable, in the

sense that the statistical fluctuation were relatively small.

In this thesis, the discrimination of difference is based on firing rate, because neurons have been found to encode information in the spike train firing rates (Dayan and Abbott, 2001).

Although this simplification is unrealistic, it allows a first analysis without the introduction of additional effects due to modulation of firing rates in the spike trains. Another important factor in the analysis is the spike train length. Naturally, in this scenario, the discrimination of the measures is expected to improve as the spike train length is increased since more information is available. In practice, however, this value is often smaller than one second. Thus, the value was chosen as a compromise between a reasonable value for actual data analysis and good statistical illustration of the properties of each measure. As most of the statistical measures were earlier investigated in the previous studies and their reliability establish. In chapter 3, we apply these measures to compare spike trains generated by our model to another model.

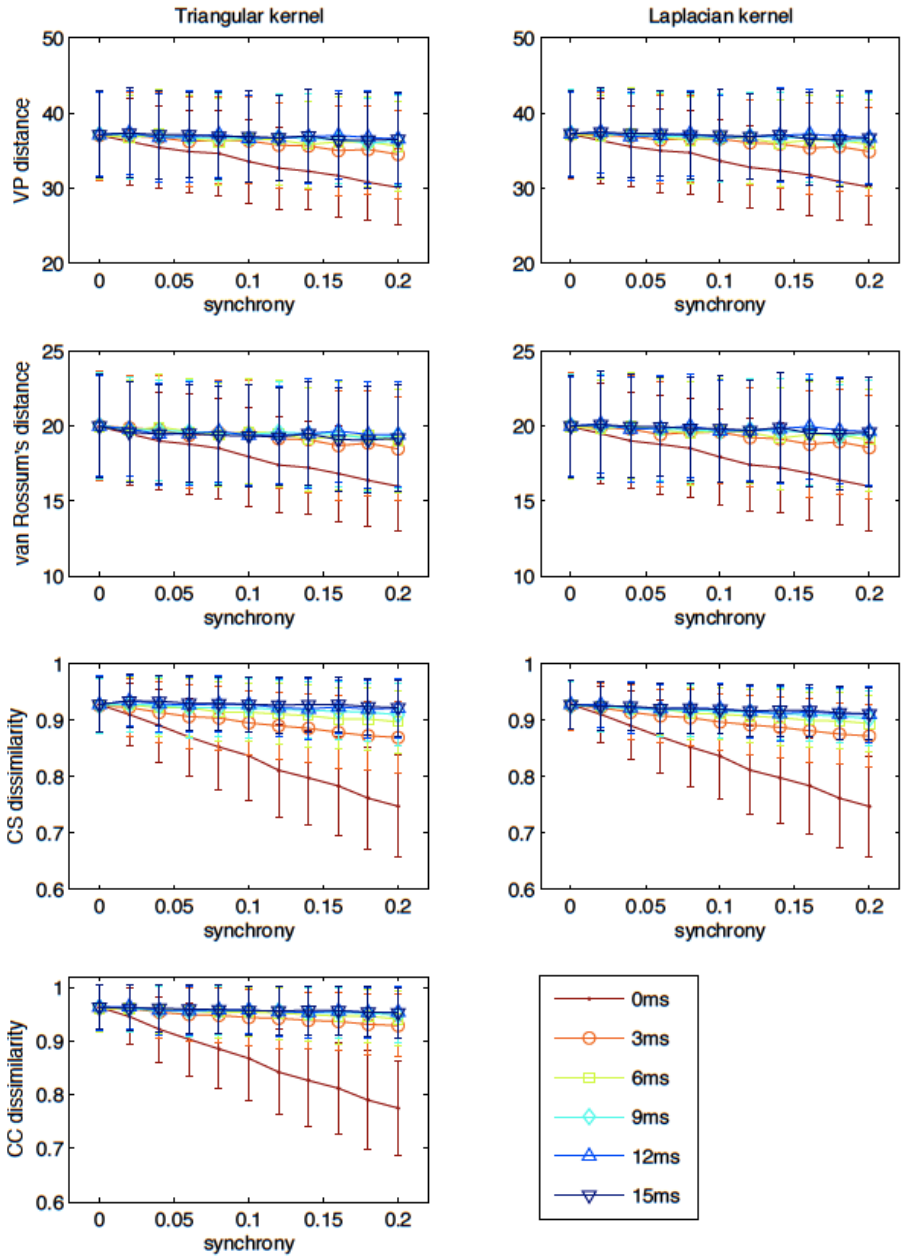

Figure 2.5: Dissimilarity measures for each kernel as a function of the synchrony of the signal among spike trains. Statistics were estimated from 1,000 randomly generated pairs of spike trains. Reproduced from (Paiva et al., 2010)

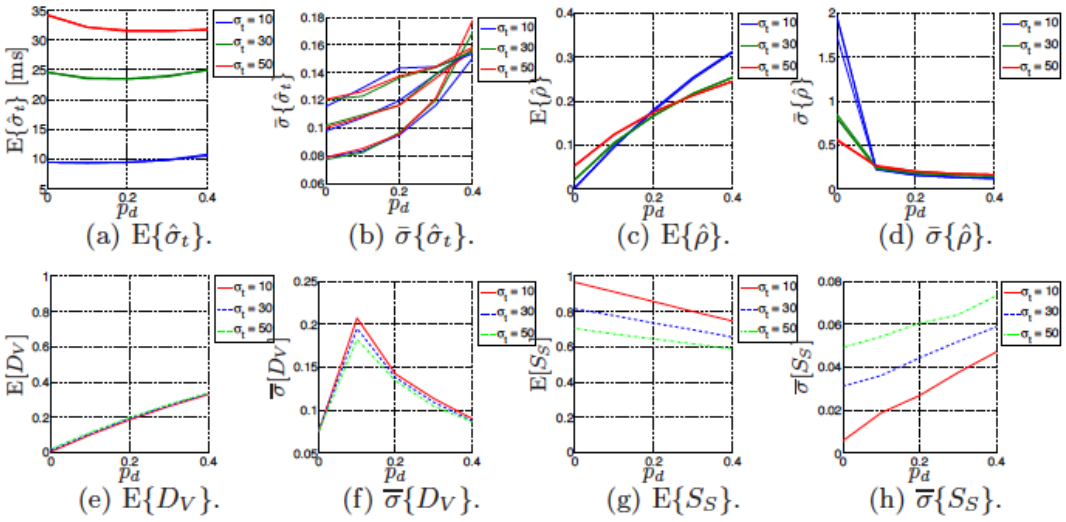

Figure 2.6: Results for Stochastic Event Synchrony (SES), Victor-Purpura metric (D_v) and Schreiber et al. measure (S_s) . Reproduced from (Dauwels et al., 2009c)

Chapter 3

Comparing Realistic Subthalamic Nucleus Neuron Models.

The original work described in this chapter was published by (Njap et al., 2011) at the International symposium on Computational Models for Life Sciences. AIP, Conference Proceedings, volume 1371, pp. 102-109, 2011, doi:http://dx.doi.org/10.1063/1.3596632 and is used with permission from the American Institute of Physics. Alterations have been made for the sake of unicity in the layout.

Abstract

The mechanism of action of clinically effective electrical high frequency stimulation is still under debate. However, recent evidence points at the specific activation of GABA-ergic ion channels. Using a computational approach, we analyze temporal properties of the spike trains emitted by biologically realistic neurons of the subthalamic nucleus (STN) as a function of GABA-ergic synaptic input conductances. Our contribution is based on a model proposed by Rubin and Terman and exhibits a wide variety of different firing patterns, silent, low spiking, moderate spiking and intense spiking activity. We observed that most of the cells in our network turn to silent mode when we increase the $GABA_A$ input conductance above the threshold of 3.75 mS/cm^2. On the other hand, insignificant changes in firing activity are observed when the input conductance is low or close to zero. We thus reproduce Rubins model with vanishing synaptic conductances. To quantitatively compare spike trains from the original model with the modified model at different conductance levels, we apply four different (dis)similarity measures

between them. We observe that Mahalanobis distance, Victor-Purpura metric, and Interspike Interval distribution are sensitive to different firing regimes, whereas Mutual Information seems undiscriminative for these functional changes.

3.1 Introduction

Deep brain stimulation (DBS) of subthalamic nucleus (STN) by means of implanted electrodes has become a well accepted technique for treatment of several movement disorders (Benabid et al., 2002; Benabid, 2007; McIntyre et al., 2004b). However, the mechanisms of the molecular and pharmacological action of periodic electrical high frequency stimulation (HFS, $f > 100\,Hz$) are still under dispute (Moser et al., 2003; Mantovani et al., 2006; Hiller et al., 2007; Mantovani et al., 2009).

To understand the network and cellular mechanisms responsible for the efficacy of HFS, several attempts have been made to mathematically model diseases related to movement disorders and other neurological disorders (Arle et al., 2008; Shils et al., 2008; Beal, 2001). In 2004 Rubin and Terman (Rubin and Terman, 2004) proposed a mechanism for HFS in Parkinsons disease (PD) based on single-compartment biophysically realistic Hodgkin-Huxley (HH) models for five interconnected subcortical nuclei. Reported firing pattern modifications in the simulated network have been intensively studied and simulated in other computer models using different approaches (Chay et al., 1995).

Since it was proposed that the GABA system is involved in the effectiveness of DBS (Moser et al., 2003; Mantovani et al., 2006; Hiller et al., 2007; Mantovani et al., 2009), our intention is to investigate this mechanism in a modified version of Rubins STN model. In detail, we added postsynaptic, GABA-related currents to the compartment receiving inhibitory stimulation-induced trans-synaptic input. Clearly, with this step we are leaving the bases of experimentally available network data and proceed on other paths to validate our model. Therefore, the current study seeks to numerically examine the extend to which both spiking models are similar or have different behavior as the synaptic input conductance fluctuates. Since both models produce spike train output, we apply different spike similarity measures to compare both biologically realistic subthalamic nucleus (STN) neuron models. Synaptic input conductances consist of two sets of ionic synaptic conductances (small and large) for action potential or spike generation.

We introduced an additional stochastic component, i.e noise, to our models so that not only different instantiations of the model are different from each other, but also to obtain more realistic simulations. Such noisy patterns are typical for many neurons in the brain (Zhang et al., 2003). Due to different ions concentration levels, the model produces irregular burst activity that can be observed during resting conditions in the basal ganglia. In the next section, we will describe the equations that define our models.

3.2 Mathematical Model

The basic model used in this paper is similar to the one described in (Rubin and Terman, 2004). It consists of five anatomical nuclei representing the external segment of globus pallidus (GPe), the subthalamic nucleus (STN), the internal segment of globus pallidus (GPi), thalamus, and cortex, where the first three nuclei belong to the basal ganglia network. We modified the STN cells in such a way as to display the possible effects of neurotransmitter GABA channels. Therefore, we used the following HH model to mathematically describe the membrane potential V of single-compartment STN neurons, given by the equation (3.1):

$$C_m \frac{dV}{dt} = -I_{Na} - I_K - I_{Ca} - I_T - I_{AHP} - I_{Leak} - I_{Syn} + C_m \eta \tag{3.1}$$

where C_m is the membrane capacitance. Incorporated ionic currents are described as follows: Na^+ current with instantaneous activation m_∞ variable and inactivation variable h; $I_{Na} = g_{Na} m_\infty^3 h\,(V - E_{Na})$.
K^+ delayed rectifier current, (high activation threshold, fast activation time constant), with activation variable n; $I_K = g_K n^4\,(V - E_K)$.
Ca^{2+} high-threshold current with instantaneous activation variable s_∞; $I_{Ca} = g_{Ca} s_\infty^2\,(V - E_{Ca})$.
Ca^{2+} low-threshold t-type current with instantaneous activation variable a_∞ and inactivation variable b_∞; $I_T = g_T a_\infty^3 b_\infty^2\,(V - E_T)$.
By using this equation, T-type currents include the effects of a hyper-polarization activated inward current.
Ca^{2+} activated voltage independent after hyper polarization K^+ current, with $\left[Ca^{2+}\right]_{in}$ the intracellular concentration of Ca^{2+} ions, and k_1 the dissociation constant of this current $I_{AHP} = g_{AHP}\,(V - E_K)\,\frac{\left[Ca^{2+}\right]}{\left[Ca^{2+}\right]+k_1}$.
Leak current $I_{Leak} = g_{Leak}\,(V - E_{Leak})$.

The gating kinetics of the ionic conductances were calculated using the following equation:

$$\frac{dn}{dt} = \frac{n_\infty - n}{\tau_n}; \qquad \frac{dm}{dt} = \frac{m_\infty - m}{\tau_m}; \qquad \frac{dh}{dt} = \frac{h_\infty - h}{\tau_h};$$
$$n_\infty = \frac{\alpha_n}{\alpha_n + \beta_n}; \qquad m_\infty = \frac{\alpha_m}{\alpha_m + \beta_m}; \qquad h_\infty = \frac{\alpha_h}{\alpha_h + \beta_h};$$
$$\tau_n = \frac{1}{\alpha_n + \beta_n}; \qquad \tau_m = \frac{1}{\alpha_m + \beta_m}; \qquad \tau_h = \frac{1}{\alpha_h + \beta_h};$$

The additional I_{syn} are inhibitory postsynaptic GABA-related currents which can be accessed both by $GABA_A$ and $GABA_B$ subtypes of GABA receptors. In this initial study, only conductance setup of $GABA_A$ is included. This conductance is modeled with the first order kinetic of the binding transmitter to postsynaptic receptors (Destexhe et al., 1994) $\frac{ds}{dt} = \alpha C\,(1-s) - \beta s$, where C is the concentration of neurotransmitter in the synaptic cleft given by: $[C] = C_{max}/\left(1 + exp\left(V - V_p\right)/k_p\right)$, α and β are the forward and backward rate constants, and s represents the fraction of open channels on the postsynaptic membrane. The postsynaptic current receiving inhibitory stimulation input is given by: $I_{GABA_A} = s_{GABA_A}\left(V_m - E_{GABA_A}\right)$; where V_m is the postsynaptic membrane potential, $g_{GABA_A}$is the peak conductance and E_{GABA_A} is the reversal potential. $C_m\eta$ is the stochastic noise current component added to our model. Simulations were performed using XPPAUT as platform developed by Bard Ermentrout and MATLAB for analysis. The numerical method used was an adaptive step fourth-order Runge-Kutta method with a maximum step width of 0.01ms for integration. Parameters describing synaptic current and membrane potential are listed in Table (3.1).

Table 3.1: Some parameters used.

Parameters	$\alpha, mM^{-1}ms^{-1}$	β, ms^{-1}	E, mV
$GABA_A$	0.53	0.184	-85
Threshold	-	-	-45
V_P	-	-	0
C_{max}	-	-	1

3.3 Methods

Since the basic problem we are facing here is the question on how similar patterns of stochastically firing cells are, we will in this section briefly describe different similarity measures. We observed simulated neuronal activity of individual cells for each realistic model for a time duration of 1000 msec. The

sequence of time occurrence of spikes $\{t_0, t_1, \ldots, t_n\}$, where $0 \leq t_n < t_1 < \ldots < t_n < T$ is called a **spike-train**. In this contribution pairs of spike trains are compared.

3.3.1 Mahalanobis Distance

The Mahalanobis distance is described in (Wright et al., 1999). It is based on correlations between variables by which different patterns can be distinguished and examined methodically. The Mahalanobis distance can be defined as a dissimilarity measure between two random vectors and of the same distribution with the covariance matrix S:

$$d(\vec{x}, \vec{y}) = \sqrt{(\vec{x} - \vec{y})^T S^{-1} (\vec{x} - \vec{y})} \tag{3.2}$$

If the covariance matrix S is the identity matrix (respectively diagonal), then the Mahalanobis distance is reduced to the Euclidean distance respectively (normalized Euclidean distance).

3.3.2 Mutual Information

Mutual information (Guiasu, 1977; Papoulis, 1984) relies on an estimation of entropy which measures the degree of uncertainty of a random variable and thereby measures how much information can be encoded with it. The entropy $H(X)$ of a discrete X random variable taking the values $a \in \chi$ with probabilities $p(a) = Pr\{X = a\}$ is defined as:

$$H(X) = -\sum_{a \in \chi} p(a) \log_2 p(a) \tag{3.3}$$

and is measured in bits. Mutual information for two random variables X and Y can be defined as a quantity that expresses the mutual dependence of two variables. Mathematically expressed as:

$$I(X, Y) = H(X) + H(Y) - H(X, Y) \tag{3.4}$$

where $H(X)$ and $H(Y)$ are marginal entropies, and $H(X, Y)$ is their joint entropy. Using the definition of entropy $H(X)$ and joint entropy and $H(X, Y)$ the mutual information can be equivalently expressed as:

$$I(X, Y) = H(X) - H(X/Y) \tag{3.5}$$

where $H(X/Y)$ is the conditional entropy. In the case of spike-trains, time is discretized into bins. Each bin has the value of 1 if a spike occurred within its time duration, otherwise its value is 0. This process is treated as stochastic with given probability for each of these two possible events. The resulting binary

string represents the spike trains and is used for entropy estimation. Entropy and mutual information are measured in bits. One significant drawback of mutual information and entropy is that both can not be estimated from correlation data, since they depend on the underlying probability distributions.

3.3.3 InterSpike Interval Distance

The Interspike Interval Distance measure is described in (Kreuz et al., 2007). It can be defined as a time-resolved measure of the firing rate of the spike train or the time between subsequent action potentials. The mean value of the ISI is calculated according to (3.6):

$$\overline{ISI} = \frac{1}{n}\sum_{i=1}^{n} ISI_i \tag{3.6}$$

3.3.4 Victor-Purpura Distance Metric

The Victor-Purpura spike metric was described in (Victor and Purpura, 1997). It defines the distance between two spike trains as the minimum cost of transforming one spike train into the other. It combines three basic operations: spike insertion, spike deletion and spike movement. The cost D_v of inserting or deleting a spike is set to one, the cost of moving a spike in time is proportional to the time shift. The time scale of the distance metric is defined by the proportionality constant C_v. If C_v is equal to zero, the distance metric D_v exactly equals to the difference in spike number, whereas large C_v the distance comes near the number of non-coincident spikes, as alternative shifting spikes it becomes more favorable to delete all non-coincident spikes of the one time series and to insert non-coincident spikes of the other. Increasing C_v the distance is transformed from a rate distance to a timing distance.

All the above similarity measures have advantages and disadvantages. They were extensively discussed and successfully implemented as analyzing tools for many spike trains in (Dauwels et al., 2009a; Rowat, 2007; Dauwels et al., 2009b).

3.4 Spike Detection

Spike detection was done by thresholding of simulated extracellular (Lewicki, 1998) potential. We determined the threshold voltage as the average of the maximum peak value and the minimum peak value of action potentials. As soon as the simulated voltage exceeds the determined threshold a spike is emitted and the depolarization is reset. This method is reguraly used for measuring neural activity, with

an advantage that it requires less hardware and software, and can obtain exactly the desired information. On the other hand it is not always possible to achieve acceptable discrimination.

3.5 Results

3.5.1 Firing Pattern

By thresholding the membrane potential V, we obtain the rastergram in Fig 3.2. Here we display 50 trials of 1000 $msec$ lengths for the input conductance 0 (top left), 0.01 (middle half) and 4 mS/cm^2 (bottom half). Spikes seem to be stochastically distributed. We begin our simulation using two different input regimes consisting of smaller and larger synaptic conductance input. We start with $g_{GABA_A} = 0$ which fully reproduced Rubins model and gradually increased the synaptic conductances with step size 0.01 mS/cm^2 up to 4 mS/cm^2, the basic bursting behavior is shown in Fig 3.1.

All our simulations showed STN neurons differ in their firing pattern depending on the synaptic parameter (GABA) strength. For large conductance inputs, this fluctuation can have very big effects on the rate of variability of firing of individual neurons. These effects depend strongly on the synaptic connectivity and neuronal mechanism. In particular, we observed four activity regimes: *Silent dominated* regime mostly when the value of synaptic conductance input is above 4 mS/cm^2, in this regime no spiking activity was observed; *Low spiking* activity regime characterized by less than 10 spikes per second *Moderate spiking* activity regime where the number of spikes per second lies between 10 and 25; *Intense spiking* activity regime where the number of spikes per second observed exceeded 25. In all our simulations, the firing pattern was mostly irregular as observed in the normal state. The analysis of qualitative firing involved taking all cells and organizing them into these four firing types. By categorizing the cells outputs based on firing rate and comparing them with the amount of inhibition in our model, Fig. 3.3. shows that almost no inhibition occurs up to conductances of 0.9 mS/cm^2. However, this qualitative picture has to be investigated more carefully, since with the increasing synaptic input conductances, the mutual information of the model almost vanishes and Mahalanobis distance metric start increasing despite seemingly comparable qualitative behavior.

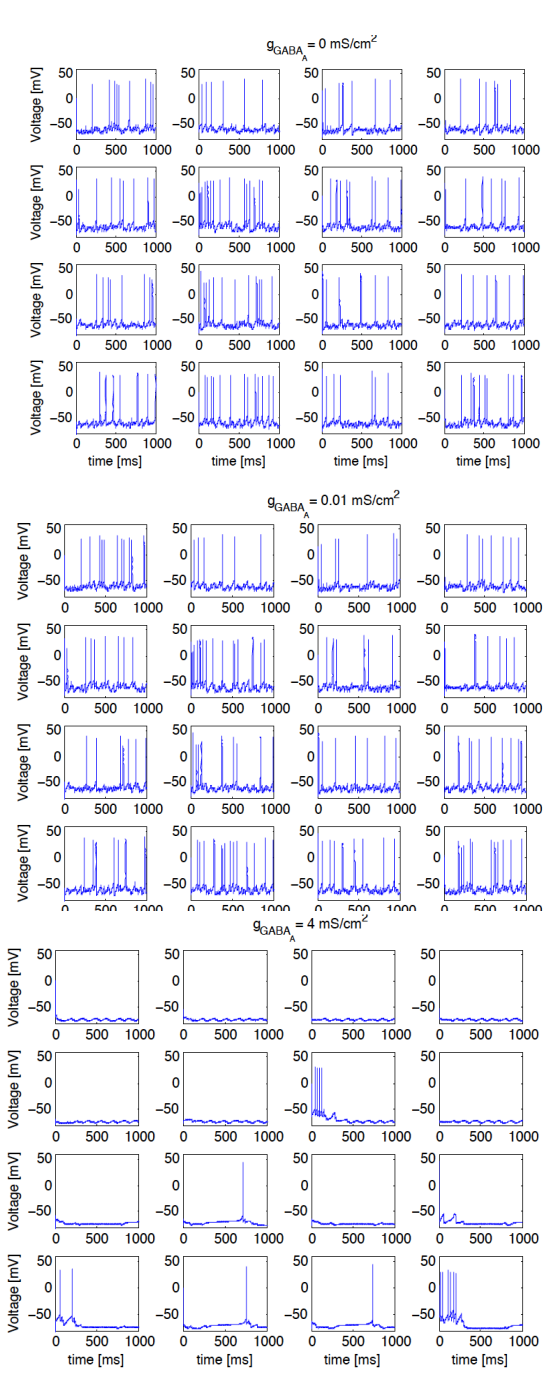

Figure 3.1: Various firing patterns exhibited by the model. Each voltage trace represents one of sixteen neurons in the STN model. Traces were simulated by using weaker or larger synaptic conductances.

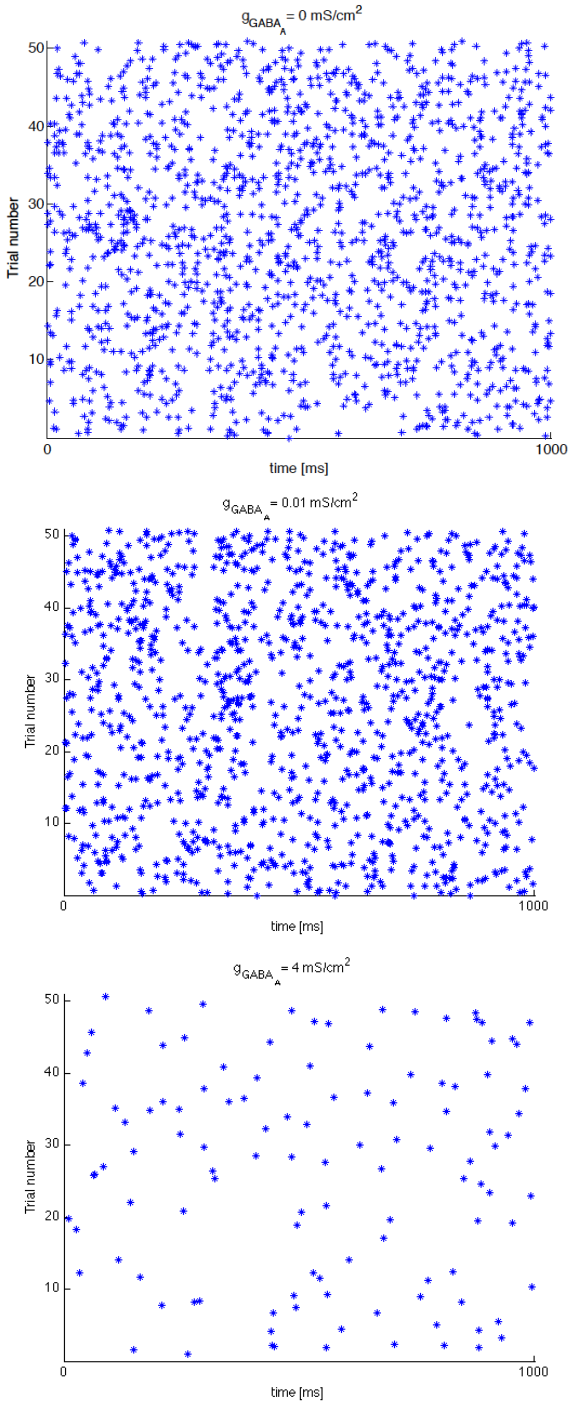

Figure 3.2: Rastergram for one cell inhibited by a synaptic conductance 0 mS/cm^2 (top half right) 0.01 mS/cm^2 (middle half) and 4 mS/cm^2 (bottom half). Spikes seem to be stochastically distributed.

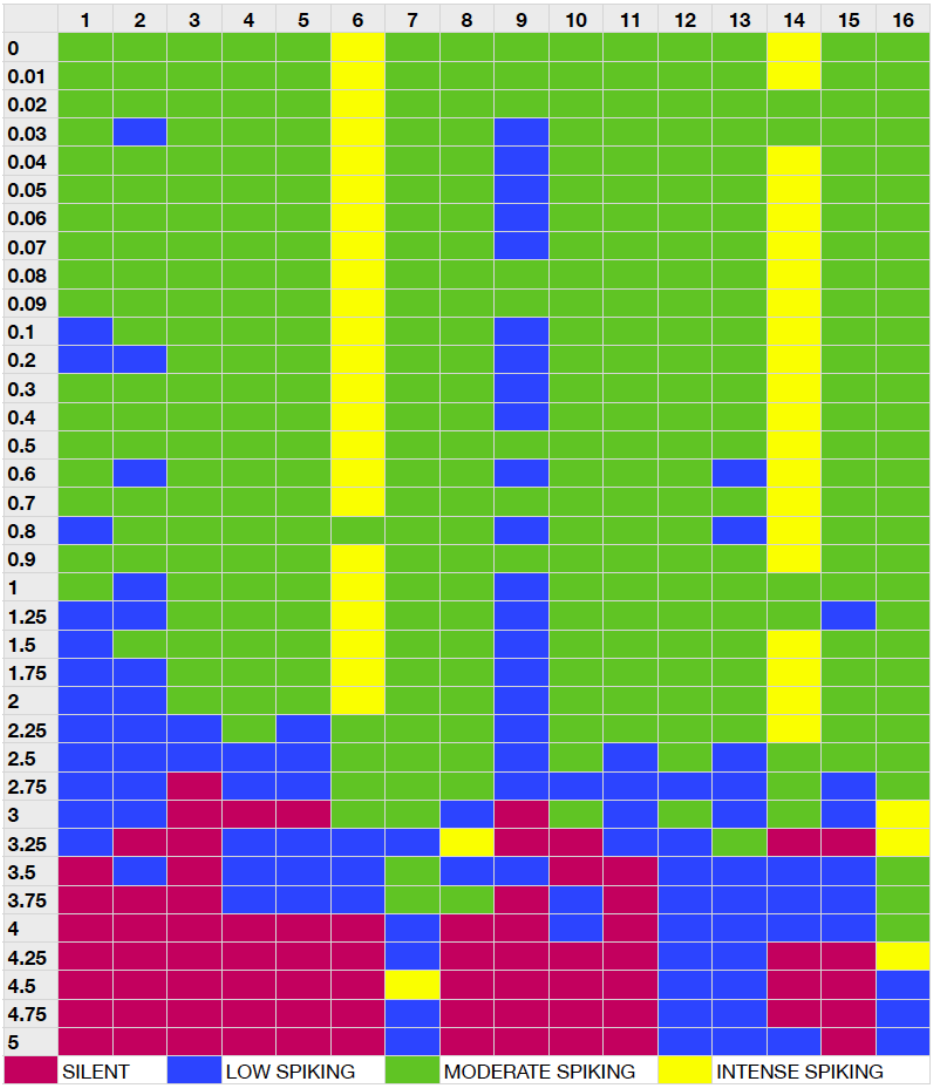

Figure 3.3: Firing types corresponding to different synaptic conductances input. Each row represents the synaptic conductances input. Each column represents an exemplary STNs cell number. Each color entry denotes the qualitative electrophysiological response of a particular cell to a level of synaptic conductance input.

3.5.2 Similarity Measures

Tests of above described similarity measures were conducted on each of the sixteen STN cells. For each synaptic conductance input, we produced several ($n = 50\,trials$) independently simulated spike trains, and calculated from them the Mahalanobis distance (*Mah_Dist*), the Victor-Purpura distance metric (*Vic_Dist*), the Mutual Information (*Mu_Info*) to the Rubins model and the Interspike interval distance (*ISI_Dist*) as the average sum of all different trials for each different cell number. Table (3.2) gives normalized average value for four metrics based on their spiketimes recorded.

Table 3.2: Normalized metrics for four different synaptic conductances input.

$GABA_A$	0	0.01	0.1	1	5
Mah_Dist	0	0.07	0.01	0.130	0.997
Vic_Dist	0	0.742	0.825	0.904	0.512
ISI_Dist	0	0.457	0.393	0.539	0.999
Mu_Info	1	0.1	0.05	0.015	0.015

Increasing synaptic input conductances, the Mutual information of the models output rapidly vanishes, the Mahalanobis distance metric, the Interspike Distance and the Victor-Purpura distance starts to increase (Fig. 3.4.). This contradicts the seemingly smooth transition from the Rubin model cell ($g_{GABA} = 0$) to our model as seen in the spike rate picture. However, up to an input conductance of $1.75\,mS/cm^2$ the further increase in all these values is quite slow, corroborating a common regime governed by the GABA-conductance. And yet, the spike rate activity here remains quite stable as seen in Fig. 3.3. Above $1.75\,mS/cm^2$ all similarity measures start to drastically change their values and, as can be seen in Fig. 3.3., the spiking activity becomes less homogeneous until most cells turn silent at values above $3.75\,mS/cm^2$.

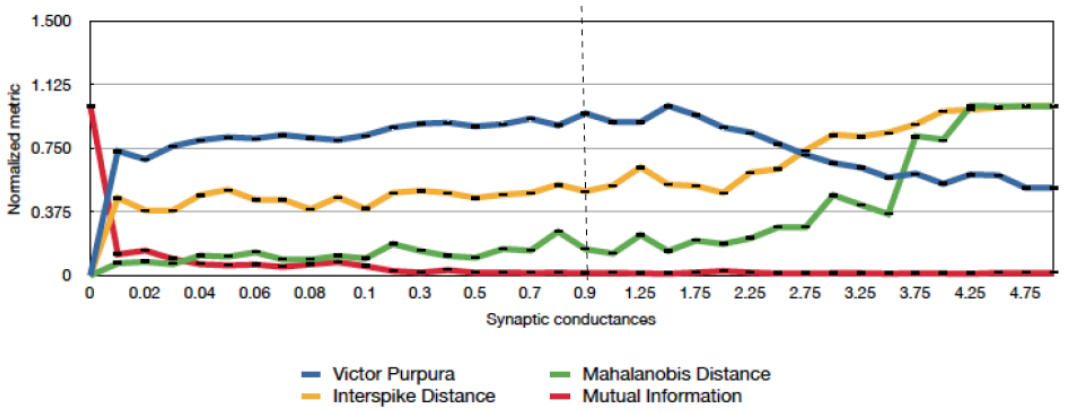

Figure 3.4: Comparison of different similarity measures for increasing synaptic input. The dashed lines represents threshold where our model behave similar to Rubins model.

3.6 Discussions and Conclusion

Our original intention was to improve an existing basal ganglia model by a GABA-mediated synaptic conductance to investigate its relevance as potential target of electrical high frequency stimulation. Not unexpectedly, the additional synaptic current g_{GABA} has a significant effect on the model neurons electro-physiological response. $GABA_A$ receptors are located on glutamatergic neurons, thus these neurons would be inhibited by increased GABA activity. In order to validate this model, we had to find a way to compare our models output to the existing model and experimental data. But how to compare stochastically produced spike trains from one model to another? So the question dealt with in this study, was to utilize existing similarity methods to monitor increasing discrepancies between the base model and ours by increasing synaptic input conductances. We found out, that besides the mutual information all three metrics are useful to detect differences in different firing regimes. Opposite to that, the standard spike rate view was to insensitive to determine a clear transition in output behavior of the model, not of one single particular cell.

All in all we are now confident that our model does not violate the assumptions found in the basic basal ganglia model of Rubin, but whether or not it will provide an alternative mechanism of action of high frequency stimulation (HFS) is subject to further investigations.

Chapter 4

Modeling Effect of GABAergic Current in a Basal Ganglia Computational Model.

The original work described in this chapter was published as: "Modeling effect of GABAergic current in a basal ganglia computational model" Authors: Felix Njap, Jens Christian Claussen, Andreas Moser, Ulrich G. Hofmann Cogn. Neurodyn. (2012) 6:333-341. Alterations have been made for the sake of unicity in the layout.

Abstract

Electrical high frequency stimulation (HFS) of deep brain regions is a method shown to be clinically effective in different types of movement and neurological disorders. In order to shed light on its mode of action a computational model of the basal ganglia network coupled the HFS as injection current into the cells of the subthalamic nucleus (STN). Its overall increased activity rendered a faithful transmission of sensorimotor input through thalamo-cortical relay cells possible. Our contribution uses this model by Rubin and Terman [*J. Comput. Neurosci.,* **16**, 211-223 (2004)] as a starting point and integrates recent findings on the importance of the extracellular concentrations of the inhibiting neurotransmitter GABA. We are able to show in this computational study that besides electrical stimulation a high concentration of GABA and its resulting conductivity in STN cells is able to re-establish faithful thalamocortical

relaying, which otherwise broke down in the simulated parkinsonian state.

4.1 Introduction

Deep brain stimulation (DBS), especially of the subthalamic nucleus (STN), utilizing chronically implanted electrodes has become an effective, though symptomatic, therapy for a wide range of neurological disorders (Benabid et al., 2002; Benabid, 2007; McIntyre et al., 2004b; stimulation for parkinsons disease study group., 2001). However the detailed working mechanism regarding molecular and pharmacological aspects is not yet fully understood. During the past decade computational neuroscience has attempted to shed light on the mechanism of DBS by numerical simulations to optimize the therapeutic outcome of DBS in movement disorders (Alejandro, 2006; Pirini et al., 2009). With this aim a cellular-based model of the basal ganglia system was implemented by (Rubin and Terman, 2004). The original model was able to reproduce the physiological and pathological activities of STN and thalamus cells (TC) in a realistic basal ganglia network and proposed such an explanation for the reduction of parkinsonian symptoms under electrical HFS. Their findings are based on increasing the firing activity of STN rather than shutting it down.

The following study utilizes the original model, but develops it further in light of recently presented neurochemical findings on the DBS rationale. Those experiments quantitatively measured extracellular neurotransmitter concentrations, and showed that electrical high frequency stimulation (HFS) induced selective -aminobutyric acid (GABA) release as a mechanistic basis of HFS (Mantovani et al., 2006, 2009; Hiller et al., 2007; Feuerstein et al., 2011). Whereas usually DBS is considered to provide excitatory input to STN neurons leading to an increased activity, we replaced it with inhibitory postsynaptic current (IPSC) exclusively conveyed by GABA (Gerstner and Kistler, 2002; Hutt and Longtin, 2010; Foster et al., 2008; Liu et al., 2010). Our current study seeks to numerically examine the thalamus' output response under DBS-related current and compare this to output response with GABAergic currents applied to the same target cells in STN instead.

4.2 Method

Our model follows up on the seminal model of the basal ganglia thalamic network by Rubin and Terman and the modified version described in our recent contribution. Each cell type in our model network is

described by a single compartment and has Hodgkin-Huxley-type spike generating currents as described previously (Njap et al., 2011). A detailed description including all parameters and nonlinear equations has been published elsewhere (e.g., (Guo et al., 2008)). The voltage in the original Rubin and Terman's original model obeys the following equation (4.1):

$$C_m \frac{dV}{dt} = -I_{Na} - I_K - I_{Ca} - I_T - I_{AHP} - I_{Leak} + I_{DBS}, \tag{4.1}$$

The model features: potassium and sodium spike-producing currents I_K, I_{Na}; a low-threshold T-type $\left(Ca^{2+}\right)$ current (I_T); a high-threshold $\left(Ca^{2+}\right)$ current (I_{Ca}); a $\left(Ca^{2+}\right)$ activated, voltage-independent after hyper polarization (K^+) current (I_{AHP}), and a leak current (I_{Leak}). All these currents are described by Hodgkin-Huxley formalism. I_{DBS} represents the deep brain stimulation current of the STN modeled with the following periodic step function (4.2):

$$I_{DBS} = i_D \left(\sin\left(2\pi t/\rho_D\right)\right)\left(1 - \theta\left(\sin\left(t + \delta_D\right)/\rho_D\right)\right), \tag{4.2}$$

where i_D is the stimulation amplitude, ρ_D stimulation period, δ_D duration of each impulse, and θ represents the Heaviside step function given by (4.3):

$$\Theta(x) = \begin{cases} 0 & \text{for } x < 0 \\ \frac{1}{2} & \text{for } x = 0, \\ 1 & \text{for } x > 0 \end{cases} \tag{4.3}$$

In the original model, during stimulation $i_{DBS}(t)$ was taken as a large positive constant and was applied directly to the neuronal membrane in the STN neuron model. In our current study the new membrane potential of each STN neuron integrates over additional ion channels and stochastic $C_m\eta$ to obtain more realistic simulations but also to account for a specific type of experimentally recorded pattern which can not be seen in purely deterministic simulations (Braun et al., 2007). It obeys the following equation (4.4):

$$C_m \frac{dV}{dt} = -I_{Na} - I_K - I_{Ca} - I_T - I_{AHP} - I_{Leak} - I_{Syn} + C_m\eta \tag{4.4}$$

where $I_{syn}(t) = g_{syn}(t)\, s\,(V - E_{syn})$ represents an inhibitory channels where s satisfies the stochastic differential equation (Higham, 2001) (4.5):

$$ds = \left[\alpha\left(1 - s\right) - \beta s\right] dt + \sigma d\eta, \tag{4.5}$$

α and β are the forward and backward rate constants, and the Gaussian white noise included is characterized by mean $< \eta = 0 >$, and variances $< \eta(t)\,\eta(0) >= 2\sigma\delta(t)$, with σ the strength of the noise. The noise strength σ decreases as the square root of the number of ions channels (Fox, 1997) (4.6):

$$\sigma = \left[\alpha(1-s) + \beta s\right] / \left[(\tau N_s)\right]^{1/2} \tag{4.6}$$

with parameters $\alpha = 1\, msec^{-1}$, $\tau = 100\, msec$, $N_s = 500$ and is chosen such that $\alpha/(\alpha+\beta) = 0.2$, σ is expressed in units of $mV^2/msec$, time in msec, currents in $\mu A/cm^2$. In all our simulations parameter values were chosen to produce reasonable visual agreement with experimental records.

The parameter E_{syn} and the function $g_{syn}(t)$ can be used to characterize different types of synapses. The parameters that describe the conductivity of transmitter-activated ion channels at a certain synapse are chosen in such a way as to mimic a time course and the amplitude of experimentally observed spontaneous postsynaptic currents. In this paper, to take heterogeneity into account the conductance current is described by the following kinetic equation (4.7):

$$g_{syn}(t) = \sum_f \bar{g}_{syn} e^{-\left(t-t^{(f)}\right)/\tau}\, \theta\left(t - t^{(f)}\right), \tag{4.7}$$

where $t^{(f)}$ denotes the arrival time of a presynaptic action potential which follow a Poisson distribution at rate 0.05 spikes/sec. $E_{syn} = -75\, mV$ is the reversal potential, $\tau = 5\, ms$ is the time constant and $\bar{g}_{syn}$ is the amplitude describing the maximal synaptic conductance of GABA. The time-dependent conductance of inhibitory synapses in deep cerebellar nuclei can be described by a simple exponential decay given by Eqn. (4.7).

In the basal ganglia, the majority of neurons uses GABA as neurotransmitter and has inhibitory effects on their targets (Chakravarthy et al., 2010a; Boyes and Bolam, 2007). For the sake of computation and simplicity, our model included only the slow component $GABA_A$ synapse. Parameter values were the same as in Rubin and Terman's model. All simulations were performed using the software XPPAUT written by G. Bard Ermentrout (Ermentrout, 2002) and MATLAB for analysis. The numerical method used was an adaptive-step fourth order Runge-Kutta method (*Qualst.RK4 in XPP*) with a typical time step of 0.01 msec.

The model network is depicted in Fig. 4.1. It consists of five anatomical nuclei representing the external segment of globus pallidus (GPe), subthalamic nucleus (STN), the internal segment of globus pallidus (GPi), thalamus, and cortex, where the first three nuclei belong to the basal ganglia network. Arrows with dashed lines indicate inhibitory synaptic connections and inputs, whereas solid lines indicate excitatory synaptic connection and inputs. In the original model GPe and GPi neurons were biased with

applied currents that varied between the normal-healthy and parkinsonian conditions, modeling changes in the strength of striatal inhibition.

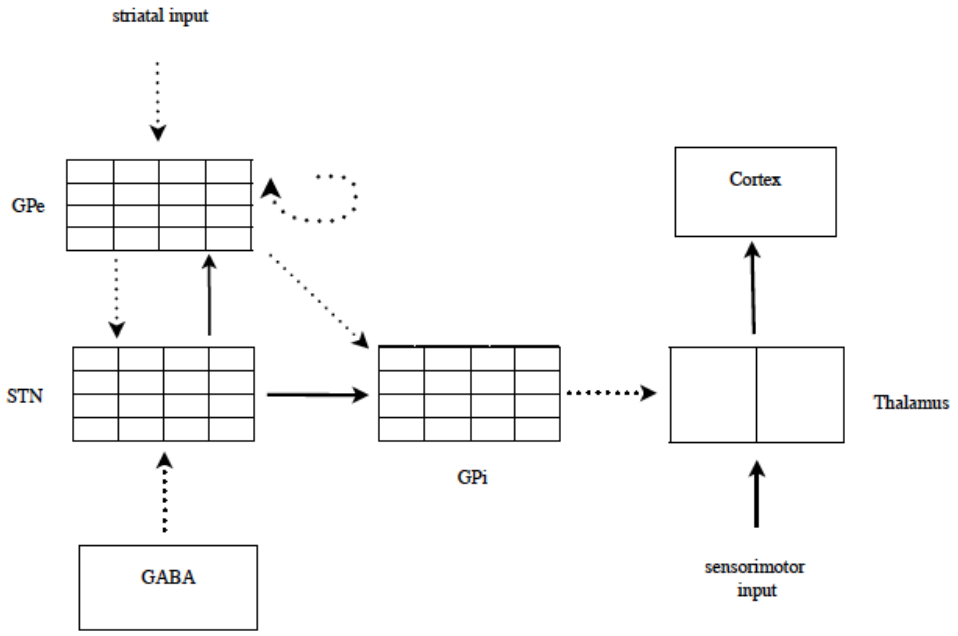

Figure 4.1: Network model consisting of sixteen STN, GPe and GPi and two TC. The thalamus receives synaptic inhibition from GPi and excitatory input, related to sensorimotor activity. GPi and GPe both receive excitatory input from STN, and GPi receives inhibition from GPe. There is interpallidal inhibition among GPe neurons. STN receives inhibition from GPe and GABAergic currents. Each STN neuron receives inhibitory input from two GPe neurons. Each GPe neuron receives excitatory input from three STN neurons and inhibitory input from two other GPe neurons. Each GPi neuron receives excitatory input from one STN neuron. Each thalamic neuron receives inhibitory input from eight GPi neurons. The thalamus is viewed as a *relay station* where cells have the unique role of responding faithfully to each excitatory sensorimotor input. GPe receives striatal input. Adapted from (Rubin and Terman, 2004).

To simulate a parkinsonian state, parameters were chosen to reproduce the behavior of experimentally recorded cells of an $1-methyl-4-phenyl-1,2,3,6-tetrahydropyridine$ (MPTP), non-human primate model of Parkinson diseases (PD) shown in (Guo et al., 2008). We then applied GABA-mediated currents onto STN cells during this parkinsonian condition and observed the direct effect on thalamus cells (TC) to relay sensorimotor input to the cortex. Secondly, as Rubin and Terman did, we

observed the thalamus' ability to faithfully relay sensorimotor input to the cortex as we slowly increased the synaptic conductance of GABA. Our model's output was compared to the optimal DBS current described in the original model. Thus we were finally able to evaluate our network model using two performance scores (*error index* and *coefficient of variation*) with the aim of measuring thalamocortical cell responsiveness to stimulus input.

4.3 Results

4.3.1 Normal and Parkinsonian firing patterns

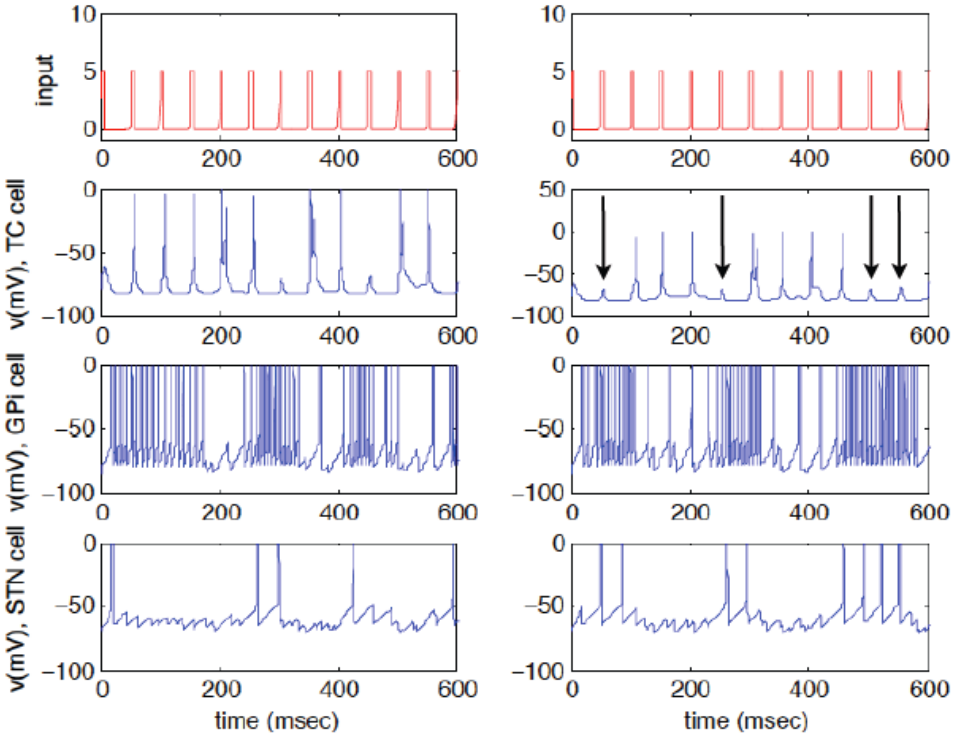

Figure 4.2: Periodic sensorimotor stimulation input and TC responsiveness in the two clinical states: normal (left) and parkinsonian (right) and corresponding GPi and STN activity under these conditions. Arrows indicate dropped responses of TC on driving input, thus indicating poor information transfer to the cortex. During the normal state, STN neurons fire irregularly whereas in parkinsonian state, each STN neuron fires in a periodic tremor-like fashion, thus leading STN neurons populations to break up into two clusters. Adapted from (Rubin and Terman, 2004).

Although the network parameters are set to produce the parkinsonian state in the absence of DBS, Rubins DBS model show that the presence of electrical DBS restores the faithful relay of inputs to the cortex by the TC. On the other hand, during parkinsonian condition, the thalamus is no longer able to relay sensorimotor input faithfully due to the bursting activity of GPi. This tonical activity may considerably influence thalamic responsiveness activity. At this stage we replaced DBS current with inhibitory postsynaptic current (IPSC) in STN cells and questioned the ability of thalamus to produce the same output. Fig. 4.3. shows that the thalamus cells produce similar network effects when replacing DBS excitatory input with the GABAergic inhibitory current at higher synaptic conductances. The loss of connectivity observed in parkinsonian state Fig. 4.2 is restored, corroborating the key role of synaptic inhibition.

4.3.2 DBS acts excitatory and $GABA_A$-type currents inhibitory

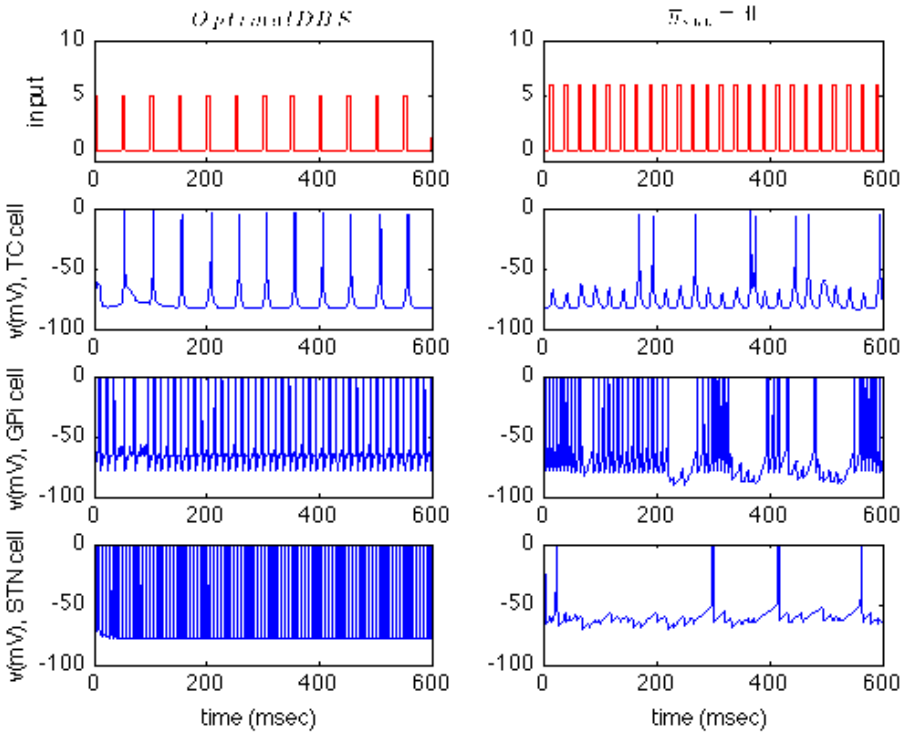

Figure 4.3: Periodic sensorimotor stimulation input and TC cells responsiveness in the optimal DBS stimulation (left) and with vanishing GABA synaptic conductance amplitude (right). Electrical HFS increases activity in the STN (Garcia et al., 2005), thus leading to increased tonic activity in GPi cells. This seemingly contradicts the idea that electrical HFS is a way of silencing the pathologically overactive indirect pathway as it is done in therapeutic lessoning (Olanow et al., 2000). Under stimulation conditions, DBS restores the thalamus ability to transmit information, whereas with vanishing synaptic conductance amplitude, TC cells are unable to transmit information to the cortex.

Thalamus cells are not able to relay information to the cortex as seen in Fig. 4.3. (right) with vanishing synaptic $GABA_A = 0$ currents. Therefore, we limited our simulations in the beginning to two different input regimes consisting of smaller and larger synaptic inputs. Increasing the synaptic conductance up to 40 pS, our simulations results show, that TC cell relay fidelity is qualitatively restored the same way as DBS is able to do Fig. 4.4. Above $\bar{g}_{syn} = 40$ our networks are no longer stable. The loss of faithful relaying quickly returns for small values of synaptic conductance see Fig. 4.5.

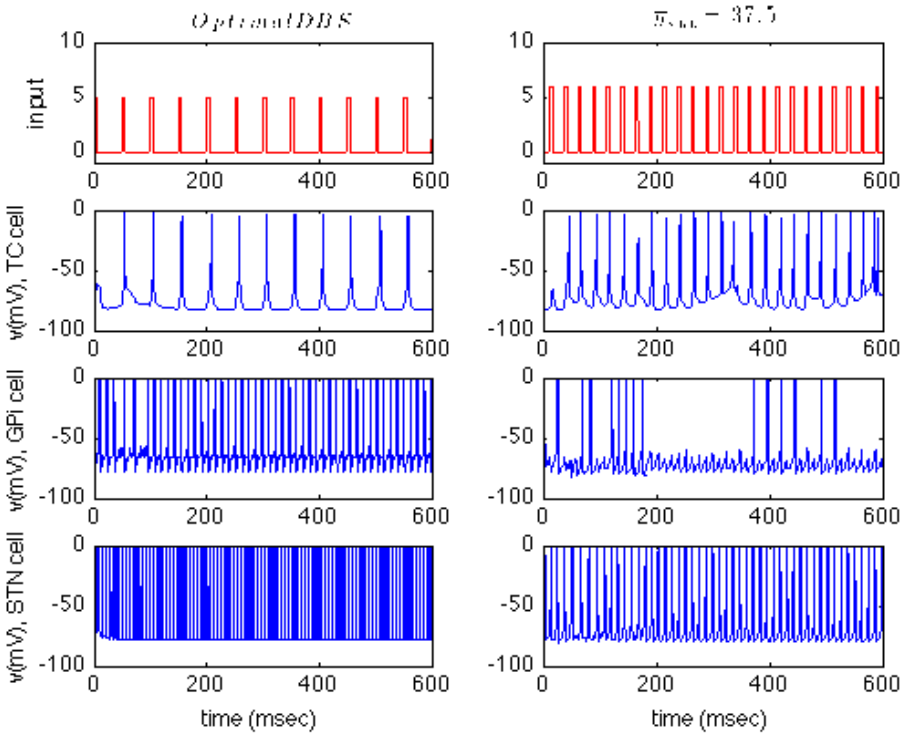

Figure 4.4: The output model membrane potential of TC, GPi and STN cells with optimal DBS stimulation (left) and GABAergic tonic inhibition (right).

In order to quantify TC cells' output in term of correct responses, we utilized two performance scores: *The error index (EI)* and the *coefficient of variation (CV)*. As Rubin and Terman defined the EI is the total number of errors divided by the total number of input stimuli. The CV is the ratio of standard deviation to the average of the inter-spike intervals.

This coefficient provides information on the output of the thalamocortical cells. By thresholding ($V_{th} = -45mV$) the membrane potential, we defined the thalamic cell spike response to each stimulus amplitude. For a perfect relay of our periodic input we expect $CV = 0$ and $EI = 0$. This ideal scenario corresponds to constant inter-spike intervals, but $EI = 0$ is not incompatible with $CV \neq 0$ (for example if pulses are relayed but timing is slightly affected). On the other hand, an $EI \neq 0$ and $CV = 0$ correspond to one stimulus pulse relayed periodically every two or more input pulses (Alejandro, 2006). Table 4.1. lists different values of CV, and EI in normal state, parkinsonian state, optimal applied DBS current and with the GABA input that seems to produce the most beneficial therapeutic effect in our simulation. To analyze the results displayed in Fig. 4.4, we successively introduced the coherence measure taken from (White et al., 1998) within and between spike trains of basal ganglia different nuclei when synaptic

Table 4.1: Averaged error index and coefficient of variation.

	Normal	**Parkinson**	**Optimal DBS**	$\bar{g}_{syn} = 37.5$
EI	0.0612	0.6265	0.1734	0.0949
CV	0.7318	0.6602	0.3087	0.3048

conductances fluctuate and computed the coherence reduction (CR) described by (Moran et al., 2011). A measure of coherence usually characterized the functional integration between the different components of the brain. The correlation or the coherence measure determines the level of synchrony and quantifies the linear correlation in time-frequency domain. Therefore, one distinguishes the magnitude square coherence function and the phase function. Spike trains were approximated by a series of square pulses of unit height and fixed width of 20% of the period of the most rapid firing cell. Each square wave is centered around the peak of the individual action potentials in the train. Then, we computed the shared area of the square pulses from each train that partly coincide in time. The cross-correlation at zero time lag was considered. This correspond to the evaluation of the shared area of the unit-height pulses. Finally, we took the coherence as the sum of these shared areas, divided by the square root of the product of the summed areas of each individual pulse train (Baker et al., 2002).

If $x(t)$ is the series of unit height pulses for the first cell over N time steps and $y(t)$ is the series of pulses for the second cell, then the coherence measure or correlation in time-domain is calculated as (4.8):

$$Coherence\ Measure = \frac{\sum_{i=1}^{N} x(t) * y(t)}{\sqrt{\sum_{i=1}^{N} x(t) * \sum_{i=1}^{N} y(t)}}, \tag{4.8}$$

Given the spike-trains $x(t)$ and $y(t)$, their Fourier transforms $X(\omega)$ and $Y(\omega)$, and complex conjugates $X^*(\omega)$ and $Y^*(\omega)$, the coherence is readily computed in the frequency domain as (4.9):

$$C_{XY}(\omega) = \frac{C_{XY}(\omega)}{\sqrt{P_{XX}(\omega) P_{YY}(\omega)}}, \tag{4.9}$$

where $P_{XX}(\omega) = X(\omega) X^*(\omega)$ is the power spectrum of $x(t)$, and $P_{XY}(\omega) = X(\omega) Y^*(\omega)$ is the cross-spectrum of $x(t)$ and $y(t)$. In this study, since both models produces spike output, $P_{XX}(\omega)$, $P_{YY}(\omega)$ and $P_{XY}(\omega)$ were computed for the mean spike trains using multi-taper estimation methods on 256 ms windows and discrete sequences every 64 ms over the trial time span. Coherences were then computed from trial-averaged spectra. We note that coherence is only meaningful at frequencies with non-vanishing power.

In all our simulation results, the spiking activity of the GPi cells reduces drastically as the synaptic conductances strength increases. The mean firing rate recorded during deep brain stimulation was 161 spikes per second, whereas with the GABA input producing the most beneficial therapeutic outcomes the mean firing rate was 40 spikes per second. Furthermore, the coherence reduction (CR) in Fig. 4.7. is in line with recently findings by (Moran et al., 2011; Wilson et al., 2011) and supports this hypothesis on declining coherence in neuronal spiking activity within and between different nuclei of the basal ganglia during STN macro-stimulation. Our results are similar to those of (Moran et al., 2011), but our explanations differ considerably. They saw a decline in coherence during stimulation. They mainly attributed the decline to the STN oscillatory decoupling from the GPi. In our work we controlled for this synaptic coupling factor, using a smaller parameter value less than 5% differences in afferent synaptic currents $g_{STN \rightarrow GPi}$ rather than in large currents (base value is $0.3 mS/cm^2$). This achieved similar relative differences in intrinsic firing rates, and we still saw a drop-off in coherence. Besides, when the synaptic coupling is extremely fast, the coupling frequently cause neurons towards anti-synchrony (Skinner et al., 1994; Wang and Rinzel, 1992).

4.3.3 Effects of different conductances

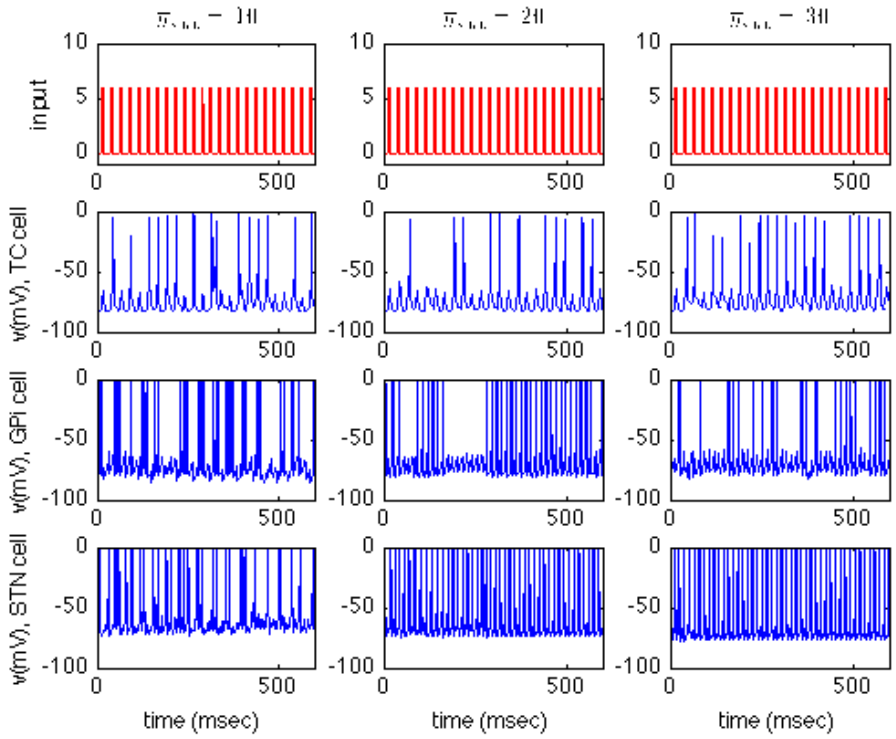

Figure 4.5: Cellular activity exhibited by the TC, STN and GPi cell models for three different synaptic conductance levels. With an increase in synaptic conductance, the relay properties of TC cells improve as can be seen on the EI and CV, respectively. EI, $CV(10) = 0.4241, 0.4851$; EI, $CV(20) = 0.3608, 0.5683$; EI, $CV(30) = 0.2089, 0.5333$.

Fig. 4.5 illustrates the model cell dynamics in dependence on synaptic conductance. One observes different effects on the relay properties of TC cells. For an increase in synaptic conductance, TC cells relay properties improve. Fig. 4.6 illustrates the effects of the synaptic conductance on the relay properties of TC cells as quantified by the error index (circles) and the coefficient of variation (stars). When taking the average of both TC cell outputs, we found that the EI decreased with increasing inhibition, resulting from a decreasing number of incorrectly transmitted responses. The coefficient of variation does not show a similar tendency to decrease with synaptic connectivity; however similarities with the error index cannot be taken much further.

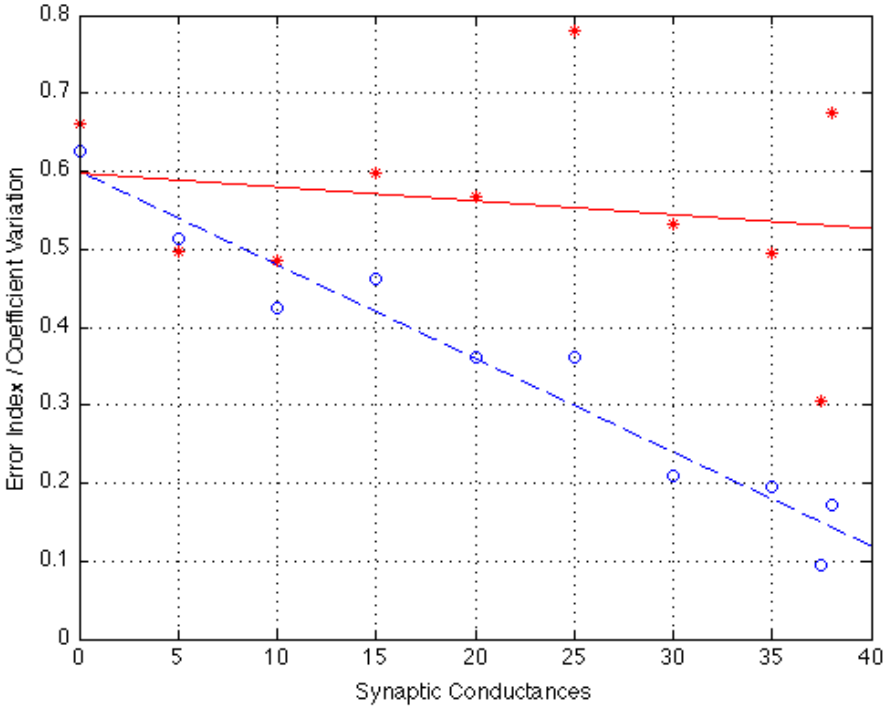

Figure 4.6: Shows average error index EI (circles) of the two thalamic cells and (CV) coefficient of variation (star) dependence of synaptic conductance (Mayer et al., 2006). Dashed and solid lines consist of linear interpolation representing lines ($y = 0.6007 - 0.0120 * x$) and ($y = 0.6007 - 0.0120 * x$) best fit which best approximates EI and CV respectively.

The mean frequency-domain coherogram in Fig. 4.7. over 50 trials is 0.4049 with $\bar{g}_{syn} = 37.5$, whereas the average coherence is 0.9921 when $\bar{g}_{syn} = 0$. The model thus exhibits a decreased coherence as the synaptic weight parameter increases. Our numerical simulations show that at gamma frequency 30-80Hz, a significant synchrony is observed, however, with heterogeneous cells, synchrony may not be possible at all frequencies. In particular, a network of this kind seems unlikely to support synchronous firing at a frequency greater than 200Hz (Fig. 4.7.), a frequency to fast to be synchronized by GABAA. The advantage of this approach is that an understanding of the complexity of the nonlinear, interacting dynamics has been obtained using previous theoretical insights on inhibitory network dynamics.

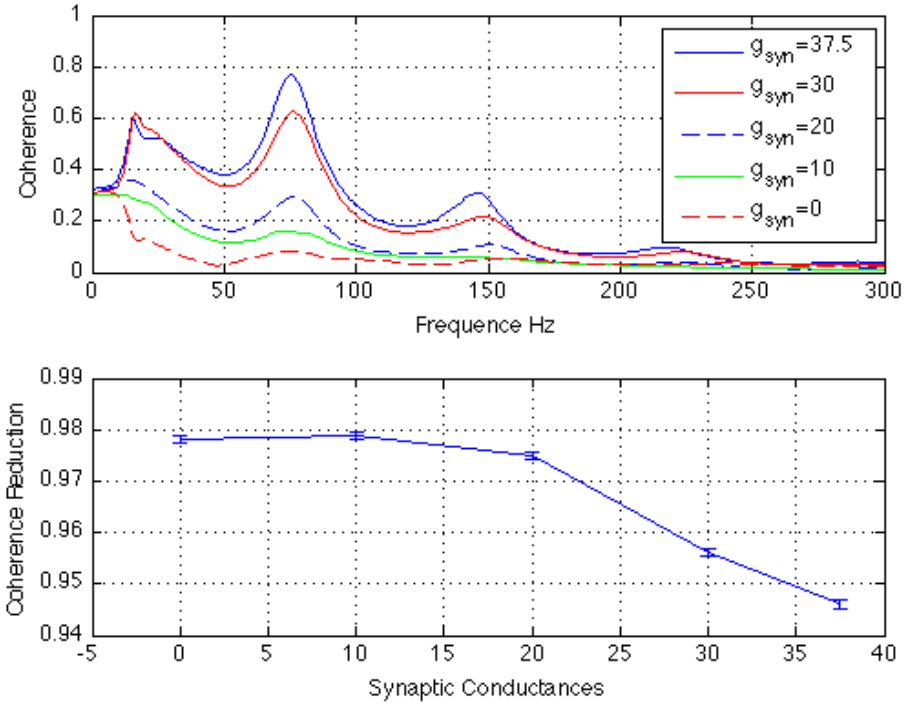

Figure 4.7: Mean coherence measure in frequency domain for GPi-STN cells (top panel) and the coherence reduction (CR) over the synapic conductances input (bottom panel).

Fig. 4.8 shows the mean coherence within the same target nucleus of the GPi cell. Significant coherence is found at a normalized frequency of 0.25 when shifting zero-frequency component to center of spectrum whereas between STN-GPi, it is found at 80 Hz. The response of the network depends on the firing frequency and the time constant of the synaptic weight. Coherence can be reduced in two qualitatively different ways depending on the parameters-either by increasing gradually the synaptic weight coupling parameter, or through suppression, the latter neurons with higher intrinsic rates fire near synchrony and keep their slower counterparts from firing.

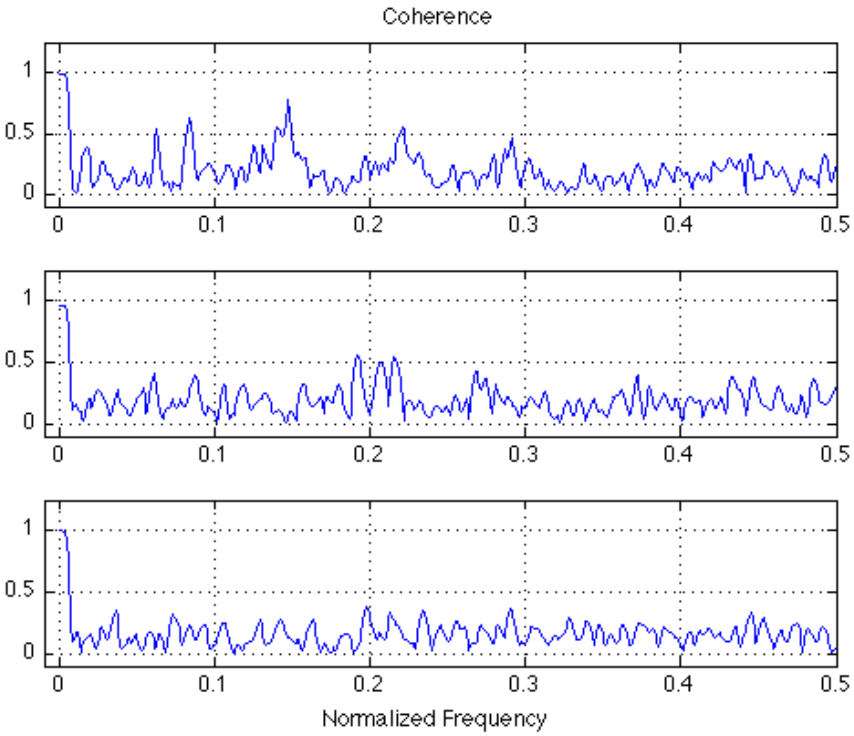

Figure 4.8: Coherence for GPi-GPi cells with the same properties but different synaptic weights as quantified by $\bar{g}_{syn}$=10 (top panel), 20 (middle panel) and 30.

4.4 Discussions and Conclusion

Recent evidence in HFS research points towards a therapeutic mechanism based on effects on the network activity due to a selective GABA release by electrical HFS (Mantovani et al., 2006, 2009; Hiller et al., 2007; Feuerstein et al., 2011). In this study, we used a computational model of the relevant neural structures to examine the effects of low and high conductance inputs in STN target cells to alleviate tentative symptoms by regularizing the pathological synaptic activity of the basal ganglia output structure, the globus pallidus internus (GPi). We used the averaged error index of the thalamic neurons as surrogate for symptom severity and found that synaptic conductance values below $\bar{g}_{syn} = 30$ did not regularize GPi synaptic activity, thus did not improve thalamic relay fidelity sufficiently. In contrast, values above $\bar{g}_{syn} = 30$ did regularize GPi activity, thus significantly improved TC neurons relay fidelity. Synchronized neural activity plays a major role in coding and reliable information transmission (Gong et al., 2010). Synchronization, however, can be enhanced depending on synaptic network connectivity

(Qu et al., 2011) in print, with the extreme case of pathological fully synchronized network activity (Pirini et al., 2009). Our study may be useful in studying the intermittent synchrony generated by moderately increased coupling strength in the basal ganglia due to the lack of dopamine and investigate the boundary region between synchronized and nonsynchronized states in PD (Park et al., 2011).

We conclude that indirect inhibition of neuronal output by means of activation of axon terminals makes the synaptic connectivity with neurons near the stimulating electrode a possible explanation of therapeutic mechanisms of actions of electrical HFS (Dostrovsky et al., 2000; Magarinos-Ascone et al., 2002).

Chapter 5

Oscillatory patterns of STN-GPe activity in Parkinson's disease.

The work described in this chapter was carried out in collaboration with the Centre for Theoretical and Computational Neuroscience, School of Computing and Mathematics, Plymouth University, United Kingdom. A manuscript was submitted to the Journal of Mathematical Neuroscience.

5.1 Introduction

We used the population-based model to study the dynamics of STN-GPe network activity under parkinsonian and heathly conditions. To explore its dynamical regime, we first introduce a geometric approach to the theory of dynamical systems. Here the notion of phace space, local and global bifurcation theory, stability theory and oscillations are briefly reviewed. All these techniques are important in the analysis of our model behavior.

5.1.1 Graphical approach

In this section, we illustrate the geometric approach by considering a one-dimensional nonlinear differential equation:

$$f(x) \equiv \frac{dx}{dt} = x - x^3 \tag{5.1}$$

The eqn. 5.1 can be solved by separating variables and then integrating. The resulting formula is not obvious and difficult to interpret. Assuming an initial condition is given $x(0) = \pi$, and we wish to find the behavior of the solution $x(t)$ as $t \to \infty$. Using the explicit form of the solution of eqn. 5.1, the answer to this question is not straightforward. In contrast, the graphical analysis provides a simple qualitative analysis of this problem as illustrated in Fig. 5.1. The differential equation $\frac{dx}{dt} = x - x^3 \equiv f(x)$ represents a **vector field**, and tells us the position of the particle at each position x.

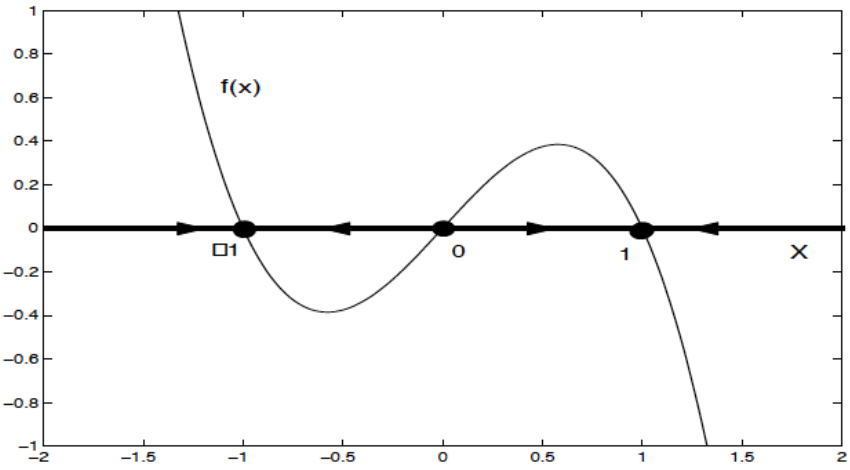

Figure 5.1: The phase space of eqn. 5.1, x is the position of an imaginary particle moving along the real line, t is time and $\dot{x}$ is the velocity of that particle.

5.1.2 Bifurcations

The qualitatively changing of a solution depending on parameter is known as a bifurcation. Four major types of local bifurcation are presented here and three of them can be explained using first-order system. The fourth major type bifurcation is so-called the *The Hopf bifurcation*, it requires at least two dimensional systems and describes how stable oscillations arise when a fixed point loses its stability (Strogatz, 2001; Terman, 2005).

Saddle-node Bifurcation

The saddle-node bifurcations is the basic mechanism by which fixed points are created and destroyed. As a parameter changes, two fixed points move towards each other, collide and mutually annihilate (Strogatz, 2001; Terman, 2005).

The first order system given by eqn. 5.2 illustrates the saddle-node bifurcation:

$$\dot{x} = \mu + x^2 \tag{5.2}$$

where μ is a fixed parameter or bifurcation, which may be any real number (positive, negative or zero). The fixed points are given when the right hand side of eqn. 5.2 vanishes, i.e. $x = \pm\sqrt{-\mu}$.
If $\mu < 0$, eqn. 5.2 has two fixed points; if $\mu = 0$ one fixed point, and if $\mu > 0$, no fixed points. To visualize the bifurcation diagram, we plot the fixed points as function the bifurcation parameter μ. We note that

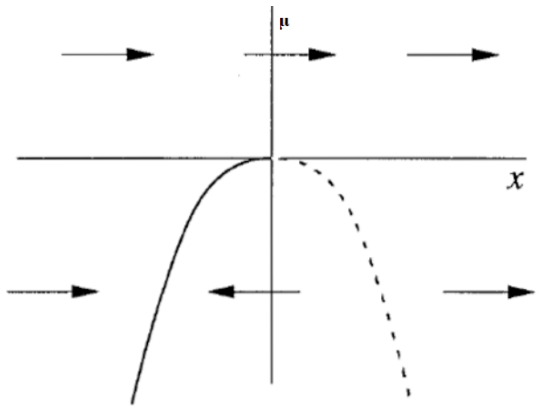

Figure 5.2: Bifurcation diagram of the saddle-node bifurcation, solid lines are used for stable points and dashed lines for unstable ones.

the saddle-node bifurcation is sometimes called a *fold bifurcation* or a *turning-point bifurcation*. Both terminologies are admitted.

Transcritical Bifurcation

The transcritical bifurcation is characterized by the change of its stability as the parameter is varied. An example that illustrates this mechanism is given by the first-order system eqn. 5.3:

$$\dot{x} = \mu x + x^2 \tag{5.3}$$

We note that the main difference between saddle-node and transcritical bifurcations is, in transcritical case, the two fixed points do not dissapear, instead there is an exchange of stability at the bifurcation point $(\mu, x) = (0, 0)$ as depicted in Fig. 5.3.

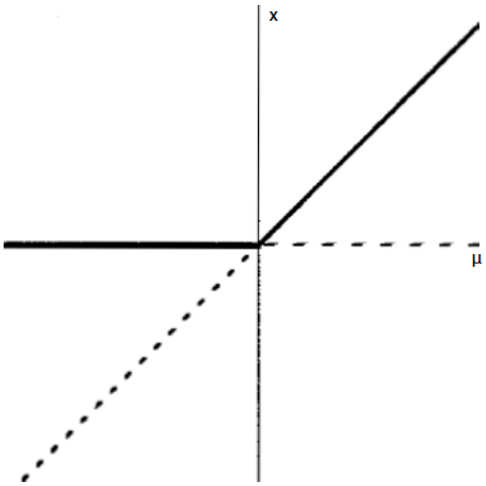

Figure 5.3: Bifurcation diagram of transcritical bifurcation, solid lines are used for stable points and dashed lines for unstable ones, the stability is switched.

Pitchfork Bifurcation

Another type of bifurcation is so-called Pitchfork Bifurcation, in this type, fixed points tend to appear and disappear in symmetrical pairs. There are two types of pitchfork bifurcation, the *supercritical pitchfork* given by the one dimensional eqn. 5.4 and *subcritical pitchfork bifurcations* given by the eqn. 5.5.

$$\dot{x} = \mu x - x^3 \tag{5.4}$$

$$\dot{x} = \mu x + x^3 \tag{5.5}$$

The bifurcation diagram for the two types of Pitchfork is depicted in Fig. 5.4

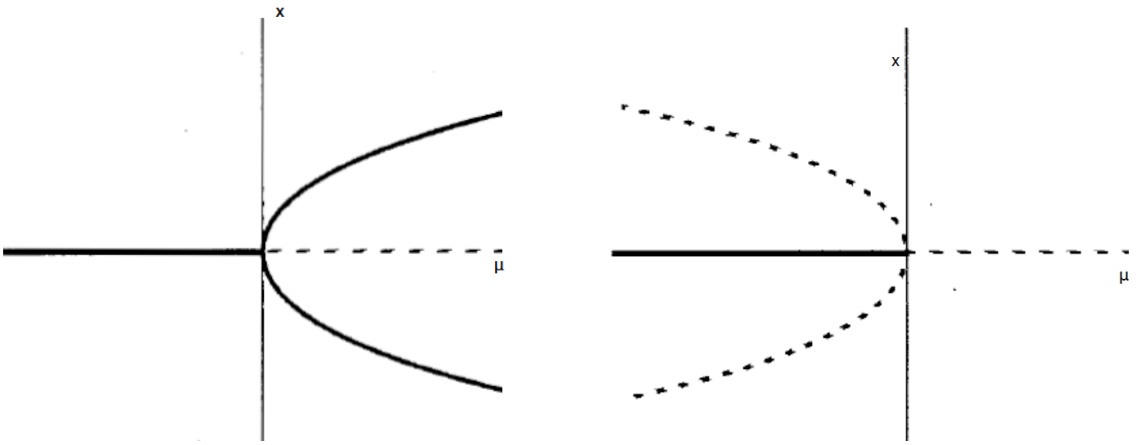

Figure 5.4: Bifurcations diagram of Pitchfork bifurcation, supercritical pitchfork bifurcation (left) and subcritical pitchfork bifurcation (right). Solid lines branches are used for stable points and dashed lines branches for unstable ones, the pitchfork is inverted.

We note that the supercritical pitchfork is sometimes called a *forward bifurcation*, and the subcritical is sometimes called an *inverted* or *backward bifurcation*. Finally, in some cases, we have two stable fixed points and this is so-called *bistable*. The existence of different stable allows for the possibility of *jumps* and *hysteresis*, in particular when there is no reversibility as a parameter is changed, *hysteresis phenomenon* is observed.

5.1.3 Higher dimensional systems

In the previous section we have seen that there exists three types of local bifurcation namely, *saddle-node, transcritical and pitchfork* bifurcations, both describing the dynamic near a fixed point as the bifurcation parameter is varying. Each of these local bifurcations can occur in higher dimensional. The major type of bifurcation in higher dimension (> 1), is *Hopf bifurcation*. We illustrate this type of bifurcation by the following example given in eqn. 5.6.

$$\begin{aligned} \dot{x} &= 3x - x^3 - y \\ \dot{y} &= x - \mu \end{aligned} \tag{5.6}$$

The above system of equations gives only one fixed point $\left(\mu, 3\mu - \mu^3\right)$ for each bifurcation parameter μ, we consider the Jacobian matrix at a given fixed points. If the Jacobian matrix does not have any eigenvalues on imaginary axis, then the fixed point is called *hyperbolic*, hence no bifurcation point. If the Jacobian matrix has purely imaginary eigenvalues (necessary condition) then there is a bifurcation point.

The following example described by eqn. 5.6 exhibits two Hopf bifurcations depicted in Fig. 5.5, as a bifurcation parameter changes, the stability of the fixed point is lost as its matching eigenvalues cross the imaginary axis (Terman, 2005). In particular the Hopf bifurcations is supercritical when the limit cycles are stable and they exist for the same parameter values as unstable fixed points, and subcritical when the limit cycles are unstable and exist for those same parameter values as the stable fixed points.

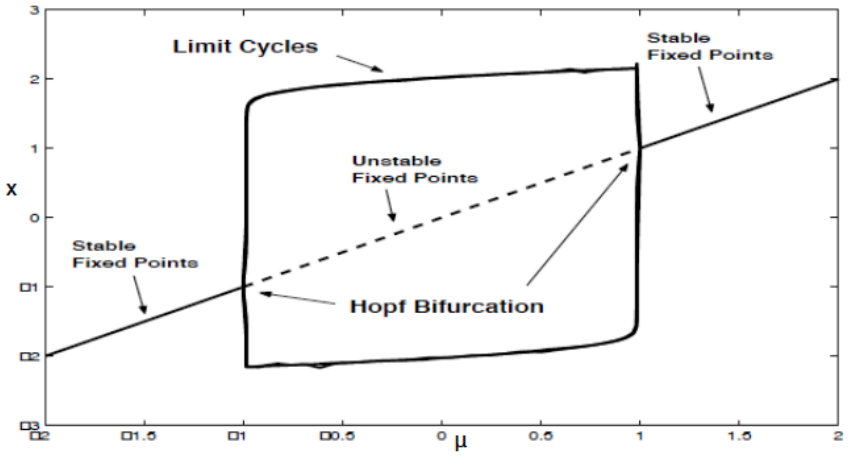

Figure 5.5: Bifurcation diagram of two-dimensional bifurcation given by the eqn. 5.6, solid lines are used for stable points and broken lines for unstable ones. Two Hopf bifurcation points can be observed.

Andronov-Hopf Bifurcation

A fixed point undergoes Andronov-Hopf bifurcation when the Jacobian matrix of the system has the sum of eigenvalues equal to zero (Borisyuk and Kirillov, 1992). If the steady state is a focus (complex eigenvalues), the Andrnov-Hopf bifurcations curve separates regions on the plane where the phase diagram contains stable or unstable focus (Borisyuk and Kirillov, 1992), and the attractor becomes a **limit cycle**. In particular when two branches of saddle-node bifurcation curve meet tangentially, it is called **Cusp bifurcation** and if the bifurcation point separates branches of sub-and supercritical Androv-Hopf bifurcations, it is called **Bautin bifurcation**. As mentioned, Hopf bifurcation are local phenomena, describing the limit cycle near a fixed point.

5.2 Bifurcation analysis of a model STN-GPe Activity

5.2.1 Introduction

In this section[1], we apply mathematical technique of bifurcation analysis to a model of STN-GPe to categorize boundary regions within the parameter space. These boundaries discriminate regions of different dynamics. As potential pacemaker, the STN-GPe network has received significant attention the last decades, the interaction between these two neurons produces synchronized oscillations (Gillies and Willshaw, 2002; Plenz and Kital, 1999) in the beta $(14-30\,Hz)$ band, in the basal ganglia of patients with Parkinson's disease. Important physiological features of the feedback between STN-GPe favor the generation of these oscillatory activities. In this study we seek the conditions under which these oscillations arise. To shed the light on the origin of beta oscillations associated with Parkinson's disease (Kuhn et al., 2006), many computatonal model have been proposed (Terman et al., 2002). All theses models provide interesting conclusions, explain experimentally observed phenomena and may help to understand and improve treatments; however, most have a drawback in that the complexity of the equations used in the model make them unsuitable for mathematical analysis. The mean field population by Wilson-Cowan equations for population dynamics (Wilson and Cowan, 1972) is used, and the bifurcation analysis gives a deeper understanding of how oscillations arise. The type of bifurcation lines separating regions with and without oscillations shows how the systems behaviour changes as it moves from an oscillatory to steady-state regime or vice versa (Borisyuk and Kirillov, 1992).

5.2.2 Mathematical Model

The model consists of two neuronal populations: the glutamatergic neurons of the subthalamic nucleus (STN) and the GABAergic neurons of the external segment of the globus pallidus (GPe). Each population connects both to itself and the other population. We include an external constant excitatory input from the cortex to the STN. Fig. 5.6 illustrates this model. Each equation describes the amount of excited neurons in the population.

[1] The original work was presented at ICMS Neurodynamics: a workshop on heterogeneity, noise, delays, and plasticity in neural systems, Edinburgh, 2012. as: *Bifurcation analysis of a model of Parkinsonian STN-GPe activity.* Authors: Robert Merrison, Felix Njap, Ulrich G. Hofmann, and Roman Borisyuk. ICMS, http://icms.org.uk/workshops/neuro2012

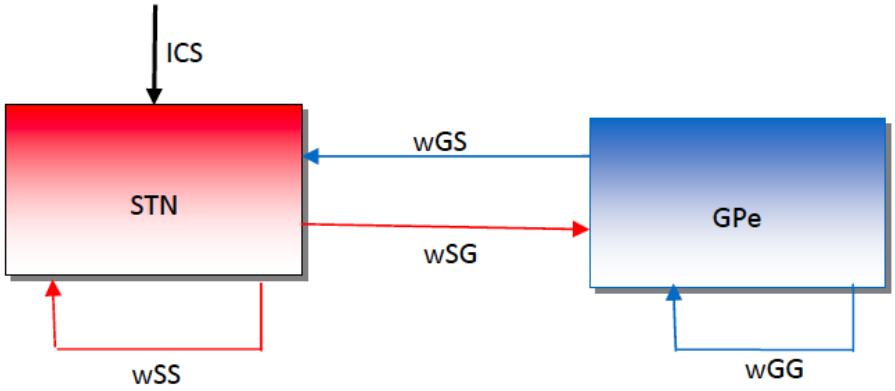

Figure 5.6: The two populations STN-GPe Excitatory-Inhibitory network, parameter ω_{ij} denotes the connection strength from i to j, I_{CS} represents constant input from the cortex to the STN.

We apply Wilson-Cowan paradigm to investigate oscillatory behaviour arising in such networks, the following dynamics described the above network model:

$$\tau_S \frac{d}{dt} STN = -STN + f_S\left(-\omega_{GS} GP + \omega_{SS} STN + I_{CS}\right) \tag{5.7}$$

$$\tau_G \frac{d}{dt} GP = -GP + f_G\left(-\omega_{GG} GP + \omega_{SG} STN\right) \tag{5.8}$$

where τ_s and τ_G are typical membrane time constants, chosen within some range as reported in some earlier contribution. 10-20 ms (Tsodyks et al., 1993), for TC cell 5-64 ms (Turner et al., 1997) and for cortical cell 7-22 ms (Anderson et al., 2000). $f_G(.)$ and $f_S(.)$ are sigmoid functions given by equation 2.14.

5.2.3 Choice of Parameters

To be specific, the weights of each connection type need to be assigned. There is a great deal of evidence from physiological experiments that can be used to determine the relative connection strengths. The connection strengths are set to those estimated in (Holgado et al., 2010). We study the bifurcations of the system under fluctuation of STN self-excitation (ω_{SS}) and cortical input I_{CS}.
To simulate the advance of Parkinson's disease (Holgado et al., 2010), weights in their study corresponding to different stages of disease progression were defined as:

$$\omega_{ij} = \omega_{ijh} + \mu \cdot (\omega_{ijd} - \omega_{ijh}) \tag{5.9}$$

Table 5.1: Estimated parameter values for synaptic connection weight.

Weight	Healthy	Disease
ω_{SG}	19.0	20.0
ω_{GS}	1.12	10.7
ω_{GG}	6.60	12.3

where ω_{ij} is the synaptic weight from nucleus i to nucleus j, ω_{ijh} the weight value corresponding to the healthy condition, ω_{ijd} the value corresponding to the diseased case, and μ a parameter that is increased from 0 to 1 as the progression of the disease.

There are three parameters in the model:

- μ scales the weights in the system between healthy and Parkinsonian values, where $\mu = 0$ corresponds to the healthy state and $\mu = 1$ corresponds to the Parkinsonian state.
- $\omega_{STN \to STN}$ (W_{SS}) is the strength of self-excitation in the STN. We do not currently have a value of this from experiments, and so we should study how the system behaves for different values.
- I_{CS} is the size of the constant input to the STN from the cortex.

5.2.4 Software Packages

A number of software packages were used for analysis. XPP was used to study phase portraits. LOCBIF and AUTO were used for numerical continuation to compute bifurcation diagrams. The dependence of oscillation frequency on parameters was visualised with NumPy / XPPy.

5.3 Results

The bifurcation diagram under Parkinsonian states ($\mu = 1$) is depicted in Fig. 5.7. It shows the system behaviour in the parameter space. Crossing the fold of limit cycles lines (dashed red line) from below (from region A to D), two limits cycle appear. An unstable one surrounds the stable spiral and a stable one surrounds that. Any trajectories starting inside the unstable limit cycle approach the fixed point and any trajectories outside of it approach the stable limit cycle. The system is therefore bistable, with some initial conditions going to the fixed point and some going to oscillations. As you approach the subcritical A-H line (moving from D to C), the unstable limit cycle shrinks around the fixed point. At

the bifurcation it joins with the fixed point, disappears, and the fixed point becomes unstable. Table 5.2 summarizes, the phase potrait of each region of the diagram:

Table 5.2: Summarized phase portrait.

	phase portrait
Region A	One stable node/spiral
Region B	One stable node/spiral, one saddle point, one unstable node/spiral
Region C	One unstable node/spiral, one stable limit cycle
Region D	Stable node/spiral, unstable limit cycle, stable limit cycle
Region E	Stable spiral/node, saddle, stable spiral/node
Region F	Unstable spiral/node, saddle, stable spiral/node, stable limit cycle

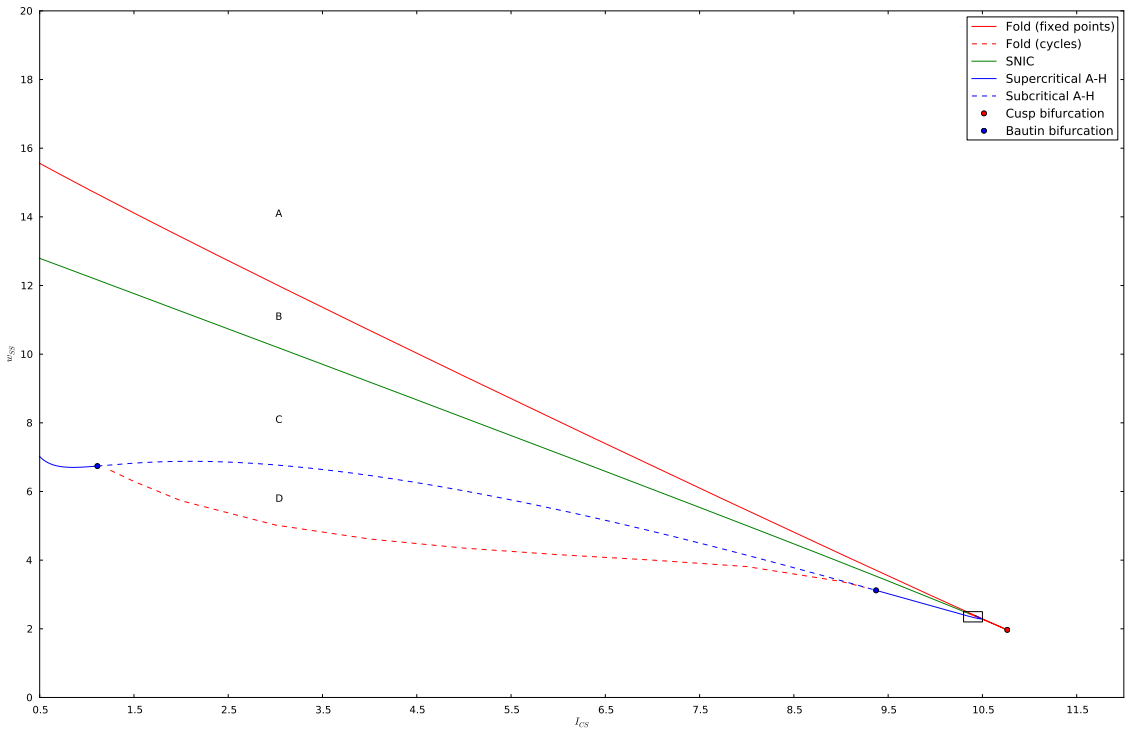

Figure 5.7: Bifurcation diagram under Parkinsonian conditions

The plot in Fig. 5.8 is the zoom version of the above plot, in which ones can cleary identify two other regions E and F.

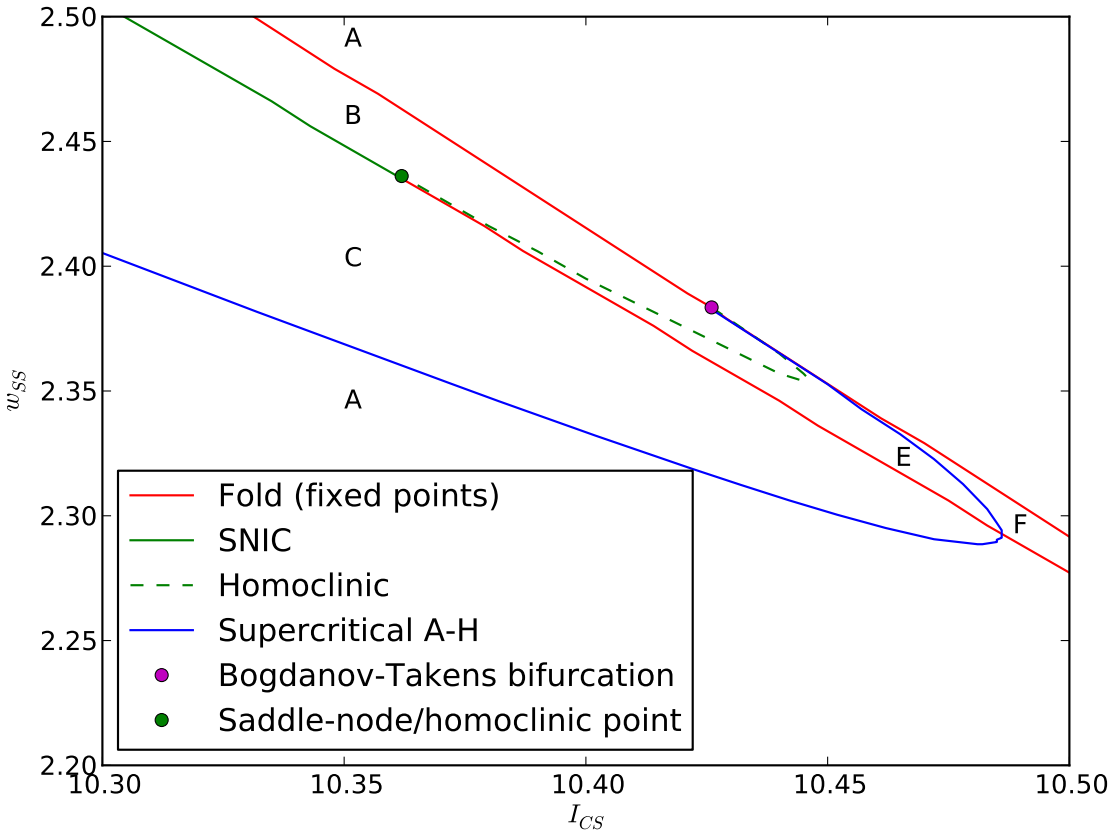

Figure 5.8: Zooming the bifurcation diagram under Parkinsonian conditions shows other regions.

We are particularly interested in region C, because examining the variation of frequency with parameters in that regions shows oscillations mostly in the beta band, as the may be correlated with symptoms of Parkinson's disease. Fig. 5.9 depicts, the phase portrait diagram in the region C.

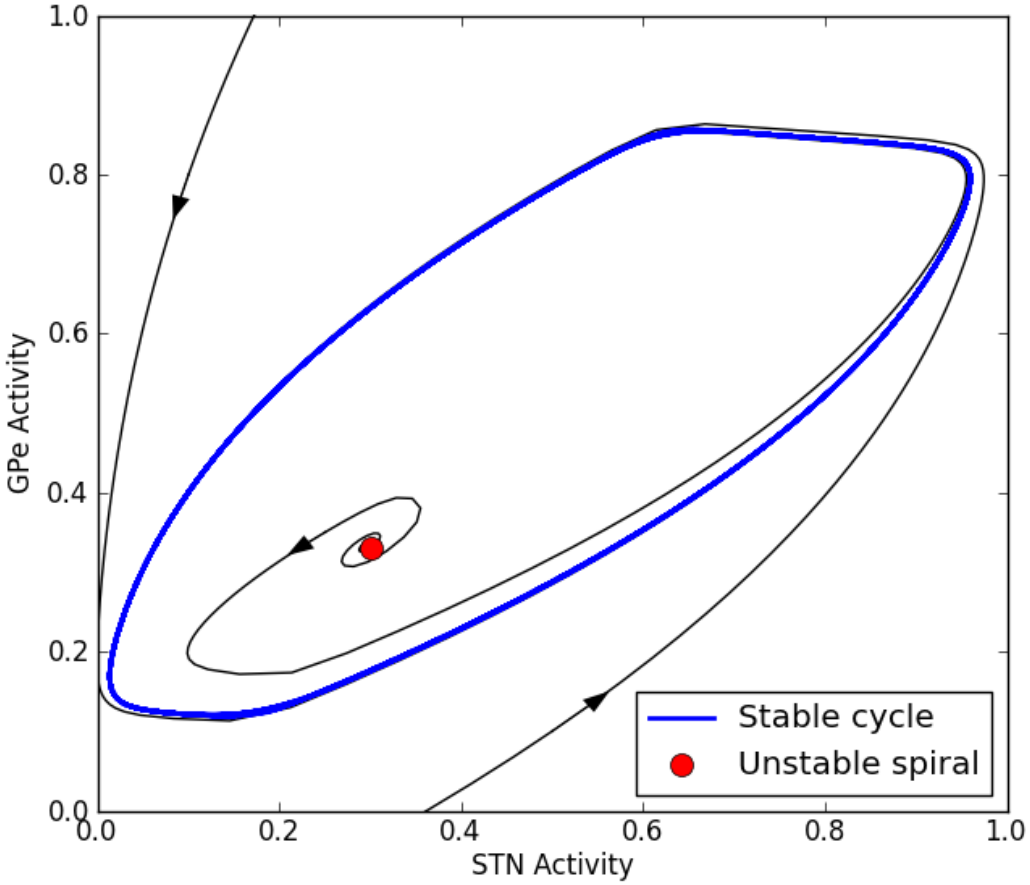

Figure 5.9: Phase portraits in region C

As the parameters move closer to the fold bifurcation at the top of region C the period of oscillation tends to ∞. For most of the period, activity is relatively constant, with brief excursions to high or low states. Most of the fold line between B and C represents a saddle node on invariant circle bifurcation where oscillations disappear. Zooming the bifurcation diagram reveals more details around the cusp point. In particular, there is a homoclinic bifurcation, shown in Fig. 5.8. None of the other regions contain oscillations. "Healthy" connection strengths do not give any parameter regions with stable oscillations.

5.4 Conclusion and discussions

A number of bifurcations (up to codimension 2) are found. In particular, a region of beta oscillations has been identified in the model under Parkinsonian conditions. No such region is present under "healthy

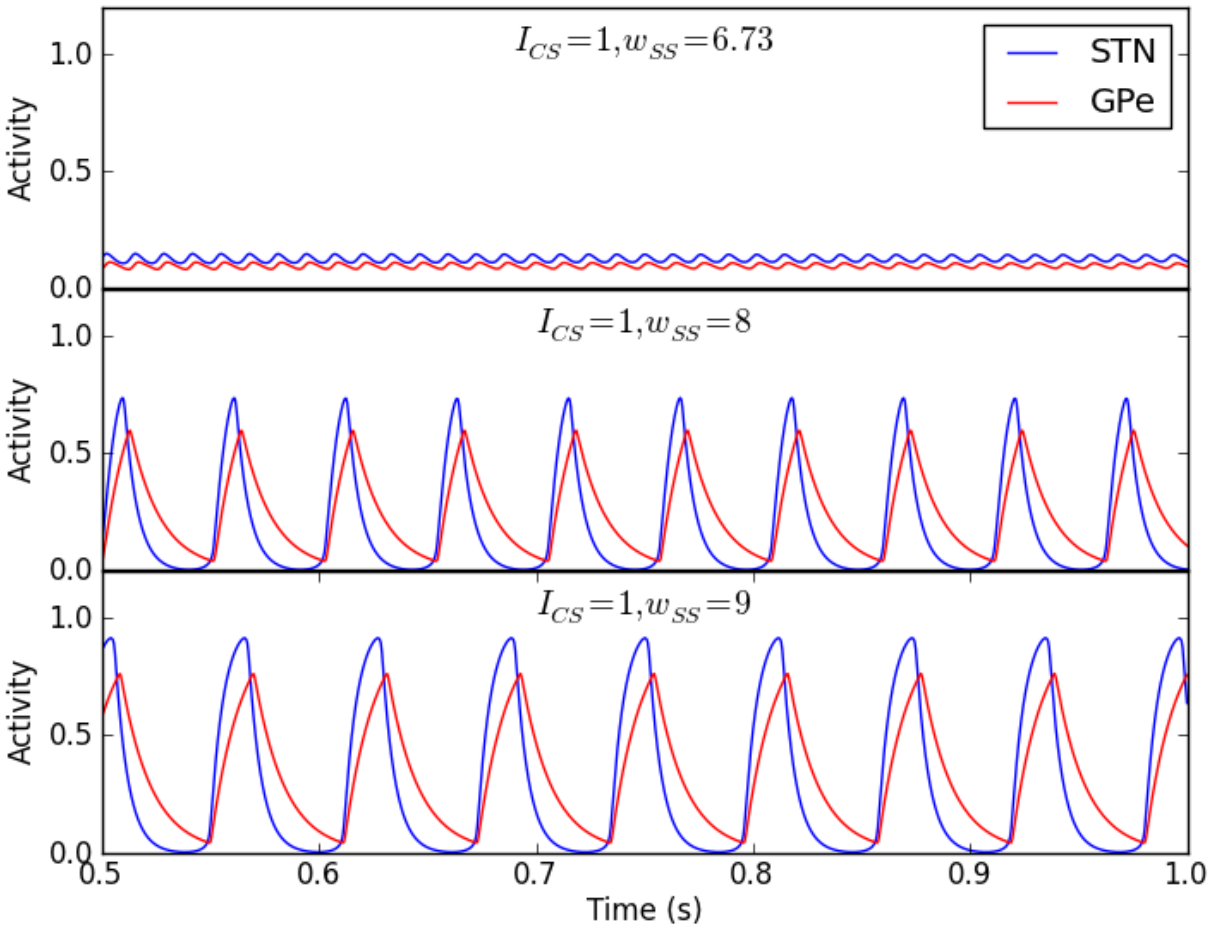

Figure 5.10: Model behaviour for different parameters

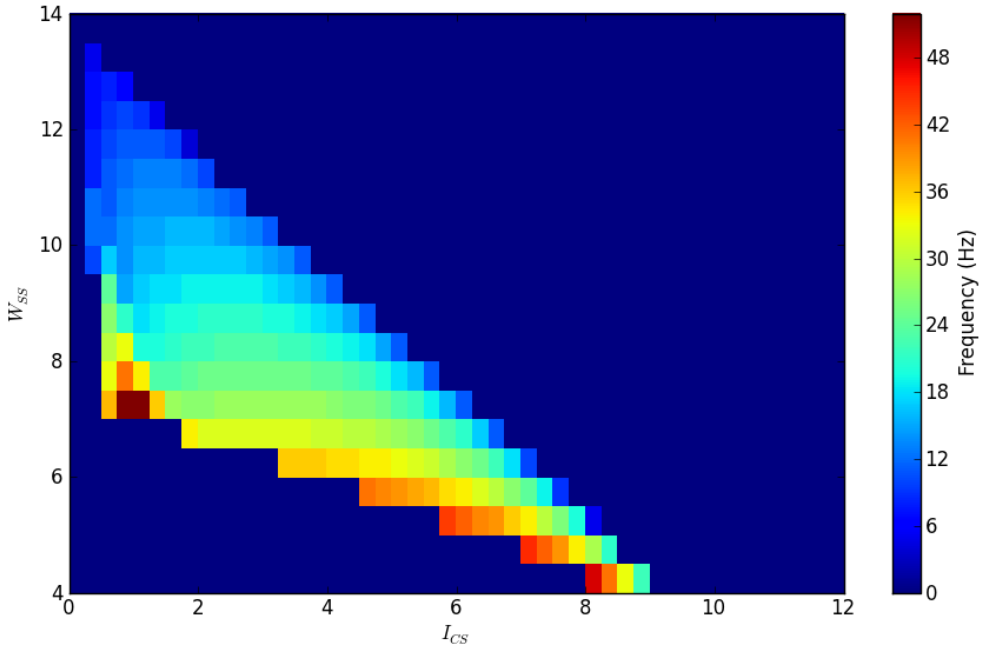

Figure 5.11: Oscillations in beta band

conditions". Under "Parkinsonian" conditions the model is able to produce beta frequency oscillations. The frequency and amplitude of these oscillations are modulated by cortical input to the STN. Bifurcation analysis has not previously been applied to a model such as this. It shows exactly how the variation of parameters controls oscillations. As with other models our approach requires STN self- excitation for oscillations. Neurophysiological data suggests that in reality such connections are limited. A new hypothesis for how oscillations arise should be formulated and tested. Preliminary work shows that adding additional populations to this model can give stable oscillations without STN self-excitation.

Chapter 6

Conclusions and Future Direction

This thesis brings together mathematical tools, modeling of neurobiological dynamics, and medical problems of interest. An extremely large amount of data and computational models in neuroscience raises new and exciting mathematical questions. Movement disorders such as Parkinsons disease affect the lives of millions of people worldwide. In order to gain insight into the pathophysiology of affected neural circuits and the effects of DBS, this thesis focuses on PD conditions and study the GABAergic neuronal target system for electrical high frequency stimulation, in the basal ganglia thalamocortical motor circuit. To this end, we incorporated a model of the $GABA_A$ receptor developed by (Destexhe et al., 1994) at synapses in our model and investigated the spiking activity of movement-related neurons in STN. We showed that the additional synaptic current and the current noise have a significant effect on the model electro-physiological responses. Examining well-established similarity measure function, we found that Mahalanobis distance, Victor-Purpura metric, and Interspike Interval distribution have a relatively high accuracy to detect functional change to stochastic generated spike trains, whereas Mutual Information performed slightly worse (ch. 3). Considering the original Rubin and Terman based computational model of basal ganglia, we demonstrated that a high concentration of the inhibiting neurotransmitter GABA together with electrical stimulation re-establishes faithful thalamocortical relaying (ch. 4). Moreover, our model showed a reduction of coherence between neurons after stimulation as recently reported by (Moran et al., 2011). The subthalamo-pallidal network is capable of self-sustained oscillations without any external oscillatory input, under some conditions (ch. 5). Our results suggest that parkinsonian brain oscillations can only rise under particlar cortical conditions, since the cortical pathway is pro-kinetic meaning that oscillations can only be seen during initiation of movement. Getting closer to the

system's parameter found in Parkinson conditions, oscillations become possible. The bifurcation analysis suggests that at some point in the progression of the disease, pauses in the constant fast tonic firing of the STN and GPe appear. Here, we note that we do not mean to imply that this constant fast tonic firing is present all the time in the healthy brain. We suggest that there may be some particular state in which this activity is seen (perhaps during movement or action selection), and in the pathological case we showed that it is disrupted in the manner described, where the firing rate drops dramatically.

6.1 Further Work

In our model we consider stochastic versions of the Hodgkin-Huxley (HH) equations, there remains an open question: the what and where the channel noise should be included in conductance-based models? Recently research by (Goldwyn and Shea-Brown, 2011) suggests different aspects of adding noise processes into HH equations, hence a more appropriate methods of incorporating channel noise might be taken into account with respect to these findings.

In another study by (Park et al., 2011), they found that the parkinsonian state lies in the boundary region between synchronized and non-synchronized states. It may be interesting to carry out more investigations to support this hypothesis, therefore, our findings call for further study of intermittent synchrony in neural systems

There are some missing neuroanatomical information to the network architecture, we believe that a precise spatial organization of the connection between STN and GPe is required. This will help to understand whether the two nuclei project on each other in a reciprocal manner or out, perhaps enabling us to roughly calculate some biologically plausible values for each synaptic connection strength. In particular, a lack of any biological evidence for self-excitation in the STN would cast doubt on our findings. It should be therefore absolutely important to understand its neuroanatomy. As the synaptic weight (synaptic plasticity) fluctuates in biological neural network, perhaps using Oja's rule or Hebbian learning that states in biological terms: *neurons that fires together, wires together*, could be relevant to adapt such fluctuations, even though there is no reported direct experimental evidence.

"What role does synaptic plasticity play in the development of excessive synchronisation? (Mallet et al.,

2008) found that only chronic dopamine depletion in rats led to excessive β synchrony and that the onset of this was delayed by several days. They suggest therefore that this synchrony is a result of plastic changes that come about slowly. They claim that stimulation in a particular pattern at multiple sites can result in changes in synaptic connectivity that reduces oscillations after stimulation is finished. It has also been found that the effects of standard DBS can sometimes persist for a short time after stimulation is switched off. Most models studied so far do not include any plasticity effects, but the experimental evidence suggests that considering these could lead to more effective treatment" (Merrison, 2011).

Modeling the direct pathway by adding a constant inhibitory striatal input could be investigated, since this would act against the excitatory hyper-direct" input to the STN. Most likely, we can predict that if this striatal inhibition is increased, therefore the cortical excitation need also to be increased to maintain oscillations, but this need to be established. Finally a more interesting research direction will consist of considering the entire basal ganglia thalamocortical circuitry, and find possible conditions under which this network could be exposed to excessive oscillations correlated with some neuropathological cases.

The experimental basis for the parameter values that were used must be checked. In particular, it is important to find out if the values used are from humans or animals. This is particularly important for time constants. If we wish to compare the frequency of oscillations in our model with those that have been observed experimentally, we must make sure that the parameters used are applicable for the source of the experimental data. Large differences in oscillation frequency have been found between humans and animals.

List of Figures

List of Tables

List of Abbreviations

AMPA: Aminomethyl-phenylacetic acid

BG: Basal Ganglia

DBS: Deep Brain Stimulation

EPN: Entopeduncular Nucleus

EPSP: Excitatory Postsynaptic Potential.

GABA: γ-Aminobutyric Acid.

GP: Globus Pallidus.

GPe: Globus Pallidus externus.

GPi: Globus Pallidus internus.

HH: Hodgkin and Huxley.

LIF: Leaky Integrate-and-Fire.

LFP: Local Field Potential.

LTP: Long-Term Potentiation.

LTD: Long-Term Depression.

MSNs: Medium Spiny Neurons.

MPTP: 1-methyl-4-phenyl-1,2,3,6-tetrahydropyridine.

NMDA: N-Methyl-D-Aspartate.

Vim: Nucleus Ventralis intermedius.

OCD: Obsessive-Compulsive Disorder.

OHDA: Hydroxydopamine.

PD: Parkinson's Disease.

PPN: Pedunculopontine Nucleus.

SN: Substantia Nigra.

SNc: Substantia Nigra pars compacta.

SNr: Substantia Nigra pars recticulata.

STN: Subthalamic Nucleus.

SMA: Supplementary Motor Area.

TAN: Tonically Active Neurons.

TC: Thalamic Cell.

UPDRS: Unified Parkinsons Disease Rating Scale.

Bibliography

Aebischer, P. and Schultz, W. (1984). The activity of pars compacta neurons of the monkey substantia nigra is depressed by apomorphine. *Neurosci. Lett.*, 50:25–29.

Albin, R., Young, A., and Penney, J. (1989). The functional anatomy of basal ganglia disorders. *Trends Neurosci.*, 12:366–375.

Alejandro, P. (2006). *Working with a computational model for high frequency stimulation.* Rapport de recherche, N RR-5890, http://hal.inria.fr/inria-00071378/en/.

Alexander, G. and Crutcher, M. (1990). Functional architecture of basal ganglia circuits: neural substrates of parallel processing. *Trends Neurosci.*, 13:266–271.

Alexander, G. and DeLong, M. (1985). Microstimulation of the primate neostriatum. ii. somatotopic organization of striatal microexcitable zones and their relation to neuronal response properties. *J. Neurophysiol.*, 53:1417–1430.

Anderson, J., Carandini, M., and Ferster, D. (2000). Orientation tuning of input conductance, excitation, and inhibition in cat primary visual cortex. *J. Neurophysiol.*, 84:909–926.

Anderson, M., Postupna, N., and Ruffo, M. (2003). Effects of high-frequency stimulation in the internal globus pallidus on the activity of thalamic neurons in the awake monkey. *J. Neurophysiol.*, 89:1150–1160.

Apicella, P., Ljungberg, T., Scarnati, E., and Schultz, W. (1991). Responses to reward in monkey dorsal and ventral striatum. *Exp. Brain Res.*, 85:491–500.

Arle, J., Mei, L., and Shils, J. (2008). Modeling parkinsonian circuitry and the dbs electrode. I. biophysical background and software. *Stereotact. Funct. Neurosurg.*, 86(1):1–15.

Ashkan, K., Wallace, B., Bell, B., and Benabid, A. (2004). Deep brain stimulation of the subthalamic nucleus in parkinson's disease 1993- 2003: where are we 10 years on?. *J. Neurosurg.*, 18:19–34.

Aubert, I., Ghorayeb, I., Normand, E., and Bloch, B. . (2000). Phenotypical characterization of the neurons expressing the D1 and D2 dopamine receptors in the monkey striatum. *J. Comp. Neurol .*, 418:22–32.

Baker, P., Pennefather, P., Oser, B., and Skinner, F. (2002). Disruption of coherent oscillations in inhibitory networks with anesthetics: Role of GABA(A) receptor desensitization. *J. Neurophysiol.*, 88:2821–2833.

Bastian, A., Kelly, V., Revilla, F., Perlmutter, J., and Mink, J. (2009). Different effects of unilateral versus bilateral subthalamic nucleus stimulation on walking and reaching in parkinsons disease. *Movement Disorders.*, 18(9):1000–1007.

Baude, A., Nusser, Z., Roberts, J., Mulvihill, E., McIlhinney, R., and Somogyi, P. (1993). The metabotropic glutamate receptor (mGluR1a) is concentrated at perisynaptic membrane of neuronal subpopulations as detected by immunogold reaction. *Neuron.*, 11:771–787.

Beal, M. (2001). Experimental models of parkinson's disease. *Nat. Rev. Neurosci.*, 2(5):325–334.

Benabid, A. (2007). What the future holds for deep brain stimulation. *Expert Rev. Med. Devices*, 4(6):895–903.

Benabid, A., Benazzouz, A., and Pollak, P. (2002). Mechanisms of deep brain stimulation. *Mov. Disorders*, 17(3):73–74.

Benabid, A., Chabardes, S., and Seigneuret, E. (2005). Deep-brain stimulation in parkinson's disease: Long-term efficacy and safety- what happened this year?. *Curr. Opin. Neurol.*, 18:623–630.

Benabid, A., Pollak, P., Gao, D., Hoffmann, D., Limousin, P., Gay, E., Payen, I., and Benazzouz, A. (1996). Chronic electrical stimulation of the ventralis intermedius nucleus of the thalamus as a treatment of movement disorders. *J. Neurosurg.*, 84:203–214.

Benabid, A., Pollak, P., Gross, C., Hoffmann, D., Benazzouz, A., Gao, D., Laurent, A., Gentil, M., and Perret, J. (1994). Acute and long-term effects of subthalamic nucleus stimulation in parkinson's disease. *Stereotact Funct Neurosurg.*, 62:76–84.

Benabid, A., Pollak, P., Louveau, A., Henry, S., and de Rougemont, J. (1987). Combined (thalamotomy and stimulation) stereotactic surgery of the vim thalamic nucleus for bilateral parkinson disease. *Appl. Neurophysiol.*, 50:344–346.

Benazzouz, A., Gao, D., Ni, Z., Piallat, B., Bouali-Benazzouz, R., and Benabid, A. (2000). Effect of high-frequency stimulation of the subthalamic nucleus on the neuronal activities of the substantia nigra pars reticulata and ventrolateral nucleus of the thalamus in the rat. *Neurosci.*, 99(2):289–295.

Berardelli, A., Rothwell, J., Thompson, P., and Hallett, M. (2001). Pathophysiology of bradykinesia in parkinson's disease. *Brain*, 124(11):2131–2146.

Bergman, H., Feingold, A., Nini, A., Raz, A., Slovin, H., Abeles, M., and Vaadia, E. (1998). Physiological aspects of information processing in the basal ganglia of normal and parkinsonian primates. *Trends Neurosci.*, 21:32–38.

Bernard, V., Somogyi, P., and Bolam, J. (1997). Cellular, subcellular, and subsynaptic distribution of AMPA-type glutamate receptor subunits in the neostriatum of the rat. *J. Neurosci.*, 17:819–833.

Betarbet, R., Sherer, T., and Greenamyre, J. (2002). Animal models of parkinson's disease. *Bioessays.*, 24:308–318.

Beurrier, C., Bioulac, B., Audin, J., and Hammond, C. (2001). High-frequency stimulation produces a transient blockage of voltage-gated currents in subthalamic neurons. *J. Neurophysiol.*, 85:1351–1356.

Bevan, M., Smith, A., and Bolam, J. (1996). The substantia nigra as a site of synaptic integration of functionally diverse information arising from the ventral pallidum and the globus pallidus in the rat. *Neuroscience.*, 75:5–12.

Bischoff, S., Leonhard, S., Reymann, N., Schuler, V., Shigemoto, R., Kaupmann, K., and Bettler, B. (1999). Spatial distribution of GABAB R1 receptor mRNA and binding sites in the rat brain. *J. Comp. Neurol.*, 412:1–16.

Bolam, J., Booth, P., Hanley, J., and Bevan, M. (2000). Synaptic organisation of the basal ganglia. *J. Anat.*, 196:527–542.

Bolam, J., Powell, J., Totterdell, S., and Smith, A. (1981). The proportion of neurons in the rat neostriatum that project to the substantia nigra demonstrated using horseradish peroxidase conjugated with wheatgerm agglutinin. *Brain Res.*, 220:339–343.

Bolam, J. and Smith, Y. (1992). The striatum and the globus pallidus send convergent synaptic inputs onto single cells in the entopeduncular nucleus of the rat: a double anterograde labelling study combined with postembedding immunocytochemistry for GABA. *J. Comp. Neurol.*, 321:456–476.

Borisyuk, R. and Kirillov, A. (1992). Bifurcation analysis of a neural network model. *Biological Cybernetics*, 66:319–325.

Bower, J. and Beeman, D. (1998). *The Book of GENESIS: Exploring Realistic Neural Models with the GEneral NEural SImulation System.* 2nd edition. Springer-Verlag, New York.

Boyes, J. and Bolam, J. (2007). Localization of GABA receptors in the basal ganglia. *Prog. Brain. Res.*, 160:229–243.

Braun, H., Huber, M., Anthes, N., Voigt, K., Neiman, A., Pei, X., and Moss, F. (2007). Interactions between slow and fast conductances in the huber/braun model of cold-receptor discharges. *Neurocomputing.*, 32(33):51–59.

Brown, P. (2003). Oscillatory nature of human basal ganglia activity: relationship to the pathophysiology of parkinson's disease. *Mov. Disord.*, 18:357–363.

Brown, P. (2006). Bad oscillations in parkinson's disease. *J. Neural Transm.*, 70:27–30.

Burbaud, P., Gross, C., and Bioulac, B. (1994). Effect of subthalamic high frequency stimulation on substantia nigra pars reticulata and globus pallidus neurons in normal rats. *J. Physiol.*, 88:359–361.

Burch, B. and Sheerin, F. (2005). Parkinsons disease. *Lancet*, 365:622–627.

Caruncho, H., Liste, I., and Labandiera-Garcia, J. (1996). GABAA receptor a1-subunit-immunopositive neurons in the rat striatum. *Brain Res.*, 722:185–189.

Chadha, A., Dawson, L., Jenner, P., and Duty, S. (2000). Effect of unilateral 6-hydroxydopamine lesions of the nigrostriatal pathway on GABAA receptor subunit gene expression in the rodent basal ganglia and thalamus. *Neuroscience.*, 95:119–126.

Chakravarthy, V., Denny, J., and Bapi, R. (2010a). What do the basal ganglia do? a modeling perspective. *Biol. Cybern.*, 103:237–253.

Chakravarthy, V., Joseph, D., and Raju, S. (2010b). What do the basal ganglia do? a modeling perspective. *Biol. Cybern.*, 103:237–253.

Charara, A., Galvan, A., Kuwajima, M., Hall, R., , and Smith, Y. (2004). An electron microscope immunocytochemical study of GABAB R2 receptors in the monkey basal ganglia: a comparative analysis with GABAB R1 receptor distribution. *J. Comp. Neurol.*, 476:65–79.

Charara, A., Heilman, C., Levey, A., , and Smith, Y. (2000). Pre-and postsynaptic localization of GABAB receptors in the basal ganglia in monkeys. *Neuroscience.*, 95:127–140.

Charara, A., Pare, J., Levey, A., and Smith, Y. (2005). Synaptic and extrasynaptic GABA-A and GABA-B receptors in the globus pallidus: an electron microscopic immunogold analysis in monkeys. *Neuroscience.*, 131:917–933.

Charles, K., Evans, M., Robbins, M., Calver, A., Leslie, R., and Pangalos, M. (2001). Comparative immunohistochemical localisation of GABAB1a, GABAB1b and GABAB2 subunits in rat brain, spinal cord and dorsal root ganglion. *Neuroscience.*, 106:447–467.

Chay, T., Fan, Y., and Lee, Y. (1995). Bursting, spiking, chaos, fractals and universality in biological rhythms. *Int. J. Bifurcation and Chaos*, 5(3):595–635.

Chen, L., Boyes, J., Yung, W., and Bolam, J. (2004). Sub-cellular localization of GABAB receptor subunits in rat globus pallidus. *J. Comp. Neurol.*, 474:340–352.

Chergui, K., Charlety, P., Akaoka, H., Saunier, C., Brunet, J., Buda, M., Svensson, T., and Chouvet, G. (1993). Tonic activation of NMDA receptors causes spontaneous burst discharge of rat midbrain dopamine neurons in vivo. *Eur. J. Neurosci.*, 5:137–144.

Chevalier, G. and Deniau, J. (1990). Disinhibition as a basic process in the expression of striatal functions. *Trends Neurosci*, 13:277–281.

Chicharro, D., Kreuz, T., and Andrzejak, R. (2011). What can spike train distances tell us about the neural code? *J. Neurosci. Methods*, 199:146–165.

Cotzias, G., Van Woert, M., and Schiffer, L. (1967). Aromatic amino acids and modification of parkinsonism. *N. Engl. J. Med.*, 276:374–379.

Dauwels, J., Vialatte, F., Weber, T., and Cichocki, A. (2009a). Metric-space analysis of spike trains: theory, algorithms, and application. *Advanced in Neuro-Information Processing*, 5506:177–185.

Dauwels, J., Vialatte, F., Weber, T., and Cichocki, A. (2009b). On similarity measures for spike trains. *Lectures Notes in Computer Science, Advances in Neuro-Information Processing*, 5506:177–185.

Dauwels, J., Vialatte, F., Weber, T., Musha, T., and Cichocki, A. (2009c). Quantifying statistical interdependence by message passing on graphs PART I: One-dimensional point processes. *Neural Computation*, 21(8):2152–2208.

Dauwels, J., Vialatte, F., Weber, T., Musha, T., and Cichocki, A. (2009d). Quantifying statistical interdependence by message passing on graphs PART II: Multi-dimensional point processes. *Neural Computation*, 21(8):2203–2268.

Dayan, P. and Abbott, L. (2001). *Theoretical Neuroscience: Computational and Mathematical Modeling of Neural Systmes.* MIT Press, Cambridge, MA, USA.

De Lau, L. and Breteler, M. (2006). Epidemiology of parkinsons disease. *Lancet Neurol.*, 6(5):525–535.

De Schutter, E. (2009). *Computational Modeling Methods for Neuroscientists.* 1st edition. MIT Press, Cambridge, MA, 432 pages.

De Schutter, E. and Bower, J. (1994). An active membrane model of the cerebellar purkinje cell. I. simulation of current clamps in slice. *J. Neurophysiol.*, 1(71):375–400.

DeLong, M. (1971). Activity of pallidal neurons during movement. *J. Neurophysiol.*, 34:414–427.

DeLong, M. (1990). Primate models of movement disorders of basal ganglia origin. *Trends Neurosci.*, 13:281–285.

Denham, M. and Borisyuk, R. (2000). A model of theta rhythm production in the septal-hippocampal system and its modulation by ascending brain stem pathways. *Hippocampus.*, 10:698–716.

Destexhe, A., Mainen, Z., and Sejnowski, T. (1994). An efficient method for computing synaptic conductances based on a kinetic model of receptor binding. *Neural Comput.*, 6:14–18.

Deuschl, G., Raethjen, J., Baron, R., Lindemann, M., Wilms, H., and Krack, P. (2000). The pathophysiology of parkinsonian tremor: a review. *J. Neurol.*, 5(247):33–48.

Deuschl, G., Raethjen, J., Lindemann, M., , and Krack, P. (2001). The pathophysiology of tremor. *Muscle Nerv.*, 24:716–735.

Dorsey, E., Constantinescu, R., Thompson, J., Biglan, K., Holloway, R., Kieburtz, K., Marshall, F., Ravina, B., Schifitto, G., Siderowf, A., and Tanner, C. (2007). Projected number of people with parkinson disease in the most populous nations 2005 through 2030. *Neurology.*, 68:384–386.

Dostrovsky, J., Levy, R., Wu, J., Hutchison, W., Tasker, R., and Lozano, A. (2000). Microstimulation-induced inhibition of neuronal firing in human globus pallidus. *J. Neurophysiol.*, 84:570–574.

Dostrovsky, J. and Lozano, A. (2002). Mechanisms of deep brain stimulation. *Mov. Disord.*, 7:S63–S68.

Ermentrout, B. (2002). *Simulating, analyzing, and animating dynamical systems: A guide to XPPAUT for researchers and student.* SIAM Press, Philadelphia, USA.

Ermentrout, G. B. and Terman, D. H. (2010). *Mathematical Foundations of Neuroscience.* Interdisciplinary Applied Mathematics, Vol. 35, 1st Edition, XV, 422 p.

Fahn, C. (2005). Does levodopa slow or hasten the rate of progression of parkinson's disease. *J. Neurol.*, 252(4):IV37–IV42.

Feuerstein, T., Kammerer, M., Lcking, C., , and Moser, A. (2011). Selective GABA release as a mechanistic basic of high-frequency stimulation used for the treatment of neuropsychiatric diseases. *Naunyn-Schmiedbergs Arch Pharmacol.*, 381(1):1–20.

Filali, M., Hutchison, W., Palter, V., Lozano, A., and Dostrovsky, J. (2004). Stimulationinduced inhibition of neuronal firing in human subthalamic nucleus. *Exp. Brain Res.*, 156:274–281.

Firestone, J., Weller, T., Franlin, G., Swanson, P., Longstreth, W., and Checkoway, H. (2005). Pesticides and risk of parkinson disease a population-based case-control study. *Arch. Neurol.*, 62:92–95.

FitzHugh, R. (1960). Thresholds and plateaus in the hodgkin-huxley nerve equations. *J. Gen. Physiol.*, 43:867–897.

Folley, P. and Riederer, P. (1999). Pathogenesis and preclinical course of parkinson's disease. *J. Neural Transm Suppl.*, 56:31–74.

Foster, B., Bojak, I., and Liley, D. (2008). Population based models of cortical drug response: insights from anaesthesia. *Cogn. Neurodyn.*, 2:283–296.

Fox, R. (1997). stochastic versions of the hodgkin-huxley equations. *Biophys. J.*, 72(5):2068–2074.

Fritschy, J. and Mohler, H. (1995). GABAA-receptor heter- ogeneity in the adult rat brain: differential regional and cellular distribution of seven major subunits. *J. Comp. Neurol.*, 359:154–194.

Gabriels, L., Cosyns, P., Nuttin, B., Demeulemeester, H., and Gybels, J. (2003). Deep brain stimulation for treatment-refractory obsessive-compulsive disorder: psychopathological and neuropsychological outcome in 3 cases. *Acta Psychiatr. Scand.*, 107:275–282.

Galati, S., Mazzone, P., Fedele, E., Pisani, A., Peppe, A., Pierantozzi, M., Brusa, L., Tropepi, D., Moschella, V., Raiteri, M., Stanzione, P., Bernadi, G., and Stefani, A. (2006). Biochemical and electrophysiological changes of substantia nigra pars reticulata driven by subthalamic stimulation in patients with parkinson's disease. *Eur. J. Neurosci.*, 23(11):2923–2928.

Galvan, A., Charara, A., Pare, J., Levey, A., and Smith, Y. (2004). Differential subcellular and subsynaptic distribution of GABAA and GABAB receptors in the monkey subthalamic nucleus. *Neuroscience.*, 127:709–721.

Garcia, L., DAllexandro, G., Bioulac, B., and Hammond, C. (2005). High frequency stimulation in parkinsons disease: more or less? *Trends Neurosci.*, 28(4):209–216.

Garcia, L., J., A., D'alessandro, G., Bioulac, B., and Hammond, C. (2003). Dual effect of high-frequency stimulation on subthalamic neuron activity. *J. Neurosci.*, 23:8743–8751.

Gerlach, M., Peter, R., and Scheller, D. (2011). Mechanisms underlying and medical management of l-dopa-associated motor complications. *Journal of Neural Transmission*, 118(12):1659–1660.

Gerstner, W. and Kistler, W. (2002). *Spiking neuron models. Single neurons, populations, plasticity.* Cambridge University Press, Cambridge,UK.

Gillies, A. and Willshaw, D.and Li, Z. (2002). Subthalamicpallidal interactions are critical in determining normal and abnormal functioning of the basal ganglia. *Proceedings of the Royal Society of London. Series B: Biological Sciences*, 269:5459–551.

Goetz, C., Tilley, B., Shaftman, S., Stebbins, G., Fahn, S., Martinez-Martin, P., Poewe, W., Sampaio, C., Stern, M., Dodel, R., Dubois, B., Holloway, R., Jankovic, J., Kulisevsky, J., Lang, A., Lees, A., Leurgans, S., LeWitt, P., Nyenhuis, D., Olanow, C., Rascol, O., Schrag, A., Teresi, J., van Hilten, J., and LaPelle, N. (2008). Movement disorder society-sponsored revision of the unified parkinson's disease rating scale (mds-uprs): scale presentation and clinimetric testing results. *Mov. Disord.*, 23(15):2129–2170.

Goldwyn, J. and Shea-Brown, E. (2011). The what and where of adding channel noise to the hodgkin-huxley equations. *PLoS Comput. Biol.*, 11(7).

Gong, H., Zhang, Y., Liang, P., and Zhang, P. (2010). Neural coding properties based on spike toming and pattern correlation of retinal ganglia cells. *Cogn. Neurodyn.*, 4:337–346.

Guiasu, S. (1977). *Information Theory with Applications*. McGraw-Hill, New-York, USA.

Guo, Y., Rubin, J., McIntyre, C., Vitek, J., and Terman, D. (2008). Thalamocortical relay fidelity varies across subthalamic nucleus deep brain stimulation protocols in a data driven computational model. *J. Neurophysiology*, 99:1477–1492.

Hall, L., Brauer, S., and Hodges, P. (2012). Implicit motor learning is impaired by levodopa, but restored by deep brain stimulation of the subthalamic nucleus. *Movement Disorders*, 27:132.

Hammond, C., Ammari, R., Bioulac, B., and Garcia, L. (2008). Latest viwe on the mechanism of action of deep brain stimulation. *Mov. Disord.*, 23:2111–2121.

Hashimoto, T., Elder, C., DeLong, M., and Vitek, J. (2001). *Responses of pallidal neurons to electrical stimulation of the subthalamic nucleus is experimental primates.* Sixth International Congress of Parkinsons Disease and Movement Disorders, Barcelona, Spain abstract 277.

Hashimoto, T., Elder, C., Okun, M., Patrick, S., and Vitek, J. (2003). Stimulation of the subthalamic nucleus changes the firing pattern of pallidal neurons. *J. Neurosci.*, 5(23):259–267.

Hauptmann, C. and Tass, P. (2009). Cumulative and after-effects of short and weak coordinated reset stimulation: a modeling study. *J. Neural Eng.*, 6:016004.

Hauptmann, C. and Tass, P. (2010). Restoration of segregated, physiological neuronal connectivity by desynchronizing stimulation. *J. Neural Eng.*, 7:056008.

Hedreen, J. and DeLong, M. (1991). Organization of striatopallidal, striatonigral, and nigrostriatal projections in the macaque. *J. Comp. Neurol.*, 304:569–595.

Heida, T., Marani, E., and Usunoff, K. (2008). The subthalamic nucleus part II: modelling and simulation of activity. *Adv. Anat. Embryol. Cell Biol.*, 199:1–85.

Higham, D. (2001). An algorithmic introduction to numerical simulation of stochastic differential equations. *SIAM review*, 43:525–546.

Hikosaka, O., Takikawa, Y., and Kawagoe, R. (2000). Role of the basal ganglia in the control of purposive saccadic eye movements. *Physiol. Rev.*, 80:953–978.

Hiller, A., Loeffler, S., Haupt, C., Litza, M., Hofmann, U., and Moser, A. (2007). Electrical high frequency stimulation of the caudate nucleus induces local GABA outflow in freely moving rats. *J Neurosci. Methods*, 159(2):286–290.

Hodaie, M., Wennberg, R., Dostrovsky, J., and Lozano, A. (2002). Chronic anterior thalamus stimulation for intractable epilepsy. *Epilepsia Psychiatr. Scand.*, 43:603–608.

Hodgkin, A. and Huxley, A. (1952). A quantitative description of membrane current and its application to conduction and excitation in nerve. *J. Physiol.*, 117:500–544.

Holgado, A., Terry, J., and Bogacz, R. (2010). Conditions for the generation of beta oscillations in the subthalamic nucleus globus pallidus network. *The Journal of Neuroscience*, 30:12340–12352.

Hsu, A., Borst, A., and Theunissen, F. (2004). Quantifying variability in neural responses and its application for the validation of model predictions. *Comput. Neural Syst.*, 15:91–109.

Hutchison, W., Dostrovsky, J., Walters, J., Courtemanche, R., Boraud, T., Goldberg, J., and Brown, P. (2004). Neuronal oscillations in the basal ganglia and movement disorders: Evidence from whole animal and human recordings. *The Journal of Neuroscience*, 42(24):9240–9243.

Hutt, A. and Longtin (2010). Effects of the anesthetic agent propofol on neural populations. *Cogn. Neurodyn.*, 4:37–59.

Izhikevich, E. (2003). Simple model of spiking neurons. *IEEE Transactions on Neural Networks*, 14:1569–1572.

Izhikevich, E. (2010). *Dynamical Systems in Neuroscience: The Geometry of Excitability and Bursting.* 2nd edition. MIT Press, Cambridge, MA, 464 pages.

Jaeger, D., Kita, H., and Wilson, C. (1994). Surround inhibition among projection neurons is weak or nonexistent in the rat neostriatum. *J. Neurophysiol.*, 72:2555–2558.

Jahr, C. and Stevens, C. (1990). A quantitative description of NMDA receptor-channel kinetic behavior. *J. Neurosci.*, 10:1830–1837.

Kandel, E., Schwartz, J., and Jessel, T. (2000). *Principles of neural science.* McGraw-Hill.

Kita, H. (2007). Globus pallidus external segment. *Prog. Brain Res.*, 160:111–133.

Kita, H. andTachibana, Y., Nambu, A., and Chiken, S. (2005). Balance of monosynaptic excitatory and disynaptic inhibitory responses of the globus pallidus induced after stimulation of the subthalamic nucleus in the monkey. *J. Neurosci.*, 25(38):8611–8619.

Klein, C. and Djarmati, A. (2011). Parkinson disease: genetic testing in parkinson disease-who should be assessed?. *Nat. Rev. Neurol.*, 1(7):7–9.

Klein, C. and Lohmann-Hedrich, K. (2007). Impact of recent genetic findings in parkinson's disease. *Curr. Opin. Neurol.*, 4(20):453–464.

Klein, C. and Schlossmacher, M. (2007). Parkinson disease, 10 years after its genetic revolution: multiple clues to a complex disorder. *Neurology.*, 22(69):2093–2104.

Klein, C., Schneider, S., and Lang, A. (2009a). Hereditary parkinsonism: Parkinson disease look-alikes-an algorithm for clinicians to PARK genes and beyond. *Mov. Disord.*, 14(24):2042–2058.

Klein, C., Schneider, S., and Lang, A. (2009b). Hereditary parkinsonism: Parkinson disease look alikes an algorithm for clinicians to PARK genes and beyond. *Mov. Disord.*, 14(24):2042–2058.

Klein, C. and Westenberger, A. (2012). Genetics of parkinson's disease. *Cold Spring Harb Perspect Med.*, 1(2).

Knight, B. (1972). Dynamics of encoding in a population of neurons. *J. Gen. Physiol.*, 59:734–766.

Koch, C. and Segev, I. (1998). *Methods in Neuronal Modeling: From Ions to Networks.* 2nd edition. MIT Press, Cambridge, MA, 687pages.

Kreuz, T., Haas, J., Morelli, A., Abarbanel, H., and Politi, A. (2007). Measuring spike train synchrony. *J. Neurosci. Meth.*, 165:151–161.

Kringelbach, M., Jenkinson, N., Owen, S., and Aziz, T. (2007). Translational principles of deep brain stimulation. *Nature Reviews Neuroscience.*, 8:623–635.

Kuhn, A., Kupsch, A., Schneider, G., and Brown, P. (2006). Reduction in subthalamic 8-35 hz oscillatory activity correlates with clinical improvement in parkinson's disease. *European Journal of Neuroscience*, 23:1956–1960.

Lacey, C., Boyes, J., Gerlach, O., Chen, L.and Magill, P., and Bolam, J. (2005). GABAB receptors at glutamatergic synapses in the rat striatum. *Neuroscience.*, 136:1083–1095.

Lamberti, P., Armenise, S., Castaldo, V., de Mari, M., Iliceto, G., Tronci, P., and Serlenga, L. (1997). Freezing gait in parkinson's disease. *Eur. Neurol.*, 38:297–301.

Lang, A. and Lozano, A. (1998). Parkinson's disease. first of two parts. *N. Engl. J. Med.*, 339:1044–1053.

Lee, R. (1989). Pathophysiology of rigidity and akinesia in parkinson's disease. *Eur. Neurol.*, 29(1):13–18.

Lees, A., Hardy, J., and Revesz, T. (2009). Parkinson's disease. *The Lancet.*, 373:2055–2066.

Levesque, M. and Parent, A. (2005). The striatofugal fiber system in primates: a reevaluation of its organization based on single axon tracing studies. *Proc. Natl. Acad. Sci. U. S. A.*, 102:11888–11893.

Levy, R., Hutchison, W., Lozano, A., and Dostrovsky, J. (2000). High-frequency synchronization of neuronal activity in the subthalamic nucleus of parkinsonian patients with limb tremor. *J. Neurosci* ., 20:7766–7775.

Lewicki, M. (1998). A review of methods for spike sorting: the detection and classification of neural action potentials. *Network*, 9(4):53–78.

Li, G., Yu, C., Lin, L., and Lu, S. (2005). Uncovering the mechanism(s) of deep brain stimulation. *Journal of Physics.*, 5:336–344.

Li, T., Qadri, F., and Moser, A. (2004). Neuronal electrical high frequency stimulation modulates presynaptic GABAergic physiology. *Neuroscience.*, 371:117–121.

Li, T., Thumen, A., and Moser, A. (2006). Modulation of a neuronal network by electrical high frequency stimulatin in striatal slices of the rat in vitro. *Neurochem. Int.*, 48:83–86.

Limousin, P., Greene, J., Pollack, P., Rothwell, J., Benabid, A., and Frackowiak, R. (1997). Changes in cerebral activity pattern due to subthalamic nucleus or internal pallidum stimulation in parkinsons disease. *Ann Neurol.*, 42:283–291.

Liu, Y., Wang, R., Zhang, Z., and Jiao, X. (2010). Analysis of stability of neural network with inhibitory neurons. *Cogn. Neurodyn.*, 4(1):61–68.

Loffler, S., Voght, S., Hofmann, U., and Moser, A. (2008). Striatal microstimulation in awake animals depends on NMDA receptor actoivity. *Biomed. Engeneer*, 53:126–128.

Lozano, A., Dostrovsky, J., Chen, R., and Ashby, P. (2002). Deep brain stimulation for parkinson's disease: disrupting the disruption. *Lancet Neurol.*, 1:225–231.

Lozano, A., Lang, A., Levy, R., Hutchison, W., and Dostrovsky, J. (2000). Neuronal recordings in parkinson's disease patients with dyskinesias induced by apomorphine. *Ann. Neurols.*, 47:5141–5146.

Magarinos-Ascone, C., Pazo, J., Macadar, O., and Buno. (2002). High-frequency stimulation of the subthalamic nucleus silences subthalamic nucleus: A possible cellular mechanism in parkinsons disease. *Neuroscience*, 115:1109–1117.

Mallet, N., Pogosyan, A., Sharott, A., Csicsvari, J., Bolam, P., Brown, P., and Magill, P. (2008). Disrupted dopamine transmission and the emergence of exaggerated beta oscillations in subthalamic nucleus and cerebral cortex. *The Journal of Neuroscience*, 18:4795–4806.

Mantovani, M., Moser, A., Haas, C., and Zentner, J. Feuerstein, T. (2009). GABA(A) autoreceptors enhance GABA release from human neocortex: towards a mechanism for high-frequency stimulation (hfs) in brain? *Naunyn Schmiedebergs Arch. Pharmacol.*, 380(1):45–58.

Mantovani, M., Van Velthoven, V., Fuellgraf, H., Feuerstein, T., and Moser, A. (2006). Neuronal electrical high frequency stimulation enhances GABA outflow from human neocortical slices. *Neurochem Int.*, 49(4):347–350.

Marsden, C. (1990). Parkinson's disease. *Lancet*, 335:948–592.

Matsumura, M., Kojima, J., Gardiner, T., and Hikosaka, O. (1992). Visual and oculomotor functions of monkey subthalamic nucleus. *J. Neurophysiol.*, 67:1615–1632.

Maurice, M., Thierry, A., Glowinski, J., and Deniau, J. (2003). Spontaneous and evoked activity of substantia nigra pars reticulata neurons during high-frequency stimulation of the subthalamic nucleus. *J. Neurosci.*, 23(30):9929–9936.

Mayer, J., Schuster, H., , and Claussen, J. (2006). The role of inhibitory feedback for information processing in thalamocortical circuits. *Phys. Rev*, 73:031908.

McIntyre, C., Savasta, M., Kerkerian-Le Goff, L., and Vitek, J. (2004a). Uncovering the mechanism(s) of action of deep brain stimulation: activation, inhibition, or both. *Clin. Neurophysiol.*, 15:1239–1248.

McIntyre, C., Savasta, M., Walter, B., and Vitek, J. (2004b). How does deep brain stimulation work? present understanding and future questions. *Expert Rev. Med. Devices*, 21(1):40–50.

McIntyre, C. and Thakor, N. (2002). Uncovering the mechanisms of deep brain stimulation for parkinsons disease through functional imaging, neural recording, and neural modeling. *Crit. Rev. Biomed. Eng.*, 30:249–281.

Meissner, W., Leblois, A., Hansel, D., Bioulac, B., Gross, C., Benazzouz, A., and Boraud, T. (2005). Subthalamic high frequency stimulation resets subthalamic firing and reduces abnormal oscillations. *Brain*, 128:2372–2382.

Merrison, R. (2011). *Modeling DBS in Parkinson's disease.* Progress Report, University of Plymouth.

Mink, J. (2003). The basal ganglia and involuntary movements: impaired inhibition of competing motor patterns. *Arch. Neurol.*, 60:1365–1368.

Mogilner, A., Benabid, A., and Rezai, A. (2001). Brain stimulation: current applications and future prospects. *Thalamus Relat. Sys.*, 1:255–267.

Montgomery, E. and Baker, K. (2000). Mechanisms of deep brain stimulation and future technical developments. *Neurol. Res.*, 2:259–266.

Montgomery, E. and Gale, J. (2007). *Mechanisms of action of deep brain stimulation (DBS).* Neuroscience and Biobehavioural Reviews, doi:10.1016/j.neubiorev.2007.06.003.

Moran, A., Stein, E., Tischler, H., and Bar-Gad, I. (2011). Decoupling neuronal oscillations during subthalamic nucleus stimulation in the parkinsonian primate. *Neurobiology of Disease*, 83:583–590.

Moro, E., Scerrati, M., Romito, L., Roselli, R., Tonali, P., and Albanese, A. (1999). Chronic subthalamic nucleus stimulation reduces medication requirements in parkinson's disease. *Neurology.*, 53:85–90.

Morris, C. and Lecar, H. (1981). Voltage oscillations in the barnacle giant muscle fiber. *Biophys. J.*, 35:193–213.

Moser, A., Gieselberg, A., Ro, B., Keller, C., and Qadri, F. (2003). Deep brain stimulation: response to neuronal high frequency stimulation is mediated through GABA(A) receptor activation in rats. *Neurosci. Lett.*, 341(1):57–60.

Nagumo, J., Arimoto, S., and Yoshizawa, S. (1962). An active pulse transmission line simulating nerve axon. *Proc. IRE.*, 50:2061–2070.

Nambu, A. (2005). A new approach to understand the pathophysiology of parkinson's disease. *J. Neurol.*, 52:suppl IV/1–IV/4.

Nambu, A. (2007). Globus pallidus external segment. *Prog. Brain Res.*, 160:135–150.

Nambu, A., Tokuno, H., Hamada, I., Kita, H., Imanishi, M., Akazawa, T., Ikeuchi, Y., and Hasegawa, N. (2000). Excitatory cortical inputs to pallidal neurons via the subthalamic nucleus in the monkey. *J. Neurophysiol.*, 4:289–300.

Nambu, A., Tokuno, H., and Takada, M. (2002). Functional significance of the cortico-subthalamopallidal hyperdirect pathway. *Neurosci. Res.*, 3:111–117.

Narabayashi, H., Miyashita, N., Hattori, Y., Saito, K., and Endo, K. (1997). Posteroventral pallidotomy: its effect on motor symptoms and scores of (mmpi) test in patients with parkinson's disease. *Parkinsonism Relat. Disord.*, 3:7–20.

Njap, F., Claussen, J., Moser, A., and Hofmann, U. (2011). Comparing realistic subthalamic nucleus neuron models. *AIP. Conf. Proc.*, 1371:102–109.

Nussbaum, R. and Ellis, C. (2003). Alzheimer's disease and parkinsons disease. *NEJM.*, 384(14):1356–1364.

Obeso, J., Olanow, C., Rodriguez-Oroz, M., Krack, P., Kumar, R., and Lang, A. (2001). Deep-brain stimulation of the subthalamic nucleus or the pars interna of the globus pallidus in parkinsons disease. *N. Engl. J. Med.*, 345:956–963.

Olanow, W., Brin, M., and Obeso, J. (2000). The role of deep brain stimulation as a surgical treatment for parkinsons disease. *Neurology*, 55(6):S60–S66.

Osborne, M. (2009). Radiofrequency neurotomy for a patient with deep brain stimulators: proposed safety guidelines. *Pain Med.*, 10(6):1046–1049.

Paiva, A., Park, I., and Principe, J. (2010). A comparison of binless spike train measures. *Neural Computing and Applications*, 19:405–419.

Paladini, C., Celada, P., and Tepper, J. (1999). Striatal, pallidal, and pars reticulata evoked inhibition of nigrostriatal dopaminergic neurons is mediated by GABA(A) receptors in vivo. *Neuroscience.*, 89:799–812.

Paladini, C. and Tepper, J. (1999). GABAA and GABAB antagonists differentially affect the firing pattern of substantia nigra dopaminergic neurons in vivo. *Neuroscience.*, 32:165–176.

Papahill, P., Levy, R., Dostrovsky, J., Davids, K., Rezai, A., Tasker, R., and Lozano, A. (1999). Tremor arrest with thalamic microinjections of muscimol in patients with essential tremor. *Ann. Neurol.*, 46:249–252.

Papoulis, A. (1984). *Brownian Movement and Markov Processes, in Probability, Random Variable, and Stochastic Processes.* McGraw-Hill, Inc., New-York, USA.

Parent, A. and Hazrati, L. (1995). Functional anatomy of the basal ganglia. I. the cortico-basal ganglia-thalamo-cortical loop. *Brain Res. Rev.*, 20:91–127.

Park, C., Worth, R., and Rubchinsky, L. (2011). Neural dynamics in parkinson brain: The boundary between synchronized and nonsynchronized dynamics. *Phys. Rev.*, 83:042901.

Parkinson, J. (1817). *Essay on the shaking palsy.* London: Sherwood, Neely, and Jones.

Pazienti, A. (2007). *Manipulations of spike trains and their impact on synchrony analysis.* PhD Thesis, University of Postdam, Germany.

Peppe, A., Gasbarra, A., Stefani, A., Chiavalon, C., Pierantozzi, M., Fermi, E., Stanzione, P., Caltagirone, C., and Mazzone, P. (2008). Acute and long-term effects of subthalamic nucleus stimulation in parkinson's disease. *Parkinsonism Relat. Disord.*, 14:501–504.

Peppe, A., Pierantozzi, M., Altibrandi, M., Giacomini, P., Stefani, A., Bassi, A., Mazzone, P., Bernardi, G., and Stanzione, P. (2001). Bilateral GPi DBS is useful to reduce abnormal involuntary movements in advanced parkinson's disease patients, but its action is related to modality and site of stimulation. *Eur. J. Neurol.*, 8(6):579–586.

Pirini, M., Rocchini, L., Sensi, M., and Chiari, L. (2009). A computational modeling approach to investigate different targets in deep brain stimulation for parkinsons disease. *J. Comput. Neurosci.*, 16:91–107.

Plenz, D. and Kital, S. (1999). A basal ganglia pacemaker formed by the subthalamic nucleus and external globus pallidus. *Nature*, 400:677–682.

Poewe, W. (2008). Non-motor symptoms in parkinsons disease. *Eur. J.Neuro.*, 15(1):14–20.

Priyadarshi, A., Khuder, S., Schaub, E., and Priyadarshi, S. (2001). Environmental risk factors and parkinson's disease: a metaanalysis. *Environ. Res.*, 86(2):122–127.

Qu, J., Wang, R., Du, Y., and Cao, J. (2011). Synchronization study in ring-like and grid-like neuronal networks. *Cogn. Neurodyn. In Press.*

Quiroga, R., Kreuz, T., and Grassberger, P. (2002). Event synchronization: a simple and fast method to measure synchronicity and time delay patterns. *Physical Review E 66.*

Ramon, y. C. (1890). *Manual de Anatomia Pathologica General (Handbook of general Anatomical Pathology).* First edition (in Spanish).

Rodriguez-Oroz, M., Rodriguez, M., Guridi, J., Mewes, K., Chockkman, V., Vitek, J., DeLong, M., and Obeso, J. (2007). The subthalamic nucleus in parkinson's disease: somatotopic organization and physiological characteristics. *Brain.*, 124:1777–1790.

Rosin, B., Slovik, M., Mitelman, R., Rivlin-Etzion, M., Haber, S., Israel, Z., Vaadia, E., and Bergman, H. (2011). Closed-loop deep brain stimulation is superior in ameliorating parkinsonism. *Neuron*, 72(2):370–384.

Rowat, P. (2007). Inter-spike interval statistics in the stochastic hodgkin-huxley model: coexistence of gamma frequency bursts and highly irregular firing. *Neural Computation*, 19:1215–1250.

Rubin, J. and Terman, D. (2004). High frequency stimulation of the subthalamic nucleus eliminates pathological thalamic rhythmicity in a computational model. *J. Comput. Neurosci.*, 16(3):211–235.

Sato, F., Lavallee, P., Levesque, M., and Parent, A. (2000). Single-axon tracing study of neurons of the external segment of the globus pallidus in primate. *J. Comp. Neurol.*, 417:17–31.

Schiff, S. (2010). Towards model-based control of parkinsons disease. *Phil. Trans. R. Soc.*, 368:2269–2308.

Schreiber, S., Fellous, J., Whitmer, J., Tiesinga, P., and Sejnowski, T. (2003). A new correlation-based measure of spike timing reliability. *Neurocomputing*, 52:925–933.

Schultz, W. (1986). Tesponses of midbrain dopamine neurons to behavioral trigger stimuli in the monkey. *J. Neurophysiol.*, 56:1439–1461.

Shils, J., Mei, L., and Arle, J. (2008). Modeling parkinsonian circuitry and the dbs electrode. II. evaluation of a computer simulation model of the basal ganglia with and without subthalamic nucleus stimulation. *Stereotact. Funct. Neurosurg.*, 86(1):16–29.

Skinner, F., Kopell, N., and Mardr, E. (1994). Mechanisms for oscillations and frequency control in network of mutually inhibitory relaxation oscillators. *J. Comp. Neurosci.*, 1:69–87.

Smith, Y. and Bolam, J. (1990). The output neurones and the dopaminergic neurones of the substantia nigra receive a GABA-containing input from the globus pallidus in the rat. *J. Comp. Neurol.*, 296:47–64.

Stefani, A., Fedele, E., Galati, S., Pepiceli, O., Frasca, S., Pierantozzi, M., Peppe, A., Brusa, L., Orlacchio, A., Hainsworth, A., Gattoni, G., Stanzione, P., Bernadi, G., Raiteri, M., and Mazzone, P. (2005). Subthalamic stimulation activates internal pallidus: evidence from cGMP microdialysis in PD patients. *Ann. Neurol.*, 57(3):448–452.

Stefani, A., Fedele, E., Galati, S., Raiteri, M., Pepicelli, O., Brusa, L., Pierantozzi, M., Peppe, A., Pisani, A., Gattoni, G., Hainsworth, A., Bernardi, G., Stanzione, P., and Mazzone, P. (2006). Deep brain stimulation in parkinson's disease patients: biochemical evidence. *J. Neural Transm.*, 70:401–408.

stimulation for parkinsons disease study group., D. B. (2001). Deep-brain stimulation of the subthalamic nucleus or the pars interna of the globus pallidus in parkinsons disease. *N. Eng. J. Med.*, 345:956–963.

Strogatz, S. (2001). *Nonlinear Dynamics and Chaos: With Applications to Physics, Biology, Chemistry, and Engineering.* Western view., Cambridge, MA, USA.

Tagliati, M., Shils, J., Sun, C., and Alterman, R. (2004). Deep-brain stimulation for dystonia. *Expert Rev. Med. Devices.*, 1:33–41.

Takakusaki, K., Oohinata-Sugimoto, J., Saitoh, K., and Habaguchi, T. (2004). Role of basal ganglia-brainstem systems in the control of postural muscle tone and locomotion. *Prog. Brain Res.*, 143:231–237.

Tass, P. (2003). A model of desynchronizing deep brain stimulation with a demand-controlled coordinated reset of neural subpopulations. *Biological Cybernetics.*, 89:81–89.

Temel, Y., Boothman, L., Blokland, A., Magill, P., Steinbusch, H., Visser-Vandewalle, V., and Sharp, T. (2007). Inhibition of 5-ht neuron activity and induction of depressive-like behavior by high-frequency stimulation of the subthalamic nucleus. *Proc Natl. Acad. Sci. U S A.*, 104(43):17087–17092.

Tepper, J., Abercrombie, E., and Bolam, J. (2007). Basal ganglia macrocircuits. *Prog. Brain Res.*, 160:3–7.

Terman, D. (2005). *Tutorials in Mathematical Biosciences I:Introduction to Dynamical Systems and neuronal Dynamics.* Springer, Heidelberg, Germany.

Terman, D., Rubin, J., Yew, A., and Wilson, C. (2002). Activity patterns in a model for the subthalamopallidal network of the basal ganglia. *J. Neurosci.*, 22:2963–2976.

Tomiyama, H., Hatano, T., and Hattori, N. (2007). Clinical molecular genetics for park8 (lrrk2). *Brain Nerve.*, 8(59):839–850.

Tronnier, V., Fogel, W., Kronenbuerger, M., and Steinvorth, S. (1997). Pallidal stimulation: an alternative to pallidotomy?. *J. Neurosurg* ., 87:700–705.

Tsodyks, M., Skaggs, W., and Sejnowski, T. (1993). Paradoxical effects of external modulation of inhibitory interneurons. *J. Neurosci.*, 17:4382–4388.

Tuckwell, H. (1988). *Introduction to Theoretical Neurobiology.* Cambridge, University Press, Cambridge.

Turner, J., Anderson, C., Williams, S., and Crunelli, V. (1997). lvlorphology and membrane properties of neurones in the cat ventrobasal thalamus in vitro. *J. Physiol.*, 505:707–726.

Tzedek, S. (2008). *A study of motor control in healthy subjects and in Parkinson's disease patients.* PhD Thesis, Massachusetts Institute of Technology, USA.

Urbano, F., Leznik, L., and Llinas, R. (2002). Cortical activation patterns evoked by afferent axons stimuli at different frequencies: an in vitro voltage-sensitive dye imaging study. *Thalamus rel. Syst.*., 1:371–378.

Van Rossum, M. (2001). A novel spike distance. *Neural Computation*, 13:751–763.

Vercueil, L., Pollak, P., Fraix, V., Caputo, E., Moro, E., Benazzouz, A., Xie, J., Koudsie, A., and Benabid, A. (2001). Deep brain stimulation in the treatment of severe dystonia. *J. Neurol.*, 248:695–700.

Victor, J. and Purpura, K. (1997). Metric-space analysis of spike trains: theory, algorithms, and application. *Nertwork*, 8:127–164.

Vitek, J. (2002). Mechanisms of deep brain stimulation: excitation or inhibition. *Mov. Disord.*, 17:S69–S72.

Vitek, J. and Giroux, M. (2000). Physiology of hypokinetic and hyperkinetic movement disorders: model for dyskinesia. *Ann Neurol.*, 47:131–140.

Waldvogel, H., Kubota, Y., Fritschy, J., Mohler, H., and Faull, R. (1999). Regional and cellular localisation of GABAA receptor subunits in the human basal ganglia: an autoradiographic and immunohistochemical study. *J. Comp. Neurol.*, 415:313–340.

Wang, W., Fang, X., Cheng, X., Jiang, D., and Lin, Z. (1993). A case-control study on the environmental risk factors of parkinson's disease in tianjin, china. *Neuroepidemiology.*, 12:209–218.

Wang, X. and Rinzel, J. (1992). Alternating and synchronous rythms in reciprocally inhibitory model neurons. *Neural Comp.*, 4:84–97.

Weinberger, M. (2009). *Oscillatory activity in the basal ganglia of patients with parkinson's disease.* PhD Thesis, University of Toronto, Canada.

Werneck, A. and Alvarenga, H. (1999). Genetics, drugs and environmental factors in parkinson's disease: a case-control study. *Arq. Neuro-Psiquiatr.*, 2(57):347–355.

White, J., Chow, C., Ritt, J., Soto-Trevino, C., and Kopell, N. (1998). Synchronization and oscillatory dynamics in heterogeneous, mutually inhibited neurons. *J. Comput. Neurosci.*, 5:5–16.

Wichmann, T., Bergman, H., and DeLong, M. (1994). The primate subthalamic nucleus. I. functional properties in intact animals. *J. Neurophysiol.*, 72:494–506.

Wichmann, T. and DeLong, M. (2006). Deep brain stimulation for neurologic and neuropsychiatric disorders. *Neuron*, 52:197–204.

Williams, D., Watt, H., and Lees, A. (2006). Predictors of falls and fractures in bradykinetic rigid syndromes: a retrospective study. *J. Neurol. Neurosurg. Psychiatry*, 77:468–473.

Wilson, C., Beverlin, B. I., and Netoff, T. (2011). Chaotic desynchronization as the therapeutic mechanism of deep brain stimulation. *Front. Syst. Neurosci.*, 5.

Wilson, H. and Cowan, J. (1972). Exictatory and inhibitory interactions in localized populations of model neurons. *Biophysical Journal*, 12:1–24.

Windels, F., Bruet, N., Poupard, A., Feuerstein, C., Bertrand, A., and Savasta, M. (2003). Influence of the frequency parameter on extracellular glutamate and gamma-aminobutyric acid in substantia

nigra and globus pallidus during electrical stimulation of subthalamic nucleus in rats. *J. Neurosci. Res.*, 2:259–267.

Wisden, W., Laurie, D., Monyer, H., and Seeburg, P. (1992). The distribution of 13 GABAA receptor subunit messenger mRNAs in the rat brain. 1. telencephalon, diencephalon, mesencephalon. *J. Neurosci.*, 12:1040–1062.

Wright, B., Rebrik, A., Emondi, A., and Miller, K. (1999). Cross channel correlations in tetrode recordings: Implications for spike-sorting. *Neurocomputing*, 27(26):1033–1038.

Yousif, N. (2005). *Computational models of the thalamocortical circuit: sleep oscillations and receptive fields.* PhD Thesis, University of Plymouth, UK.

Yung, K., Ng, T., and Wong, C. (1999). Subpopulations of neurons in the rat neostriatum display GABAB R1 receptor immunoreactivity. *Brain Res.*, 830:345–352.

Zhang, M., Goforth, P., Bertram, R., Sherman, A., and Satin, L. (2003). The Ca2+ dynamics of isolated mouse beta-cells and islets: implications for mathematical models. *Biophys J.*, 84(5):2852–70.